Locking Strategies IJmuiden

Developing and validating a method to quantify the effects of restrictive locking measures on both salt intrusion and vessel waiting times

J.W.E. de Ruiter

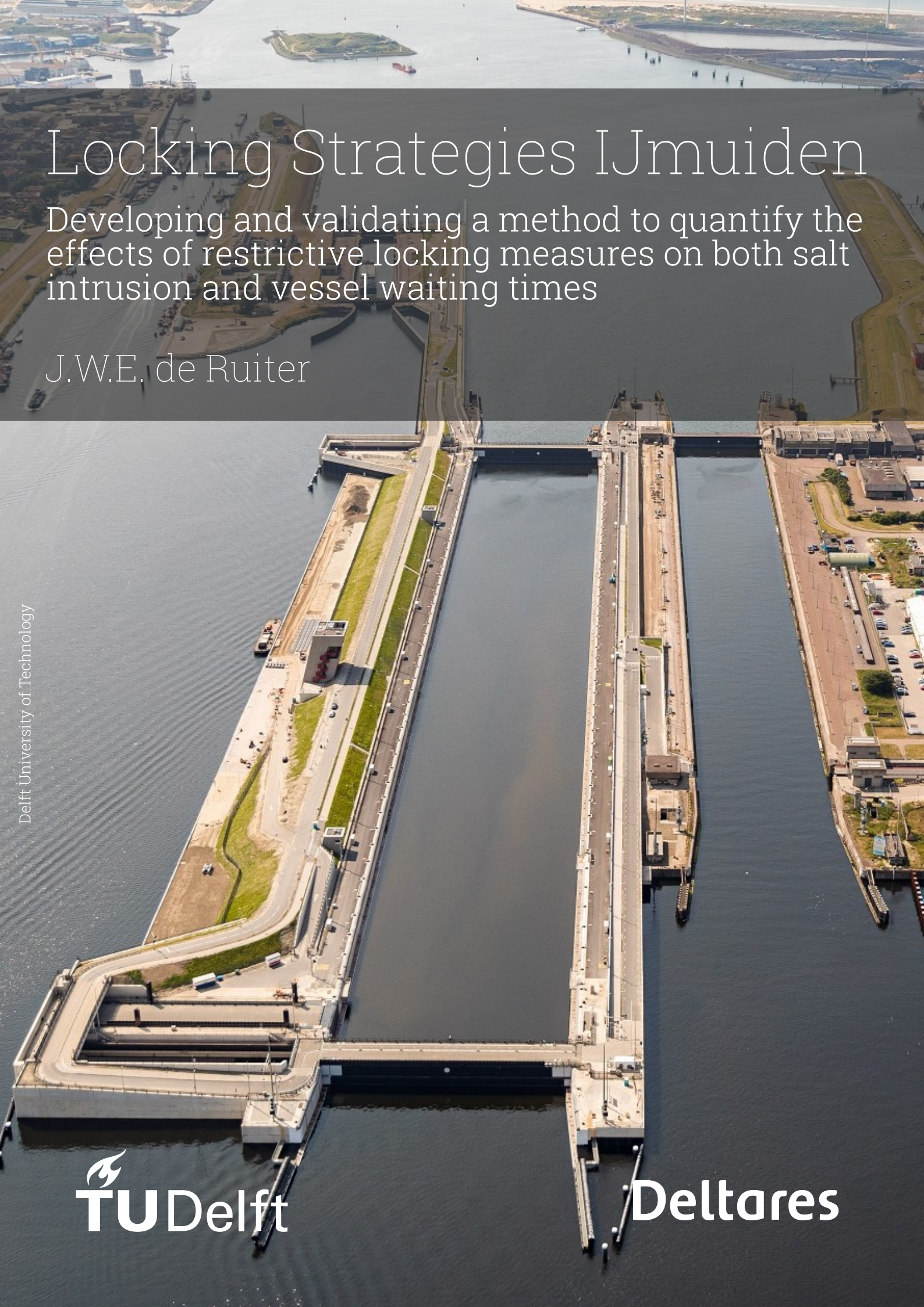

Delft University of Technology

TU Delft

Deltares

Locking Strategies IJmuiden

Developing and validating a method to quantify the effects of restrictive locking measures on both salt intrusion and vessel waiting times

by

J.W.E. de Ruiter

to obtain the degree of Master of Science
at the Delft University of Technology,
to be defended publicly on Friday August 29, 2025 at 13:00.

In collaboration with:

Deltares

Student number:	4484568	
Project duration:	November 2023 – August 2025	
Thesis committee:	Prof. dr. ir. M. van Koningsveld,	TU Delft, chair
	Ir. A.J. van der Hout,	TU Delft, Deltares, supervisor
	Ir. F.P. Bakker,	TU Delft
	Dr. T.S.D. O'Mahoney,	Deltares
	Dr. ir. W.M. Kranenburg,	TU Delft

Front cover image of the Sea lock IJmuiden by Rijkswaterstaat (2023b)

TU Delft

Preface

This thesis concludes my Master in Hydraulic Engineering at the Faculty of Civil Engineering and Geosciences at the TU Delft. It has been the most challenging project of my academic career so far, and the path to finishing it has been far from straightforward. I underestimated how time-consuming certain aspects would be, such as understanding and debugging the two models and, at times, simply finding the right words to put on paper. Completing this work would not have been possible without the support of many people, to whom I am deeply grateful.

First and foremost, I would like to thank my thesis committee. Arne van der Hout, for his daily supervision at both Deltares and TU Delft and for his consistent guidance in setting up a strong research foundation. Floor Bakker, for his extensive help with data provision, model setup, debugging in Python, and even a trip to the IJmuiden lock complex. Mark van Koningsveld, for serving as chair of the committee, for his valuable feedback, and for helping me sharpen my ideas and put them into writing. Tom O'Mahoney, for his constructive feedback on the validation of the Zeesluisformulering. And Wouter Kranenburg, for his insightful comments that helped raise the overall quality of this thesis. And of course, Deltares for having me as an intern and introducing me to the professional field for the first time.

Finally, I owe much to my family and friends for their unwavering support throughout my time in Delft. They believed in me during the moments when I almost did not believe in myself, and for that I am truly thankful. Without them, this achievement would not have been possible. I now look forward with excitement to the opportunities and adventures ahead.

J.(Jikke) W.E. de Ruiter
Rotterdam, August 2025

Abstract

Sea locks are a barrier between sea water and fresher inland water, allowing for control of inland water levels. They help maintain navigability for vessels, ensuring the connection of hinterland ports to the global shipping network. At the same time, they ensure the continued availability of drinking water, fresh water for agriculture and industry, and contribute to ecological stability by regulating water quality. However, the locking operations needed for vessel passings lead to salt intrusion and thus a reduction in the water quality of the inland waters. With climate change, longer periods of drought and an increase in sea water levels are expected, which increases the salt intrusion. And the growth of the global vessel industry means larger locks are needed to ensure navigability of the increasing vessel sizes, which increases the salt intrusion even more. We observe that measures taken by governments to reduce salt intrusion around locks require insight into both shipping impacts and salt exchange effects. Currently there seem no methods available to quantify how operational measures to reduce salt intrusion around locks impact both the shipping performance and salt levels behind the lock. This thesis investigates how we can overcome this gap in literature.

A first step is to identify how vessels pass shipping locks. We identify the important events that make up the entire lock passage procedure of a ship. Specifically we distinguish: approach, doors open, sailing in, doors closing, levelling, doors opening, sailing out and doors closing again. Next, we identify how the hydrodynamic processes that occur during the locking process influence salt intrusion. The most impactful hydrodynamic processes that occur are taking place between doors opening and closing, and during levelling.

Next we investigate what models are available to simulate both the shipping events and the salt exchange events. While there are several modelling concepts out there, we conclude that for the challenge at hand it is most suitable to use the mesoscopic agent-based traffic simulation model OpenTNSim to simulate vessel passages through locks. We couple this with the semi-empirical salt exchange model called the Zeesluisformulering. The main reason to choose this combination is that a discrete event agent based nautical traffic model captures exactly those events that drive the salt exchange estimates of the Zeesluisformulering. By combining both methods we get a new method that allows us to quantify how salt intrusion mitigation measures affect shipping performance and salt levels intrusion through the lock.

To determine how well the proposed combination of models works in practice we apply it to a real world case. For this thesis we select as our case location the Sea Lock IJmuiden, which at this point is the largest sea lock in the world. The lock complex in IJmuiden is suitable as a case, in February and March of 2023 salt intrusion measurements have been taken by Deltares and Rijkswaterstaat. During this period we also know what ships passed the locks, based on records taken by maritime students of the Amsterdam University of Applied Sciences. Based on these data sources we can test if the combination of models is capable of reproducing the observed behaviour.

A first step in the validation of our approach is to check to what extent the observed vessel passages trigger the observed salt intrusion patterns. We ran the Zeesluisformulering for the period of the salt measurements and created an estimate of the salt masses passing the lock. Next we compared the simulation prediction with the observed values. It turned out that the model was systematically under predicting the actual salt intrusion. Potential causes for this are an oversimplified representation of the lock exchange hydrodynamics, external parameters such as wind and currents, and the characteristics of the salt measurements (weighted averages as lock chamber concentrations and selected averaging methods for the harbour basins). For the IJmuiden case it was found that applying a correction factor of 1.65 to the propagation velocity of the exchange current after door opening was effective to match the predicted salt intrusion with the observations. For the current state of the ZSF a location specific correction factor should be derived. In the future the correction factor can be replaced by improving the representation of the hydrodynamic processes.

With the now corrected ZSF the discrete event agent based nautical traffic model is capable of estimating the salt intrusion caused by locking vessels with sufficient accuracy. This allows us now to use it to quantify the effect of different salt intrusion mitigation strategies. To demonstrate the methods capability we compare two strategies: 1. vessels are locked according to the normal IJmuiden locking procedure, and 2. vessels are clustered to reduce the number of locking operations. By changing the time interval by which vessels are clustered, we can now quantify both the impact on shipping delays and the resulting intruded salt mass as a function of the clustering interval. The results demonstrate that we now have a method that is able to quantify how measures to reduce salt intrusion around locks impact both the shipping performance and salt levels behind the lock, which was the gap in literature we aimed to overcome.

While the method presented here is indeed capable to quantify the effect of different strategies, several issues remain. The accurate representation of the clustering on the vessel trajectories had to be manipulated, given the current state of the OpenTNSim package. This is something that can and should be improved for future applications. Also the validation and the application of the correction factor are quite case specific. For future applications the ZSF should be improved to better represent the velocity of the exchange current to get a better general applicability.

Despite these obvious potential improvements, the work in this thesis clearly demonstrated that it is possible to quantify the salt intrusion caused by traffic passing through a sea lock.

Contents

1 Introduction

1.1. Background

Sea locks serve as a vital barrier between salty sea waters and fresher inland waters, playing a critical role in regulating water levels, navigability, and ensuring the protection of essential inland resources. Sea locks are indispensable to the global shipping industry, as they maintain navigability for vessels by ensuring water levels in inland waterways remain high enough for safe and efficient passage. They also allow ships to pass through hydraulic structures such as dams or dikes, facilitating connections between inland ports and the global shipping network. This connection is critical for the movement of goods and raw materials that fuel the global economy. By controlling water salinity and quality, sea locks help maintain ecological stability, support agricultural irrigation, and provide fresh water for industrial processes and drinking supplies. These functions are crucial for preserving ecosystems, sustaining livelihoods, and supporting economic activities that depend on clean and controlled water sources. By balancing the need for environmental protection with the demands of international trade, sea locks ensure that inland waterways remain both a sustainable resource and a vital component of the shipping and logistics infrastructure.

The locking operations required for vessel passage through sea locks often lead to salt intrusion, which reduces the water quality of inland waters and can result in restricted water use and freshwater shortages for drinking, agriculture, and industry. This issue is becoming increasingly pressing due to two major factors: climate change and socio-economic development. Climate change is intensifying pressures on inland and coastal waterways. Rising sea levels and prolonged droughts are leading to reduced river discharges, which in turn exacerbate saltwater intrusion in estuarine systems, complicating water management and navigation (United Nations, 2024). At the same time, the rapid growth of the global shipping industry has driven a steady increase in vessel sizes, as reported by (Merk et al., 2015). To accommodate these larger vessels, waterways have required significant infrastructure upgrades, such as the construction of new, larger locks in the Panama Canal and European seaports like Terneuzen and IJmuiden (Webuild Worldwide (2025); Buitendijk (2025); Port of Amsterdam (2023)). These trends place significant pressure on lock design, which must now simultaneously address the hydrological impacts of climate change and the operational demands of an expanding and increasingly oversized global fleet. Larger and more frequently operated locks allow more saltwater to enter inland waterways, further intensifying the effects of climate change. As waterborne trade volumes continue to expand, these combined factors are expected to drive greater salt intrusion, posing significant challenges for water resource management, ecological stability, and the sustainable operation of inland waterways. Addressing these issues will require innovative lock designs and operational strategies to balance the demands of global trade with the protection of vital freshwater resources.

Salt intrusion through sea locks is already a significant problem worldwide, posing challenges for water quality, ecological stability, and economic activity. One prominent example is the IJmuiden lock complex on the Dutch North Sea coast, a critical gateway to the Port of Amsterdam and its hinterland connections. Low river discharges during droughts have previously forced temporary adjustments to the locking

regime to reduce the salinity of the North Sea Canal. This was done by clustering vessels during limited operational hours to minimize the number of daily lock operations (Port of Amsterdam, 2023). However, the unpredictability of these adjustments caused delays, prompting some vessels to bypass the Port of Amsterdam altogether (Cruise Port Amsterdam, 2022), resulting in economic losses for the region. With the commissioning of the new Sea Lock IJmuiden, which is significantly larger than the existing locks in the IJmuiden lock complex to accommodate growing vessel sizes, salt intrusion and its impacts on vessel delays and port economics are expected to increase further if no mitigation measures are implemented.

Similarly, the Panama Canal lock complex faces significant challenges related to salt intrusion. This vital shortcut between the Atlantic and Pacific Oceans connects to upstream freshwater reservoirs and lakes, which are crucial water supplies for Panama. Lock operations there not only reduce freshwater volumes, but also degrade water quality due to salt intrusion. To mitigate these impacts, the number of vessels allowed to transit and their maximum draught are restricted, with even stricter limits during droughts (MercoPress, 2024). These measures, while necessary, come with economic consequences for Panama due to lost toll revenues and a possible ripple effect of delays across global shipping due to the importance of this key trade route.

Together, these examples highlight the need for balancing environmental protection, water management, and global trade demands. However, there is still a significant lack of understanding about how exactly mitigation measures affect salt intrusion and vessel performance. While the mechanisms by which adjustments to lock operations influence salt intrusion are somewhat understood, the full extent and dynamics of their consequences on shipping performance remain unclear. This knowledge gap creates challenges for effectively managing lock operations, as the interplay between reducing salt intrusion and maintaining efficient vessel transit is not well quantified. Addressing this uncertainty is essential to ensure that mitigation strategies are both environmentally and economically sustainable, minimizing the trade-off between protecting freshwater resources and supporting the global shipping industry.

1.2. Problem statement

The problem statement of this research focuses on the need to quantify the effects of restrictive locking measures on both salt intrusion and vessel waiting times. By understanding these effects, the most effective mitigation measures could be implemented in time, potentially avoiding the need for severe restrictions on lock operations in the future. However, to the best of the researcher's knowledge, these impacts have not yet been comprehensively studied, and existing methods in the literature are found to be limited. A critical challenge lies in the inability to analyse shipping performance and salt intrusion together, making it exceedingly difficult to determine the effectiveness of combinations of mitigation measures. To address this gap, a modelling framework is required that simultaneously quantifies the impact of countermeasures on both the reduction of salt intrusion and the increase in vessel delays. Such an approach is essential for designing balanced and effective strategies to mitigate salt intrusion while maintaining efficient shipping operations.

1.3. Research objective

The objective of this research is to develop an approach that addresses current limitations by integrating a logistical simulation model for vessel passage with a hydrodynamic model for salt intrusion at locks. By coupling these two types of models into a unified framework, the research aims to enable the quantification of the effectiveness of salt intrusion mitigation measures on both shipping performance and salt intrusion. This integrated approach will provide a comprehensive understanding of how various countermeasures impact the balance between maintaining efficient vessel operations and reducing salt intrusion, ultimately supporting the development of sustainable and effective strategies for lock management.

1.4. Research question

To achieve our research objective we aim to answer the following research question:

How can shipping delays and salt intrusion as a result of locking operations be quantified, to be able to compare the effects of realistic locking strategies?

To answer this main question we ask ourselves the following sub-questions:

1. What locking processes take place during the passing of ships through locks and how do they affect the salt intrusion?
2. What models are suitable to quantify the effect of locking strategies on vessel passage and salt intrusion for a real world example, and how can these models be coupled?
3. How well does the salt intrusion model perform compared to measurements and how can this performance be improved?
4. How can the coupled model be used to compare the effect of alternative locking strategies?

1.5. Research scope

This research focuses exclusively on logistical locking operations, excluding any structural modifications to the lock infrastructure. The analysis is limited to a single case study: the IJmuiden lock complex, with only one lock considered at a time: Sea Lock IJmuiden. Furthermore, the scope is restricted to the passage of sea-going vessels, since they represent the most critical category in terms of both operational impact and salt intrusion, due to their size and frequency of passage.

1.6. Report structure

The structure of this thesis is as follows: Chapter 2 describes the theory of locking, detailing both the logistics of vessels passing through a lock as well as the salt intrusion for the different locking processes. This answers the first sub-question. Additionally it describes possible operational salt intrusion mitigation measures. Chapter 3 provides the selection of suitable models and a description of the chosen models, including the input and output data needed. It also describes how the chosen models can be coupled, answering the second sub-question. Chapter 4 introduces the IJmuiden Lock Complex as the case study to represent a real world example. It details the layout of the lock complex, the water system around it and the monitoring and consequences of salt intrusion. It also describes the key aspects needed for traffic modelling and salt exchange modelling. In Chapter 5 the accuracy of the Zeesluisformulering will be determined by comparing model calculations to field measurement data of IJmuiden. With these results, a correction of the Zeesluisformulering is proposed to improve the ZSF model to make salt intrusion predictions at the Sea Lock IJmuiden more accurate. This answers the third sub-question. In Chapter 6 OpenTNSim will be used to simulate locking strategies. With OpenTNSim the vessel delays of the strategies are determined and the simulations are then used as input for the ZSF to calculate the salt intrusion for each strategy. Chapter 7 contains the discussion and conclusions, which will be followed up with some recommendations for future research.

2

Theory of lock operation

To enable the quantification of shipping delays and salt intrusion under various locking strategies, it is essential to understand how vessels pass through locks, how locking operations drive salt exchange, and how these processes interact. This chapter provides the theoretical basis for understanding the operation of shipping locks, focusing on both the logistical and hydrodynamic aspects of the locking cycle. It concludes with the identification of the interface between logistics and salt transport, which forms the foundation for the coupled modelling approach.

2.1. Logistics of vessel passage through locks

Understanding the logistics of vessel passage through locks begins with identifying the main components of a lock area and their respective functions. The movement through these components is then described from the perspective of a vessel, including interactions with other vessels, such as opposing traffic and the clustering of multiple vessels within the lock chamber. Finally, the cyclic process of locking is considered from the operator's point of view, highlighting the influence of operational decisions.

2.1.1. Lock area components

From a logistical perspective, not only the lock chamber but also the approach areas play a crucial role in efficiently managing vessel traffic. Nowadays, commercial shipping lock areas are designed for an optimal efficient locking process (Kooman & De Bruijn, 1975). Figure 2.1 illustrates one side of a typical layout of a commercial shipping lock area, highlighting its most important components, which are clarified below.

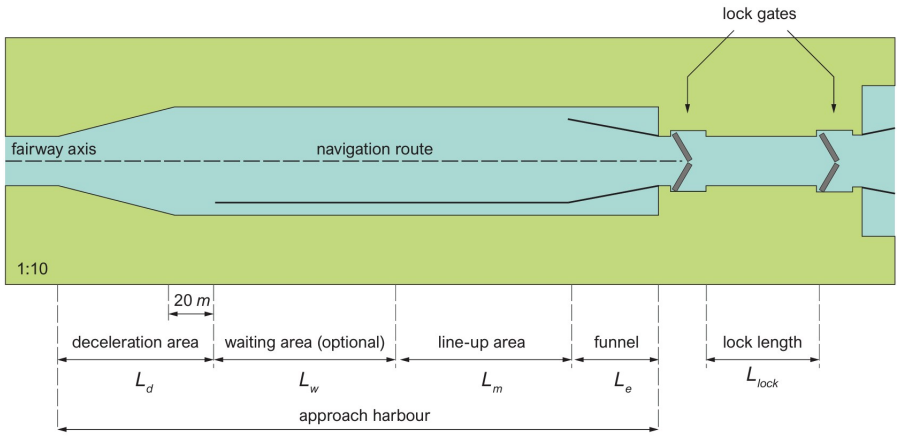

Figure 2.1: Lock area elements (from Van Koningsveld et al. (2023) by TU Delft - Ports and Waterways is licenced under CC BY-NC-SA 4.0, originally by RVW (2020))

The lock chamber is the main and central component of a lock system. It is enclosed by lock doors on either end, which open and close to allow vessels to enter and exit, while the water level inside the chamber is adjusted through controlled filling and emptying. According to Kooman and De Bruijn (1975), efficient locking requires the cross-section of the chamber to be rectangular and it's width constant and equal to navigable width at the lock doors.

The approach area of a lock is typically straight and in line with the lock chamber and consists of multiple elements. As vessels approach a lock, they enter the deceleration area where they begin to slow down in preparation for a controlled entry. Vessels arriving early may need to stop in the waiting area, either due to ongoing operations or traffic management considerations. Vessels remain there until a spot in a locking operation is assigned to them. A waiting area by the lock itself is optional as waiting in anchorage areas or on the quay are often an availability, especially for sea-going vessels. Adjacent to this is the line-up area, where vessels queue in the correct order before entering the lock chamber, ensuring an orderly and efficient passage. Before reaching the lock itself, vessels pass through the funnel, a structure designed to guide vessels towards the lock entrance.

2.1.2. Vessels passing through the lock system

The passage of a single vessel through a lock can be described from the perspective of the vessels' skipper. Often a tracking diagram, as illustrated in Figure 2.2, is used for this. Such a diagram displays the vessel's behaviour during the locking process and depicts the passage time and experienced delay.

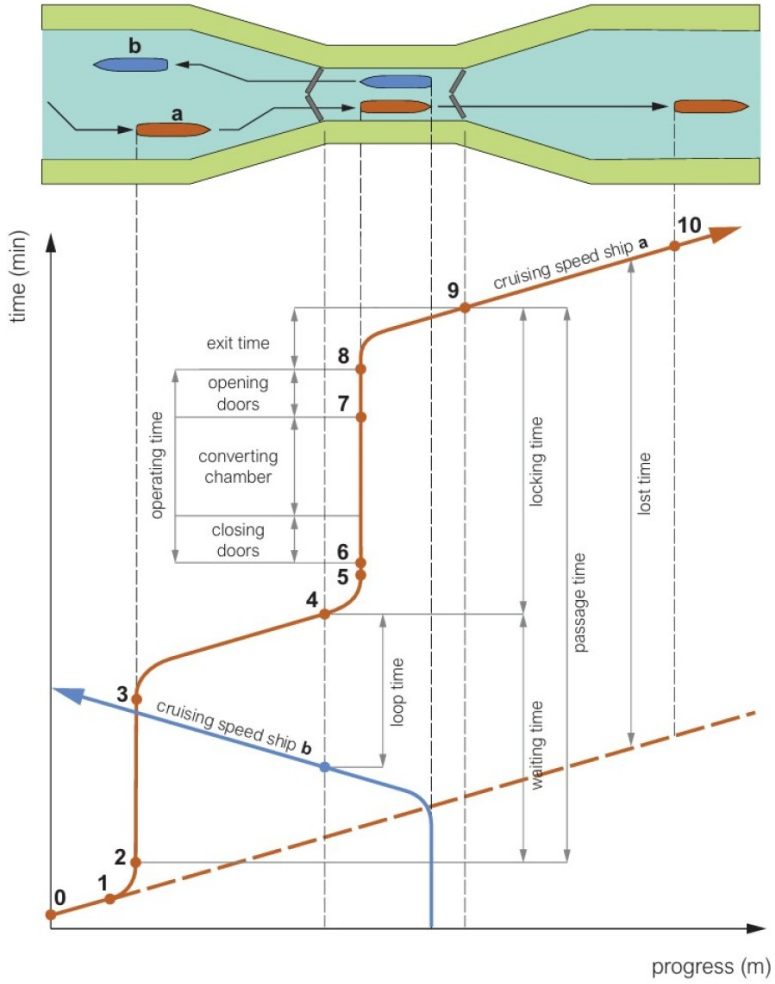

Figure 2.2: Tracking diagram for a single vessel passing a lock (from Van Koningsveld et al. (2023) by TU Delft - Ports and Waterways is licenced under CC BY-NC-SA 4.0)

In the tracking diagram in Figure 2.2 the red and blue vessel (a and b respectively) are passing the lock in opposite directions. According to Van Koningsveld et al. (2023), the passage of the red vessel can be separated in the following phases:

- $(0 \rightarrow 1)$ approaching at cruising speed,
- $(1 \rightarrow 2)$ slowing down to full stop and mooring in the waiting area,
- $(2 \rightarrow 3)$ waiting in lay-by until the lock can be entered,
- $(3 \rightarrow 4)$ speeding up and entering the lock chamber, once the last ship leaving the lock has passed
- $(4 \rightarrow 5)$ slowing down to full stop and mooring in the lock chamber,
- $(6 \rightarrow 8)$ door closing once all vessels are in, levelling process, unmooring whilst other door is opening
- $(8 \rightarrow 9)$ once the door is open: speeding up and leaving the lock chamber,
- (9) ship stern passes the exit lock sill,
- $(9 \rightarrow 10)$ leaving the other lock area and continuing the journey at cruising speed.

Delay

To determine the efficiency of a lock, one can look at the delay of vessels. In the tracking diagram depicted in Figure 2.2, the original path of the red vessel at cruising speed is used to determine the delay caused by the presence of the lock and the blue vessel.

However, in order to compare the efficiency of different locking strategies, the definition of vessel delay must be adapted. In this study, delay is defined as the difference in passage time compared to the most efficient possible passage. This adjusted definition allows for a consistent comparison across various operational strategies. The tracking diagrams shown in Figure 2.3a and Figure 2.3b provide a visual representation of how delay is interpreted within the context of this research, illustrating the delay caused by clustering and by oncoming traffic respectively. How much delay a vessel experiences is dependent on whether the lock is already accessible on the approaching side and whether clustering of vessels occurs. The most efficient possible passage, represented by the blue dashed line, is defined as immediate entry upon arrival at the lock without interacting with other traffic (i.e. no clustering and no oncoming traffic).

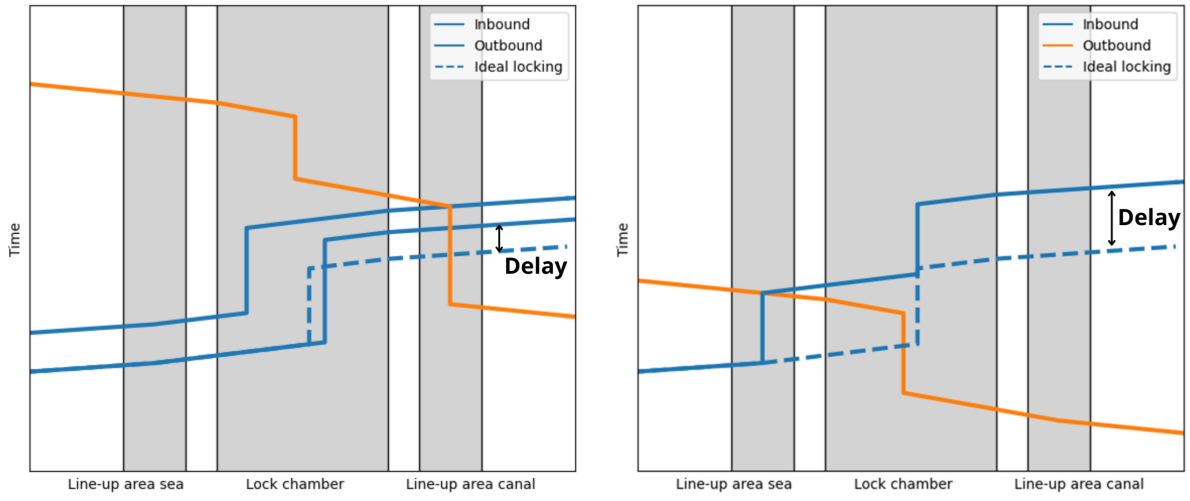

(a) Delay due to clustering

(b) Delay due to oncoming traffic

Figure 2.3: Tracking diagram depicting clustering and delay

Clustering

In a single locking operation, the simultaneous passage of multiple vessels is referred to as clustering. This interaction is illustrated in the tracking diagram in Figure 2.3a by the solid blue lines. Vessels enter the lock chamber one by one, and the locking process begins once the final vessel is inside the lock. After the opposite door opens, vessels exit the lock sequentially. Any vessels waiting to enter must do so only after the entire group has passed.

Whether clustering takes place depends on several factors. One key factor is whether multiple vessels physically fit within the lock chamber, which is determined by the chamber dimensions, vessel sizes, and the clearance required for safe mooring. Another factor is logistical availability, such as the presence of linesmen, tugboats, and pilots, as well as the readiness of the hinterland to process the arriving vessels.

Clustering reduces the total number of locking operations, which helps to lower salt intrusion levels (as will be discussed in Section 2.3). However, it also introduces delays, since vessels must wait for others to arrive before a locking cycle can begin.

2.1.3. Locking cycle

The passage of vessels can also be viewed from the perspective of the lock operator. When looking at multiple lock passages back to back, elements of the locking process are repeated. The cyclic process of a complete sequence of operations from one side of the lock to the other and back is called a locking cycle. The recurring series of events of the locking cycle as described by Rijkswaterstaat (1973) are listed below. They are summarised in a schematic diagram in Figure 2.4.

1. the stern of the last ship of the previous locking cycle passes the lock sill on exit,
2. the stern of the first ship of the new cycle passes the lock sill while entering the lock chamber,
3. the stern of the last ship of this cycle passes the lock sill, so door closing can begin,
4. the doors are closed and the water level in the lock chamber can be adjusted to that at the exit side,
5. the water level in the chamber is (almost) adjusted and the exit doors can be opened,
6. the exit doors are open and the stern of the first ship leaving passes the lock sill,
7. the stern of the last ship leaving passes the lock sill and the operation in opposite direction can begin when this ship has passed the waiting area.

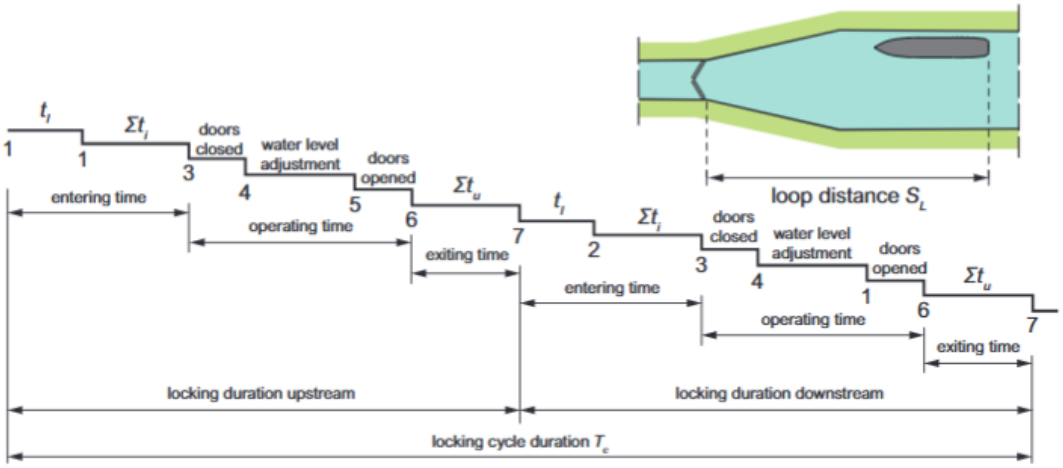

Figure 2.4: Locking cycle components (from Van Koningsveld et al. (2023) by TU Delft - Ports and Waterways is licenced under CC BY-NC-SA 4.0, originally by Rijkswaterstaat (1973))

The locking cycle can be divided into distinct phases based on the movements of the lock doors and the associated water level changes. It consists of four main phases: two phases involve levelling, where the water level in the lock chamber is raised or lowered to match the adjacent water level on either side of the lock, and two phases involve the opening of the lock doors to allow vessels to enter or exit the chamber. The sequence of these phases, as applied in this study, is illustrated in Figure 2.5. The operation is simplified by assuming that the time required to move the doors is reduced to an instantaneous moment.

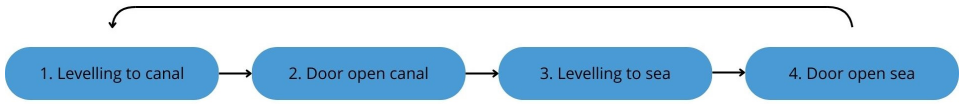

Figure 2.5: Locking cycle phases

Now that the logistical phases of the locking process have been defined, the next step is to describe the hydrodynamic processes that occur during each of these phases.

2.2. Salt intrusion through locks

In the previous section, it was determined that the locking cycle can be divided into four phases, separated by the movement of the lock doors. In this section, the hydrodynamic processes causing salt fluxes during each of these phases are examined. Salt intrusion is defined as the net salt flux from the lock chamber into the canal. The relevant water fluxes and mechanisms for each phase are outlined, along with an indication of which directly contribute to salt intrusion.

The four phases of the locking cycle are illustrated in Figure 2.6, distinguishing between low and high sea water levels compared to the canal water level. During the first phase, the water level in the lock chamber is raised or lowered to the canal level. During the second phase the doors open at the canal side, allowing vessels to exit and enter the lock. During the third phase, the lock chamber water level is raised or lowered to the water level at sea. During the fourth phase the doors at the sea side open, allowing vessels to exit and enter the lock. Within these phases, there are three categories of hydraulic processes that create salt fluxes: *levelling*, *lock exchange* and *ship influences*.

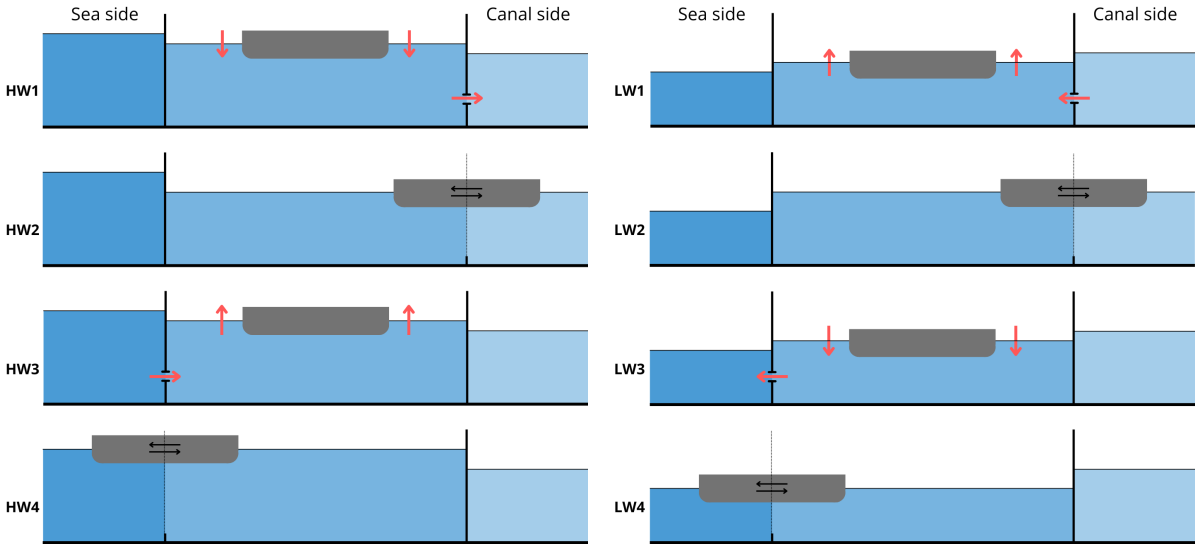

(a) Around low water **(b)** Around high water

Figure 2.6: Schematic of the locking phases around low and high water. HW1/LW1: Levelling to the canal side, HW2/LW2: Door open phase at the canal side, HW3/LW3: Levelling to the sea side, HW4/LW4: Door open phase at the sea side.

2.2.1. Levelling

During the levelling phase, the lock doors are closed and the water level is either increased by allowing water to enter the lock chamber or decreased by allowing water to exit the lock chamber. This can be achieved by opening the lock valves in the doors, as is the case at Sea Lock IJmuiden. The water movement always occurs over the lock door at the side where the water level in the lock chamber needs to be matched to. The volume of water used for levelling, called the lockage prism, equals the product of the water level difference between the lock and the sea or canal times the horizontal lock chamber area. According to Kerstma et al. (1994) the transferred salt mass during this phase depends on this

lockage prism and the salt concentration of the displaced water. When assuming a homogeneous situation, the salt concentration of the displaced water is the salt concentration of the lock chamber. In case of a stratified situation, the salt concentration depends on the position of the levelling valves. The closer the valve is located to the chamber floor, the larger the salt concentration of the displaced water will be.

Figure 2.7 illustrates the water fluxes in the four different levelling situations that can occur. In Figure 2.7a levelling of the lock to the canal during low water at sea is illustrated. Freshwater from the canal is used to raise the water level in the lock, creating a freshwater wedge along the surface of the lock. The influx of freshwater increases the water volume in the lock and as a result, the salt concentration of the lock chamber decreases. Levelling to the canal side during high water at sea is depicted in Figure 2.7b. The water level of the lock chamber is lowered by relieving water into the canal, resulting in a water flux in the form of a saltwater wedge propagating along the canal floor. If the water in the chamber is considered homogeneous, the salt concentration in the lock chamber remains the same. When this is not the case, a levelling system closer to the chamber floor results in a saltier water flux, which decreases the salt concentration in the lock chamber. In Figure 2.7c the water level in the lock chamber is levelled to the seaside during low water by relieving water into the sea. Here, a wedge propagates along the sea surface. Again, if the situation is considered homogeneous, the salt concentration of the lock remains the same, while a stratified situation with a lower located levelling system has a saltier water flux and thus decreases the salt concentration in the lock chamber. Figure 2.7d illustrates the water displacement due to the levelling of the lock chamber to the seaside during high water at sea. Saltwater is let into the lock chamber to raise the water level, which causes a saltwater wedge to propagate along the lock chamber floor. The salt concentration in the lock chamber increases due to the saltwater flux.

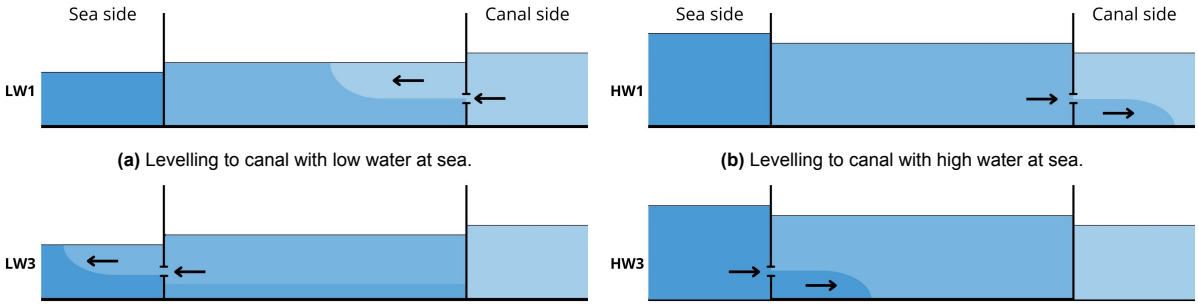

(a) Levelling to canal with low water at sea.

(b) Levelling to canal with high water at sea.

(c) Levelling to sea with low water at sea.

(d) Levelling to sea with high water at sea.

Figure 2.7: Different situations of salt intrusion during levelling with a salty sea and freshwater canal. Locking phase numbers corresponding to those in Figure 2.6. Adjusted from Deltares (2011).

Since salt intrusion is only stated to occur when salt water flows from the lock chamber into the canal, this is only the case when the lock chamber is levelled to the canal during high water at sea (Figure 2.7b). Something to keep in mind is that in the case of sea locks, previous salt intrusion has likely made the water of the canal brackish. When levelling to the canal during low water at sea (Figure 2.7c), the water flux into the lock chamber causes salt extraction from the canal into the lock chamber, although the salt concentration of the canal will not be affected by this.

2.2.2. Lock exchange

Before opening the lock doors, a difference in salt concentrations between the lock chamber and the harbour basin on the other side of the door is present. When the lock doors are opened, the salt and fresh water start to interact. Since salt water is heavier than fresh water, it sinks directly to the bottom. Kerstma et al. (1994) states that during this process, the potential energy in the water is converted into kinetic energy, which causes the salt water to start moving as a wedge along the bottom. As the salt wedge propagates along the bottom, an equally large fresh water wedge moves in the opposite direction. According to Deltares (2011) the propagation speed of the wedge depends on the salt concentration difference between the lock chamber and harbour basin and on the water depth, and the height of the wedge depends on the water depth above the lock sills. Therefore, the displaced salt mass is

dependent on the salt concentration difference, the sill depth and the duration of the opened doors.

As with the levelling, there are multiple situations of lock exchange. The first situation is the opening of the doors on the canal side of the lock, see Figure 2.8a. In this case, the salt wedge intrudes the canal along the bed, while the fresh water wedge moves into the lock chamber until it reaches the closed lock door on the other side. Due to mass inertia the salt wedge keeps moving. When the door is open long enough, the amount of salt water in the lock chamber depletes and the tail of the salt wedge starts dragging fresh water. This causes the lock chamber to fill with even more fresh water. When the lock has sills, a residual of salt water may remain on the lock chamber floor. The inward flux of fresh water and the outward flux of salt water decreases the salt concentration of the lock chamber.

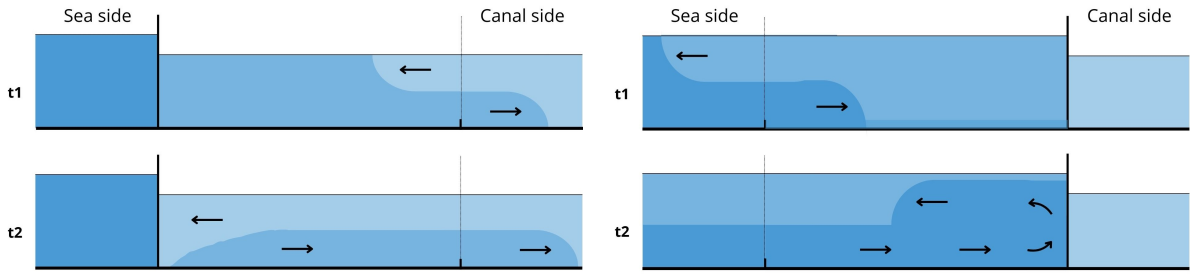

(a) Lock exchange at the canal side

(b) Lock exchange at sea side

Figure 2.8: Lock exchange development when lock doors are open. Adjusted from Deltares (2011).

The second scenario is the opening of the lock chamber doors on the sea side, see Figure 2.8b. Here, the salt wedge intrudes the lock chamber while the fresh wedge exits toward the sea and spreads out as a top layer, increasing the salt concentration of the lock chamber. When the salt wedge reaches the closed lock door on the other side of the lock chamber, it is pushed upward and the potential energy created by this is then converted back into movement. This causes the wedge to reflect back toward the open lock door. When the lock door is open long enough, the salt wedge travels back to sea leaving a top layer of fresh water. Closing of the lock door stops the growth of the salt wedge and internal waves can occur as a result of reflection against the now closed door.

When the water level at sea changes as a result of the tide while the lock door is open, the water level in the lock chamber also changes. This also translates to a water flux: rising tide at sea fills the lock chamber with sea water, lowering tide at sea draws the water of the lock chamber out into the sea.

As stated before, salt intrusion occurs when there is a salt flux from the chamber to the canal. For lock exchange this is only the case when the lock doors are opened on the canal side.

2.2.3. Vessel influences

A vessel passing through a lock causes water displacements, which has an influence on the salt intrusion. A distinction between two types of displacement can be made: *static displacement* and *dynamic displacement*.

Static displacement

Static displacement is the effect of a stationary vessel in a lock on the water in a lock chamber. A vessel lying at rest in water takes up a certain volume of water called the underwater volume of the vessel (or displacement). Deltares (2011) states that when a vessel is located in a lock, the volume of the lock chamber is decreased by the vessels underwater volume, which leads to a more rapid increase and decrease in salt concentration when an equal amount of salt mass would be exchanged. For example, when the lock fills up with fresh water while levelling toward the canal side during low water, the presence of a larger vessel results in a greater decrease in the salt concentration of the lock chamber than with a smaller vessel. Consequently, when the doors on the canal side are opened, the difference in salt concentration is smaller, resulting in a less strong lock exchange between the canal and the lock chamber.

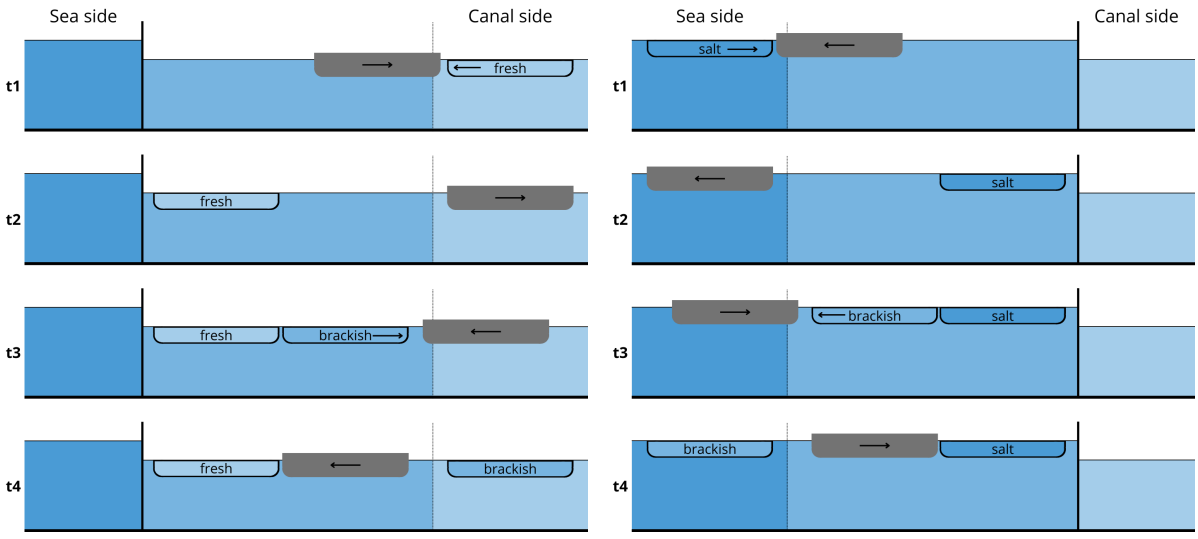

(a) Displacement at canal side

(b) Displacement at sea side

Figure 2.9: Dynamic displacement of water by vessels entering and exiting the lock. Adjusted from Deltares (2011)

Dynamic displacement

The displacement of water resulting from the entering or exiting of a vessel is defined as dynamic displacement. Deltares (2011) divides this further into two distinct categories: displacement caused by the movement of the vessel itself and displacement resulting from the use of the vessel's propellers. The first of these contributions is illustrated in Figure 2.9. A vessel moving through water pushes water in front of it away, while creating a void that suctions water behind it. Upon exiting a lock, the vessel's underwater volume is replaced by an equal volume of water sucked into the lock. Vice versa, when a vessel enters a lock, the volume of water is expelled from the lock.

From Figure 2.9 it can be concluded that only vessels entering the lock from the canal side cause salt intrusion. Vessels exiting the lock on the canal side do cause an extraction of salt from the canal, but this has no direct influence on the salt concentration of the canal.

The second dynamic displacement contribution is the influence of the propeller operations. When a vessel enters the lock it uses its propeller to slow down and come to a halt. This causes a suctioning of water from the direction of the open lock door and a movement of water to the closed lock door. Vice versa, when a vessel accelerates to exit the lock, the propeller pushes water to the closed lock door and suctions water from the direction of the open lock door. Whether the propeller operations contribute to salt intrusion is difficult to estimate, since it depends on the depth and speed of the vessel and the relative location of the propeller to the moving salt tongue.

2.3. Operational salt intrusion mitigation measures

Now that the logistical elements of locking, and the hydrodynamical salt intrusion processes have been identified, an investigation can be conducted into the potential mitigation measures that could be employed. For the purpose of this research, only those measures that can be implemented by modifying lock operations (i.e. vessel composition, door operations and operational hours) will be considered. The theoretical impact of these measures on the salt intrusion and potential delays for vessels will be outlined.

2.3.1. Reduced door open times

The amount of salt water exchanged when the lock doors are open depends on the duration that the doors are open. Closing the doors faster will stop the momentum of the salt tongue and thus reduces the salt intrusion. The effect of this is enhanced with repetition. When limiting the salt exchange on one side lock will decrease the change in density in the lock chamber. When opening the doors on

the other side of the lock, the density difference between that side and the lock will have decreased as well. This in itself will slow down the lock exchange. If again the door open time is reduced, the salt exchange is again limited and the lock density changes will be smaller. When this is repeated over multiple locking cycles, the chamber density will vary around the mean harbour basins density (PIANC, 2021). This measure does not have an impact on vessel delays, but it can have impact on the vessel safety, i.e., there can be an increase in risk that a vessel hits an opening door that malfunctions.

2.3.2. Vessel clustering

Clustering of vessels means postponing lock operations until the lock is filled with vessels, which reduces the amount of locking cycles needed. It almost certainly results in delays for vessels, but whether clustering of vessels will lead to a significant decrease in salt intrusion is not a certainty. Generally, salt intrusion decreases when the amount of locking cycles decreases, but because clustering affects multiple hydraulic processes this is not a linear relation. Decreasing the number of cycles decreases the total lockage prism thus reducing the amount of salt water that can enter the lock to raise the water level. Furthermore, filling the lock with vessels increases the vessel volume in the lock, which in its turn decreasing the volume of salt water in the lock. Finally, more vessels in the lock means longer door open times and more lock exchange (PIANC, 2021).

2.3.3. Limited operational hours

When limiting the operational hours of a lock, the number of locking cycles per day is limited as well. This forces the clustering of vessels to keep up with the traffic supply. Again, whether this will lead to a reduction in salt intrusion is not a certainty. The implementation of this strategy can differ from one main operating block to several operating blocks throughout the day. With fixed operational hours the vessels will know better what to expect at the moment they arrive at the locking complex. For vessels, arriving outside of operational hours automatically results in delays and causes the formation of a queue for other oncoming vessels. An added benefit of this strategy is a reduction in the required workers at the locking complex.

2.3.4. Levelling around low water

When scheduling the block(s) of limited operational hours around low tide when the sea level is below the canal level, the lock chamber will be filled with fresh water from the canal to raise the water level and lowering of the water level is done by emptying to sea, thus eliminating the salt water locking prism. Filling the lock with fresh water from the canal also reduces its density, resulting in a slower lock exchange at the canal side. This could decrease the salt intrusion when the lock doors are closed in time. However, since levelling only results in water movement from canal to sea it causes loss of fresh water, which might not be an option in drought periods (PIANC, 2021). Levelling around low water is a specific application of limiting the operational hours, except the operating block(s) move daily with the phases of the tide.

2.4. Interfaces between logistics and hydrodynamics

The preceding sections have provided insight into the logistical processes of vessel passage through locks, the hydrodynamic mechanisms driving salt intrusion, and the operational measures that may mitigate salt intrusion. Distinct phases within the locking cycle have been identified, each associated with specific vessel behaviour and mechanisms of salt exchange.

These insights form the basis for selecting appropriate modelling concepts in the next chapter. The goal moving forward is to identify and evaluate models capable of representing the critical interface aspects, so that the effects of alternative locking strategies can be reliably assessed. Figure 2.10 provides a visual summary of these requirements, illustrating the separation of locking phases by door movement and interaction of lock and vessels in triggering next events. It also highlights how vessel delays (in red) and salt intrusion (in blue) coincide within the locking process, presenting the dynamics that a suitable model must represent.

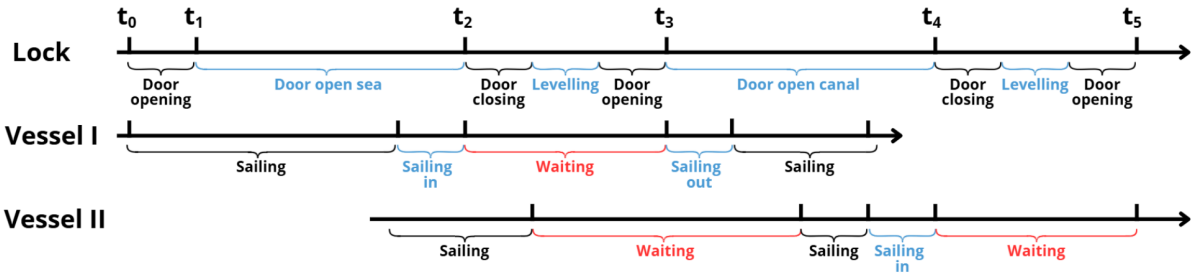

Figure 2.10: Time discretization requirement of coupled model

3

Models

The previous chapter has provided an insight into the logistical and hydrodynamic aspects of the locking process. Building on this theoretical foundation, the current chapter focuses on the modelling approach used to assess the effectiveness of operational mitigation strategies. First, a selection of suitable models is made, considering both the logistical simulation of vessel traffic and the hydrodynamic representation of salt intrusion. Then, the selected models are discussed in greater detail, including their underlying principles, required inputs, and generated outputs. This provides the basis for coupling the models in a later stage of the research and applying them to the selected case study.

3.1. Model overview

To simulate the impact of operational strategies on both vessel logistics and salt intrusion, appropriate models must be selected that reflect the key processes identified in the previous chapter. The goal is to identify models that are not only accurate, but also flexible enough to be coupled and to support the evaluation of alternative locking strategies.

3.1.1. Vessel behaviour models

According to Van Koningsveld et al. (2023), simulation models can be classified as microscopic, mesoscopic, or macroscopic, depending on their level of detail. This classification reflects both their spatial resolution—from local to national scale—and their temporal resolution, ranging from time steps of seconds to several hours. Bakker (2025) has done a detailed research into the usability of these different types of models:

Microscopic models simulate behaviour of individual vessels and their interactions with other vessels and infrastructure in high detail, with a focus on single port components as the cause for waiting. Although the estimations of waiting times are great, using microscopic models for large fleets and/or full port networks is rarely done due to the significant computational power needed.

Mesoscopic models strike a balance in scale and detail. They are able to simulate large fleets but limit the detail of behaviour to larger events. Using schematised networks, the computational power is limited, while still able to keep track of individual vessel behaviour.

Macroscopic models describe vessel flow in aggregate terms, focusing on system-level trends rather than individual movements. They are useful for assessing general system efficiency and throughput. However, their coarse resolution limits the ability to capture detailed operational processes. These models typically do not incorporate realistic hydrodynamics, dynamic accessibility rules, or berth availability, making them unsuitable for accurately quantifying vessel waiting times or lock-specific delays.

The coming paragraphs will describe the micro-, meso-, and macroscopic simulations models which are listed below:

- Microscopic: SIMDAS

- Mesoscopic: SIVAK, SHIPMA, OpenTNSim, BIVAS, NODUS
- Macroscopic: BASGOED

SIMDAS
SIMDAS was developed by Rijkswaterstaat (1986) and simulates individual vessel movements in detail, capturing interactions such as encountering and overtaking manoeuvres on a vessel-by-vessel basis. This level of detail allows for the analysis of dynamic behaviour on the waterway at high temporal and spatial resolution. The model is designed to simulate traffic flow on specific sections of inland waterways, including straight reaches, bends, and intersections. By resolving the precise positions of vessels over time and modelling their interactions, SIMDAS can be used to assess the capacity of waterway segments and identify potential congestion effects. This makes it a valuable tool for evaluating operational strategies, infrastructure design, or policy decisions aimed at improving traffic efficiency and safety on inland waterways.

SIVAK
SIVAK (SImulatiepakket voor de VerkeersAfwikkeling bij Kunstwerken) is a simulation system originally built in the programming language PROSIM, but with the newest model built in Simio. Since 1990 it has been used by Rijkswaterstaat to analyses the vessel traffic at waterway infrastructures, and can be used to design new infrastructures and to identify and prevent bottlenecks in a waterway network (Bijlsma & van der Schelde, 2019). The simulations are done by creating networks of waterways connected by nodes, with bridges, sluices or narrowings serving as infrastructures on those waterways. The model is not open-sourced, which makes it a less accessible and also less flexible since coupling a salt model is a more difficult process.

SHIPMA
The SHIPMA model, first developed in 1992 by MARIN and Deltares, is an open-source fast-time simulation tool designed to model vessel manoeuvring behaviour in ports and fairways. It simulates individual vessels using an autopilot system capable of track-keeping and harbour manoeuvring, including typical operations such as turning, reverse sailing, and berthing (MARIN & Deltares, 2025). The model incorporates vessel-specific hydrodynamic derivatives obtained from scale model tests or calculations, and accounts for environmental factors such as wind, waves, and currents. Because SHIPMA simulates individual vessel movements and interactions with port infrastructure in detail, it operates at a mesoscopic scale, providing insight into intermediate-level behaviours suitable for evaluating port design, channel layouts, and terminal configurations. This level of detail allows it to capture realistic vessel manoeuvring patterns while remaining computationally efficient.

OpenTNSim
OpenTNSim (Open source Transport Network Simulation) is an open-sourced Python package developed by Delft University of Technology (Baart et al., 2022). It is a mesoscopic discrete-event model that simulates traffic in port and waterway systems using a network of nodes and edges. By assigning infrastructure and hydrodynamics to the nodes and edges and adding sailing vessels to interact in the network, the behaviour of the vessels can be modelled and analysed. OpenTNSim contains a lock module capable of clustering vessels, which allows the simulation of vessel behaviour around locks.

BIVAS
BIVAS is a mesoscopic inland waterway transport (IWT) simulation model developed to support policy analysis related to traffic loads, infrastructure use, and network resilience (Van Koningsveld et al., 2023). It is designed to assess the effects of blockages, management strategies, and maintenance scenarios on traffic performance across the IWT network. Based on trip demands from origin-destination pairs (typically derived from the BASGOED model), BIVAS calculates whether trips can be executed and simulates them accordingly—without resolving individual vessel movements. This allows for realistic flow estimations at the network level while maintaining computational efficiency. For detailed simulations near critical infrastructure such as locks and bridges, BIVAS is complemented by SIVAK, and for detailed interactions on waterway segments, by SIMDAS.

NODUS
NODUS is a macroscopic freight transport simulation model developed at the Center for Operations Research and Econometrics (CORE) of UCLouvain (Jourquin, 2022). It is designed for strategic analysis of multimodal and intermodal transport flows across large-scale networks. As a macroscopic model, it operates at an aggregated level, focusing on freight flows rather than individual vehicles. NODUS applies the “Virtual Networks” methodology, which merges modal choice and network assignment into a single step. This makes it well-suited for applications such as regional transport planning, infrastructure evaluation, and environmental policy analysis. The software supports GIS standards, handles large datasets through parallelized algorithms, and offers an open API for scripting in Python, R, or Java, allowing integration with various data platforms and workflows.

BASGOED
BASGOED (Basismodel voor Goederenvervoer) is a macroscopic freight transport model developed by Rijkswaterstaat for use in the Netherlands (Van Koningsveld et al., 2023). It is designed to make long-term forecasts—typically over a 15–30 year horizon—of goods transport volumes across the national network. The model estimates how much freight is produced and consumed, what portion requires transportation, and the most likely origin-destination combinations. Based on sector-specific growth projections, travel times, and costs, BASGOED distributes transport demand across road, rail, and inland waterways. It predicts total transported tonnage per cargo type and modality, and for road transport, it also provides estimates of the number of trips.

Conclusion
For this research it is necessary that individual vessel behaviour can be distinguished to be able to see the influence on the caused delay on individual vessels. It is also of importance of the traffic model to be able to compute an entire port network and a large size fleet. For this reason, a mesoscopic approach is selected for the logistical modelling in this research. Out of the mesoscopic models, OpenTNSim, a Python-based, open-source model, is chosen due to its flexibility, ease of integration with salt intrusion mechanisms, and the accessibility of expert knowledge.

3.1.2. Salt intrusion models
Hydraulic models are essential tools for simulating and understanding water movement in natural and engineered systems. Bakker (2025) suggest that they can be categorized into three main types: data-driven models, schematized models, and process-based (or physics-based) models.

Data-driven (or empirical models) in hydrodynamics use historical measurements—such as water levels, flow velocities, and precipitation—to identify patterns and make predictions using statistical or machine learning techniques. These models are particularly effective for hind-casting, anomaly detection, and long-term trend analysis when large datasets are available. However, because they do not explicitly represent the underlying physical processes, they are limited in their ability to predict outcomes under changing conditions, such as infrastructure modifications or climate change. Additionally, they often offer limited spatial resolution and may struggle with extrapolation beyond the range of the training data.

Schematic (or semi-empirical) models represent hydrodynamic systems using simplified, idealized structures such as channels, reservoirs, pumps, or control gates, often based on engineering judgment and empirical relationships. These models combine basic physical principles with calibration to observed data, allowing for practical and relatively efficient simulations. They are especially useful in applications like flood forecasting, drainage system design, and operational planning, where full physical detail is unnecessary or impractical. While more flexible and interpretable than purely data-driven models, their accuracy depends heavily on the quality of schematization and calibration, and they may not capture complex or rapidly changing hydrodynamic interactions in detail.

Proces-based (or numerical) hydrodynamic models simulate water movement by solving the governing physical equations—typically the Navier-Stokes or Saint-Venant equations—that describe fluid motion. These models offer high accuracy and can represent complex processes such as tidal dynamics, salinity intrusion, and stratification. However, their precision comes at the cost of requiring detailed input data (e.g., bathymetry, boundary conditions) and significant computational resources. Depending on the

spatial resolution and complexity of the system, different model dimensions can be used—such as 1D, 2DH, 2DV, and 3D—which are discussed in more detail below.

1D Models One-dimensional (1D) models average flow properties over width and depth, making them suitable for long, narrow channels or rivers where cross-sectional variability is minimal. They are often used for large-scale network analysis, such as estimating salt intrusion in extensive river or canal systems. These models are computationally efficient, allowing for long simulations and quick scenario testing. However, their simplified structure limits their ability to represent local hydraulic details—especially near structures like sluices or bifurcations.

2D Vertical (2DV) Models 2DV models resolve vertical variability while averaging over width, making them well-suited for simulating vertical stratification and sluice exchanges in cross-sectionally uniform channels. They are valuable when vertical gradients, such as salinity or temperature layering, are important—especially near hydraulic structures. However, the added vertical resolution significantly increases computational demands, particularly in systems with many interacting sluices or doors.

2D Horizontal (2DH) Models 2DH models average over depth but resolve horizontal flow patterns across a surface, making them ideal for estuaries, floodplains, and tidal basins where lateral variability is significant. These models can simulate complex features like flow separation, eddies, or wetting and drying in shallow areas. They are widely used in flood modelling and coastal dynamics but require more computational power and detailed bathymetric data than 1D models.

3D Models Three-dimensional models provide the most detailed representation by resolving both vertical and horizontal variations in flow and water quality. They are essential in highly stratified or morphologically complex environments such as estuaries, ports, or fjords, where both surface and bottom processes interact. 3D models are often used for environmental impact assessments, sediment transport, and detailed design near hydraulic structures. Their complexity comes with high data requirements and long computation times, making them best suited for site-specific, high-stakes applications.

Within this category are Computational Fluid Dynamics (CFD) models, which solve the full Navier–Stokes equations without relying on the hydrostatic assumption. This means they can capture small-scale details such as turbulence, vortices, and density-driven flows that standard models cannot. CFD models are extremely accurate for studying local processes around locks, sluices, or ship-induced flows, but their heavy computational demands make them less practical for large areas or long simulation periods.

The coming sections will discuss some actual examples of schematic and process/physics based models.

- schematic: SWINLOCKS, WANDA-Locks, Zeesluisformulering (ZSF)
- process/physics based (1D, 2D-V and 3D): SOBEK, Delft3D, WAQUA

SWINLOCKS

SWINLOCKS (Salt Water Intrusion through Navigation LOCKS) is a specialized simulation tool developed to model the interaction between saltwater intrusion and navigation through sluices or locks in estuarine and tidal systems (Jongeling, 2003). The model focuses on quantifying how lock operations contribute to the transport of saline water into freshwater systems (Wijsman, 2011). SWINLOCKS uses a simplified, yet physically-based approach to represent the exchange of water and salt during the locking process, accounting for processes such as flushing, leakage, and density-driven mixing. The model is typically integrated into broader schematic or operational water management models to support decision-making around sluice operation timing, freshwater conservation, and shipping schedules. Its main strength lies in enabling the evaluation of trade-offs between maintaining navigational access and limiting salt intrusion, especially in vulnerable delta areas like the Netherlands where freshwater availability and salinity control are critical. However, this source-code is not openly available.

WANDA-Locks

In 2010 Deltares developed a tool called the Zoutlekmodel (ZLM, translation: salt leakage model) to study the salt intrusion at specifically the Volkeraksluizen in The Netherlands. In 2013 this model was adapted to make it more generic and it was then housed in WANDA to make it easier in use, which

resulted in the WANDA-Locks model (de Groot & Vreeken, 2016). WANDA-Locks models the fresh-salt exchange at the lock doors during the locking process by displaying in 1D the accurately calculated 3D density flows. Validation of the WANDA-Locks has been done by means of measurements at the Stevinsluis and Krammerjachtensluis (both in The Netherlands). The validations showed that the WANDA-Locks model is capable of accurately predicting the salt transport for a locking cycle series for 5 days.

Zeesluisformulering

The Zeesluisformulering (ZSF, translation: sea-lock formulation) is an open-sourced tool and the current salt intrusion tool of Deltares (Deltares, 2019). It was developed as a result of the need to be able to link salt intrusion models to other models such as a salt dispersion model, after it was concluded that WANDA-Locks was insufficiently applicable (Weiler & Burgers, 2018). The ZSF is described in formulas that simplify salt intrusion through locks, while also representing in a simplified way the in reality varying locking operations like cycle frequency and door open times. Currently the ZSF has already been translated into a Python module, but it is suitable for a wider range of programming languages. The ZSF has not been validated with measurement data, but instead simulations have been compared to WANDA-Locks simulations for simple scenario's.

SOBEK

SOBEK is a modelling suite developed by Deltares for simulating surface water flow, water quality, and sediment transport in integrated river, urban, and rural water systems (Deltares, 2025b). It is particularly well-suited for 1D and 1D/2D coupled simulations, making it widely used in flood forecasting, drainage design, polder management, and sewer system analysis. SOBEK can model open-channel flow, pipe flow, and overland flow, and supports complex hydraulic structures such as weirs, pumps, sluices, and culverts. It is known for its ability to represent control strategies and operational rules, making it ideal for real-time decision support and operational water management. The model is often used in the Netherlands for simulating polder systems, combined sewer overflows, and flood defence assessments. Like Delft3D, SOBEK is evolving into the D-HYDRO Suite, which aims to unify hydrodynamic modelling capabilities under a flexible, modern framework with better integration of 1D, 2D, and 3D processes.

Delft3D

Delft3D is a numerical modelling software developed by Deltares for simulating water movement and related processes in coastal, riverine, estuarine, and lake environments. It solves the fundamental equations governing fluid flow, typically the shallow water equations, and is capable of modelling complex hydrodynamic behaviour, including tides, currents, waves, sediment transport, water quality, and morphological changes (Deltares, 2025a). Delft3D supports both 2D depth-averaged (2DH) and 3D hydrodynamic simulations, allowing for detailed analysis of vertically and horizontally varying flows. Its modular structure enables users to couple different physical processes, making it suitable for a wide range of applications—from flood forecasting and salt intrusion analysis to environmental impact studies and coastal engineering. More recently, Delft3D Flexible Mesh (Delft3D FM) has been introduced, allowing for unstructured grids that provide greater flexibility in representing complex geometries such as estuaries, ports, and urban water systems.

WAQUA

The WAQUA model is an application developed by Rijkswaterstaat to simulate water levels, flow velocities, and the transport of substances in open water bodies by averaging over the depth (IPLO, 2025). It is efficient for large-scale application and can help identify the effects of interventions in water systems. Implementation of simulations with WAQUA is done in combination with a SIMONA-package.

Conclusions

Given the goals of this study—namely simulating multiple lock operations over extended periods and capturing vessel movements—a schematized modelling approach is the most suitable for now. We opt for the Zeesluisformulering (ZSF) to quantify salt exchange processes during lock operations. The ZSF offers a practical balance between accuracy and computational efficiency, reproducing measurements with reasonable precision while allowing for short runtimes. This makes it well-suited for integration into logistical simulations involving many vessels and events. Additionally, because the ZSF is implemented

in Python, it can be directly coupled with the mesoscopic traffic model discussed in Section 3.1. For end users who require insight into the spatial extent of salt dispersion, the ZSF output can be added as a source term to more detailed 1D or 2D hydrodynamic models. This layered approach offers both scalability and flexibility, aligning well with the broader objectives of this research.

3.2. Selected model combination

As concluded in Section 3.1, the two models selected are the OpenTNSim vessel simulation model and ZSF hydrodynamic model. Coupling of these two models has first been suggested before by Bakker and van Koningsveld (2024).

3.2.1. OpenTNSim model

The lock module in OpenTNSim models the logistical interaction between vessels and locks in inland waterway networks. It simulates how vessels move through lock systems, accounting for waiting behaviour, levelling operations, and spatial constraints, and produces detailed vessel and lock activity logs. The most relevant elements of the model can be divided into three parts: governing logistics, model input, and model output. These elements will be discussed in the coming paragraphs.

Governing logistics

In an OpenTNSim network, the infrastructure is represented by a series of nodes and edges. Nodes mark important locations such as entry and exit points, detection zones, locks, and waiting areas, while edges represent the waterways connecting these points, defined by attributes like length and sailing speed. Vessels move through the network by following predefined routes composed of these nodes and edges. Their travel times are calculated based on sailing speed and edge length.

With the use of the locking module, locks can be added to edges of the network. The locks are spatially discretised into five core components: outer and inner waiting areas, line-up areas, and the lock chamber itself. Vessels move through the lock in eleven sequential phases, which are similar to those in Figure 2.2 of Subsection 2.1.2: from arriving at a distance from the lock, to waiting, lining up, locking in, levelling, and finally exiting the system. Vessel movements are guided by detection nodes that register arrivals at specific lock areas. These nodes trigger the next phase in the operation, such as opening lock doors or initiating levelling. A vessel arriving at the lock will wait for following vessels going in the same direction that are within the detection zone and will fit inside the lock together. Lock levelling only begins after all vessels have entered and the doors have closed. Similarly, vessels exit the lock one-by-one, and only when the previous vessel has passed the line-up or waiting area can the next begin its movement.

In the locking module, the levelling time is calculated by repeatedly determining how much the water level difference (denoted as *z*) decreases over each small time step. For each step, the model estimates how much the head difference reduces, based on the flow through the lock's opening. This flow depends on the discharge coefficient, opening area, chamber size, and gravity. The process continues, updating *z* at every interval, until the remaining difference between water levels inside and outside the lock is small enough—specifically, when it falls below 0.05 meters. The total levelling time is the sum of all these time steps needed to reach that point. The change in *z* for each time step is calculated using the formula:

$$dz = \left(\sqrt{H} - \frac{C_d A_o \sqrt{2g}}{2LW}\left(t + \frac{\Delta t}{2}\right)\right)^2 - \left(\sqrt{H} - \frac{C_d A_o \sqrt{2g}}{2LW}\left(t - \frac{\Delta t}{2}\right)\right)^2 \tag{3.1}$$

where H is the initial head difference, C_d is the discharge coefficient, A_o is the valve opening area, L and W are the lock's length and width, g is gravitational acceleration, t is time, and Δt is the time step.

Model input

The simulation takes as input the vessel arrival times at network entry points and uses predefined sailing speeds over the transport graph to estimate arrival times at locks. Additionally, hydraulic data

(such as water levels and discharge) are required to calculate levelling durations. The configuration of locks, vessel types, and operational parameters are also part of the input.

- Geospatial data: port network, lock geometry, levelling system
- AIS-data: vessel dimensions, arrival time, speed and route
- Hydrodynamic data: water-levels

Model output

The model produces two main types of logs: vessel logbooks and lock logbooks. Vessel logbooks, detailing the time of arrival at each network node, the time spent at waiting and line-up areas, and each step of the lock passage. Lock logbooks, registering the timing of door operations, levelling activities, and vessel entry/exit sequences.

3.2.2. Zeesluisformulering

The Zeesluisformulering (ZSF) can estimate salt fluxes between a lock chamber and the lock harbour basins. In the ZSF there are already 3 salt intrusion measures implemented: bubble screen, water screen, flushing. However, since these are not operational measures, these are disregarded in this report. Furthermore, the ZSF contains equations used for calculating average operational parameters. However, this research focuses on the implementation of operational strategies, which means these parameters are time-dependent. Thus these equations are disregarded as well. The most relevant elements of the model can be divided into three parts: general works, model input, and model output.

The ZSF consist of simplified formulations, based on assumptions, that enable the estimation of mass fluxes during the distinct phases of the locking cycle. These distinct phases are schematized in Figure 3.1.

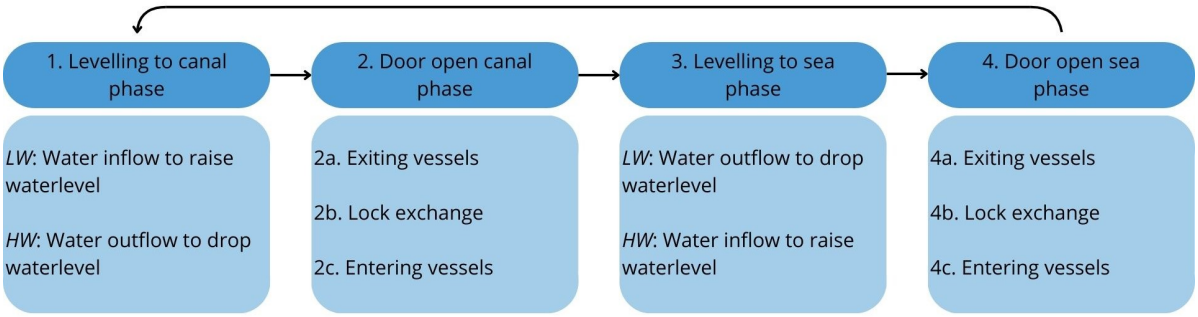

Figure 3.1: Zeesluisformulering locking phases

General works

The ZSF formulation uses assumptions to simplify the processes of salt intrusion (Weiler & Burgers, 2018). Below the general assumptions are listed:

- only the lock chamber is taken into account (not the harbour basins)
- quantities are averaged over a phase
- well-mixed conditions apply in the harbours basins and in the lock chamber
- fully stratified exchange current (without mixing) is believed to develop
- there is an individual sequence of sub-operations between which no currents exchange
- resulting discharges and salinity are uniformly distributed over width, length and depth

Further more, the boundary of the phases is halfway through door movement. The equations which are used can be found in Appendix A.

Input parameters

The transport of salt through a lock system depends on a range of input parameters, which can be grouped into four main categories: geometry, boundary conditions, operational parameters, and initial conditions. Each of these categories contains specific variables that define the physical and dynamic setup of the model. These are outlined below.

Spatial data
Geometry and bathymetry parameters define the structural layout of the lock and the adjacent basins, forming the spatial foundation for the model. The following data is needed:

- dimensions of the lock (length and width) [m]
- bottom levels (lock and harbour basins) [m NAP]
- sill levels [m NAP]

Boundary conditions
Boundary conditions describe the hydraulic and salinity context of the system and influence the direction and magnitude of salt transport.

- water levels in harbour basins [m NAP]
- salt concentration in harbour basins [kg/m^3]

Operational parameters
Operational inputs define the vessel movement and lock operation dynamics that directly affect the timing and scale of salt exchange.

- door open times per phase [s]
- volume of upstream and downstream vessels [m^3]

Initial conditions
Initial conditions describe the salinity state of the lock at the start of the simulation.

- salt concentration of the lock chamber [kg/m^3]

These parameters together provide the necessary input for simulating salt intrusion through a lock in a simplified yet representative manner.

Output data

The output of the ZSF consists of key hydrodynamic and salinity-related variables that are essential for quantifying salt intrusion. These variables are used to evaluate the salt fluxes during each phase of the locking cycle and to assess the impact of different locking strategies. The main output parameters are:

- M: mass fluxes of salt [kg]
- Q: discharges of water [m^3/s]
- S: salt concentration [kg/m^3]

3.2.3. Coupling

An agent-based traffic model such as OpenTNSim can be integrated with a schematic salt intrusion model like the Zeesluisformulering through one-way coupling, where the output of the traffic model is used as input for the hydraulic model. OpenTNSim generates detailed vessel and lock logbooks, including door operations, levelling durations, and vessel entry/exit sequences. From these logs, key operational parameters, such as door open times per phase and vessel volumes from upstream and downstream, can be extracted and supplied to the salt intrusion model. This allows for traffic-driven simulation of salt exchange at locks, providing a dynamic representation of vessel-induced salt transport that supports the central goal of this thesis: quantifying the impact of lock operations on salt intrusion under realistic traffic conditions.

3.3. Conclusion

With the selection and description of the OpenTNSim and ZSF models complete, the next step is to apply these tools to a real-world case study. To do so, specific data inputs must be identified and prepared to enable a representative simulation of the case study. Based on Bakker et al. (2024), OpenTNSim requires geospatial data, AIS-data, and hydrodynamic data to simulate logistics accurately. According to Weiler and Burgers (2018) local hydrodynamic data, lock geometry, and operational parameters are essential for the ZSF to quantify salt fluxes during the locking process. The following chapter focuses on the selected case study and outlines how these data sources are gathered and configured to support the combined simulation framework.

4

Case Study: IJmuiden

The IJmuiden lock complex was chosen as a case study due to its significance for both navigation and water management, and its sensitivity to salt intrusion. In 2022, several issues arose during a period of drought, prompting questions from pilots, Rijkswaterstaat, and the Port of Amsterdam about the necessity and effectiveness of the measures implemented at the time. These challenges are expected to intensify with the recent opening of the Sea Lock IJmuiden, the largest sea lock in the world, which was also used for the measurement campaign conducted by Deltares at the beginning of 2023. This comprehensive dataset is available for validating the ZSF (Zeesluisformulering) and will enable testing of operational measures aimed at balancing navigation efficiency and salinity control.

This chapter describes the IJmuiden lock complex, including its elements, the surrounding water system, and the effect and monitoring of salt intrusion. It also presents the key data required for the traffic model, followed by the key data for the salt intrusion model.

4.1. The IJmuiden lock complex

The IJmuiden lock complex is located along the coast of the Dutch province North-Holland. The complex has been the barrier between the North Sea and the North Sea Canal since 1876 and nowadays consists of multiple locks, a pumping station and discharge sluices, with a selective withdrawal dam under construction, see Figure 4.1.

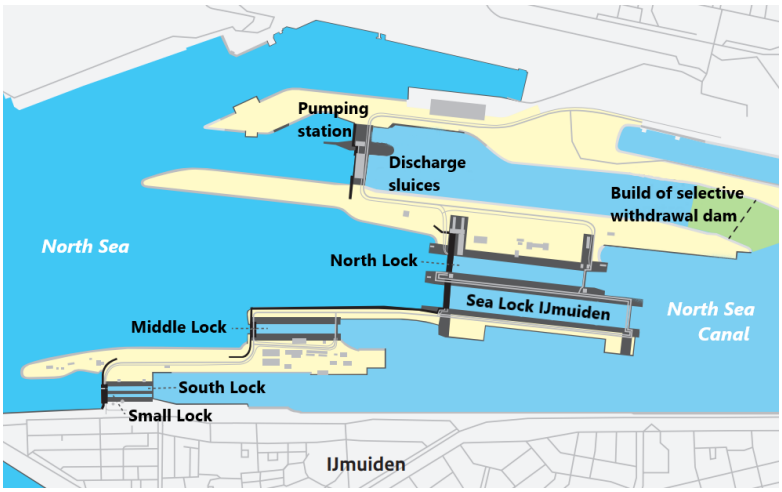

Figure 4.1: Layout of the IJmuiden Lock Complex. Adjusted from (Rijkswaterstaat, 2021)

Locks

When the North Sea Canal was first connected to the North Sea, the IJmuiden lock complex consisted of just the Small Lock and the South Lock (Rijkswaterstaat, 2023b). Over the years several locks have been added to keep up with the growth and development of maritime transport. The Middle Lock was added in 1896, and in 1929 the North lock was completed. In 2022, the most recent lock was opened: the Sea Lock IJmuiden. This lock was built to take over operations from the almost 100 year old North Lock and is prepared for an increase in ship sizes and rising sea water level for the next 100 years.

With a length of 545 m, a width of 70 m and a depth of 17.75, Sea Lock IJmuiden is the largest sea lock in the world. According to Port of Amsterdam (2023) ships up to 339 meters long, 57 meters wide and 13.75 meters deep are permitted to enter, guided by bow and stern tugboats. Because of its low lock chamber floor and thresholds, it can be used regardless of the tide and thus giving increased access to the North Sea Canal, the Port of Amsterdam and other hinterland connections (Rijkswaterstaat, 2023b).

Discharge sluices and pumping station

On the north side of the IJmuiden complex discharge sluices and a pumping station are located. During lower tidal water levels, seven discharge sluices can relieve a total maximum discharge of 500 m^3/s from the North Sea Canal. During higher tidal water levels, 6 pumps can pump a total maximum discharge of 260 m^3/s into the North Sea. Yearly a combined volume of about 4.6 billion m^3 water is discharged through the station to relieve the discharge of the North Sea Canal to the North Sea and to regulating the water level of the North Sea Canal (Rijkswaterstaat, 2023b).

Selective withdrawal dam

With the increase in size from the North Lock to the Sea Lock IJmuiden comes an increase of salt intrusion into the North Sea Canal. To mitigate the effect of increased salt intrusion in the canal, a selective withdrawal dam is being built in the water branch leading to the spillway station. This dam has a gap underneath resulting in the heavier, salter water at the bottom of the water column to be extracted. Until construction of the dam is completed, the Sea Lock IJmuiden cannot be in full-time use. Because of this the North Lock will remain in operation, determining case by case whether the Sea Lock IJmuiden needs to be used (Rijkswaterstaat, 2023a).

4.1.1. Water system

Starting in Lobith, one of the major rivers of the Netherlands, the Rhine, enters the country from Germany. Via the main part of the Amsterdam-Rijnkanaal, which flows from the Nederrijn to Amsterdam, and via the North Sea Canal, which connects Amsterdam to IJmuiden, one branch of the Rhine flows into the North Sea. This makes the North Sea Canal an important navigational route between the North Sea, the Port of Amsterdam and other hinterland connections. Besides carrying discharge from the Rhine, several water boards, see Figure 4.2, use the North Sea Canal and Amsterdam-Rijnkanaal as a runoff for excess water or to retrieve water from in periods of drought (Rijkswaterstaat, 2022). In total an area of 2300 km^2 drains through the IJmuiden complex toward the North Sea, most of which goes through the discharge sluices and pumping complex. As mentioned before, the complex is responsible for regulating the water level of the North Sea Canal and the Amsterdam-Rijnkanaal. However, due to connections to surrounding water bodies, required water depths for navigation and limited clearance heights at some bridges and locks, there is little deviation in the water level of the canal. Rijkswaterstaat (2021) aims to maintain a target water level of -0.4 m NAP, with margins that range from -0.3 m NAP till -0.55 m NAP where no problems are to be expected.

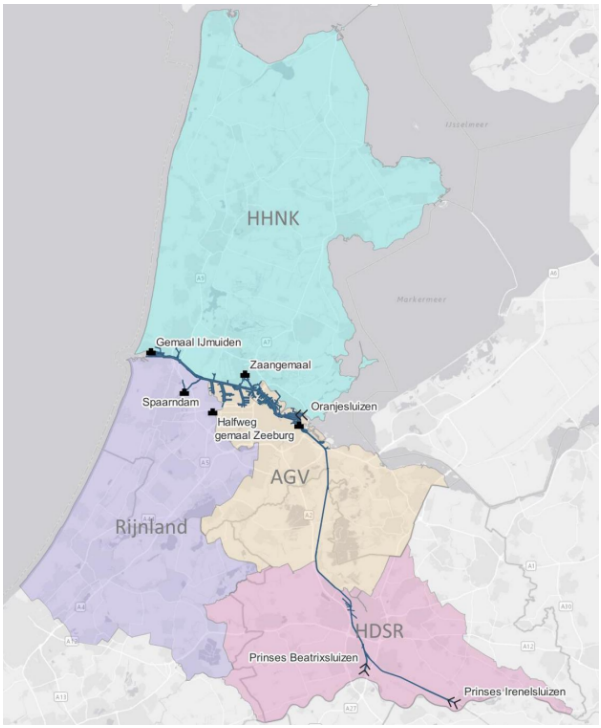

Figure 4.2: North Sea Canal, Amsterdam-Rijnkanaal and surrounding waterboards (Rijkswaterstaat, 2022)

On the outside of the IJmuiden complex the water level is determined by the tide of the North Sea. The mean tide with an average water level of 0.04 m NAP, a mean high tide of 1.01 m NAP and a mean low tide of -0.68 m NAP (Rijkswaterstaat, 2021). During spring tide the mean high water spring level is 1.16 m NAP and the mean low water spring is -0.75 m NAP. According Kortlever et al. (2018), whenever the sea level reaches above 3.90 m NAP or below -1.65 m NAP the doors are closed and the lock is out of use.

4.1.2. The problem with salt

Rijkswaterstaat (2022) describes the different uses of the water in the North Sea Canal and Amsterdam-Rijnkanaal and the consequences that come along with an increase in salinity. One of the main water users experiencing damage as a result of salinity increase is the surrounding nature. In adjacent canals and waters, the ecology needs to be protected and as a result, there is a limit to the amount of salt that can infiltrate in these areas. Another important use of water extraction is the agricultural sector. During growing seasons, dependent on the weather, water is needed for irrigation and maintaining the water table. A salinity increase in the water can damage the crops, although it depends on the crop how much salt can be tolerated. The last main usage of the extracted water is drinking water. At multiple locations along the Amsterdam-Rijnkanaal water is extracted for the production of drinking water. These production locations are not suitable for desalination of water, and therefore it is important to limit the salt intrusion to these locations. Figure 4.3 illustrates the adjacent waters, nature areas and agricultural zones as well as the drinking water extraction point closest to IJmuiden. Even though there are mostly negative effects of salt intrusion in the North Sea Canal, it also has a positive side. It creates a transition between the salter seawater and the brackish inland waters, which is advantageous for the ecology of the canal. Keeping the right balance of salinity of the canal is important and thus monitoring the salinity is needed to keep a hold on the salt intrusion.

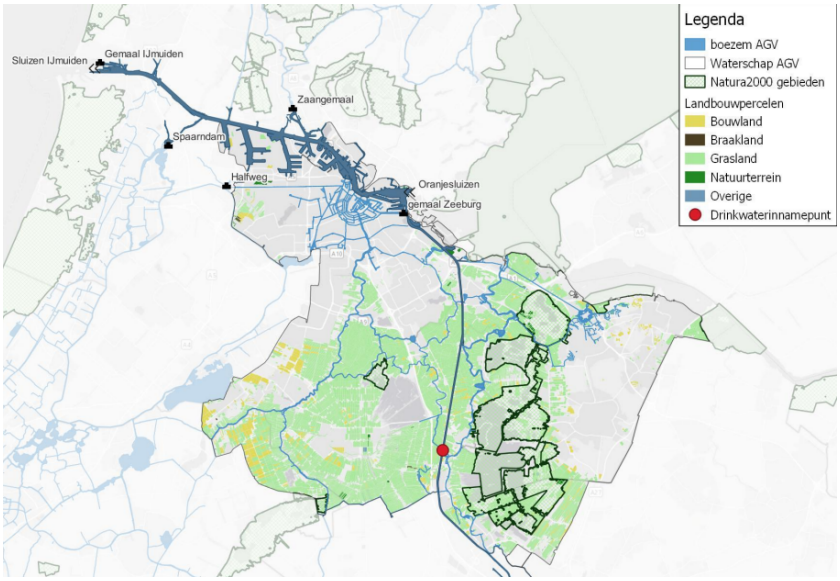

Figure 4.3: North Sea Canal and Amsterdam-Rijnkanaal water uses (Rijkswaterstaat, 2022)

Even though the entirety of the North Sea Canal and Amsterdam-Rijnkanaal form the larger area impacted by salt intrusion, this research focuses exclusively on the source of that intrusion: the IJmuiden lock complex. In other words, while the broader problem area is acknowledged, this study is limited to understanding and quantifying the salt exchange that occurs at the locks themselves. An additional step would be required to simulate how this salt propagates through the larger canal and river network, but that falls outside the scope of the present work.

Salt monitoring

Salt that enters a canal does so as a tongue of salt that moves along the bottom of the canal as salt water is heavier than fresh water. Figure 4.4 illustrates how the water in the North Sea Canal is stratified and how far salt water penetrates, using salt concentrations in the canal. Along the North Sea Canal, 11 sensors have been installed at 5 locations, see Figure 4.5, which monitor the salt concentrations of the water. By taking the unweighted 5-day moving average of the measured concentrations a so-called Z5-value is calculated.

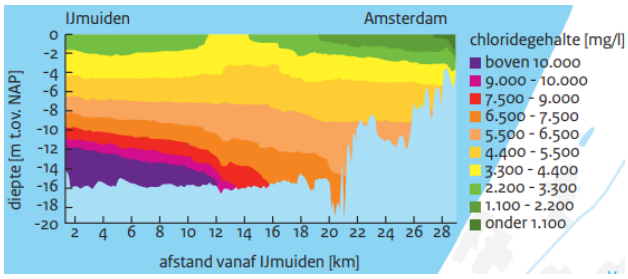

Figure 4.4: Salt intrusion North Sea Canal (Rijkswaterstaat, 2021)

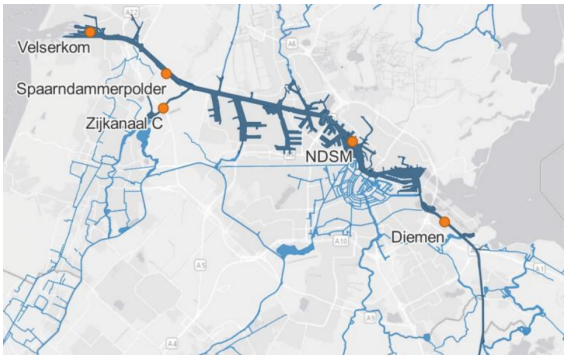

Figure 4.5: Salt monitoring locations (Rijkswaterstaat, 2022)

For the salt intrusion in the Amsterdam-Rijnkanaal the monitoring point in Diemen, the most upstream monitoring point in Figure 4.5, is an important location. It has been determined by Rijkswaterstaat (2021) that the 5-day moving average discharge at Diemen needs to be at least 25 m^3/s, and even 35 m^3/s until the selective withdrawal dam is finished. This is needed to keep the salt tongue from reaching further upstream and causing irredeemable damage to nature.

Rijkswaterstaat is responsible for monitoring the Z5 salinity index and will impose corresponding salt intrusion mitigation measures IJmuiden must adhere to. The higher the Z5 values, the stricter these measures will be. These measures may include a limitation on the number of locking operations per day or even a restriction on operational hours, both of which require vessel clustering.

4.2. Key aspects for traffic modelling

As concluded in Subsection 3.2.1, the OpenTNSim models take the following information as input: geospatial data, vessel data and hydrodynamic data. This section will describe how this data is obtained. It will also describe some IJmuiden specific logistical details needed for locking and clustering.

4.2.1. Geospatial data

Port network

OpenTNSim requires a schematization of the waterway network, consisting of nodes and edges, to model vessel movements. For IJmuiden, the available data from Rijkswaterstaat's Fairway Information System (FIS), is retrieved from vaarweginformatie.nl. The retrieved data does not contain a edge for the Sea Lock IJmuiden, so this will be added manually. To focus the analysis on locking strategies, a simplification of the network has been introduced. Instead of including the entire port network and coastal region, the network only covers the area from the 5-mile zone around the harbour entrance to the Houtrak. These points are chosen as such because in reality if a vessel passes these locations they are confirmed by the lock planner in the locking schedule. The full model network is displayed in Figure 4.6. To comply with a decreased network, virtual waiting areas are added to the immediate vicinity of the locks. This simplification allows the model to capture the relevant dynamics of locking operations. Longer vessel routes can be added for future simulations, but are right now outside of the scope of this research. An example of more comprehensive network simulations are demonstrated in Bakker (2024) by means of open system.

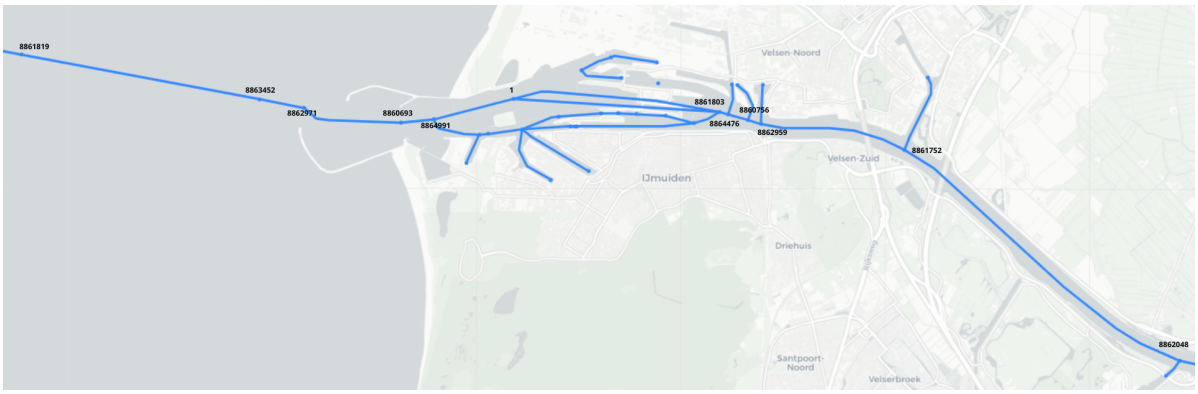

Figure 4.6: FIS Port network of OpenTNSim

Lock geometry and levelling system

OpenTNSim uses basic lock geometry to determine the levelling time. Equation 3.1 takes into account the length and width of the lock. Beside that, the length, width and depth are also used to determine which and how many vessels can fit into the lock. The basic dimensions are shown in Figure 4.7.

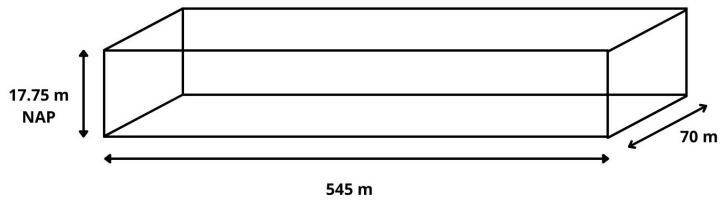

Figure 4.7: Main dimensions Sea Lock IJmuiden

Besides dimensions, OpenTNSim also needs information on the levelling system to determine how long the levelling operations take. According to Kortlever et al. (2018) Sea Lock IJmuiden is equipped with rolling doors on either side of the lock, which take 4.5 minutes to open or close. Within each of these doors 16 valves are located with their centre line at a height of -10.25 m NAP. Each valve has a width of 2.2 m and a height of 3.0 m opened and closed by lifting hydraulic gates. For the levelling calculation of Equation 3.1 this means a total opening area of 16*2.2*3 m^3. Kortlever et al. (2018) also states that the discharge coefficient needed is 0.42.

4.2.2. Vessel data

For the locking strategies, AIS data is used to create a representative ship fleet by selecting all vessels that passed through the Sea Lock IJmuiden or North Lock. The AIS dataset provided is from the period of January 2023 until March 2023. The dataset provides detailed information necessary for the model, including vessel dimensions, sailing speeds, and the arrival times of vessels at the lock complex, both inbound and outbound. This data forms the basis for simulating vessel traffic and evaluating different locking strategies.

Dimensions

While all vessels in the dataset have at least some dimensional data, not all required dimensions (length, width, or draught) are always available. To address these gaps, missing values are filled by estimating the missing dimension based on the average of vessels with similar known characteristics. For example, if a vessel's length is missing, it is approximated using the average length of vessels with a comparable width. This approach ensures that the dataset is as complete as possible for use in the simulation, while maintaining consistency with observed vessel characteristics.

Speed

The sailing speeds of all vessels within the network are visualized in Figure 4.8, with a distinction made between inbound and outbound traffic. This figure illustrates the variation in speed along the different routes through the system. Based on the AIS data, a trend line is fitted separately for each direction, representing the typical sailing behaviour of vessels. The resulting average sailing speeds are then assigned to the corresponding network edges in the model. This approach ensures that the vessel movement in the simulation reflects realistic conditions observed in practice.

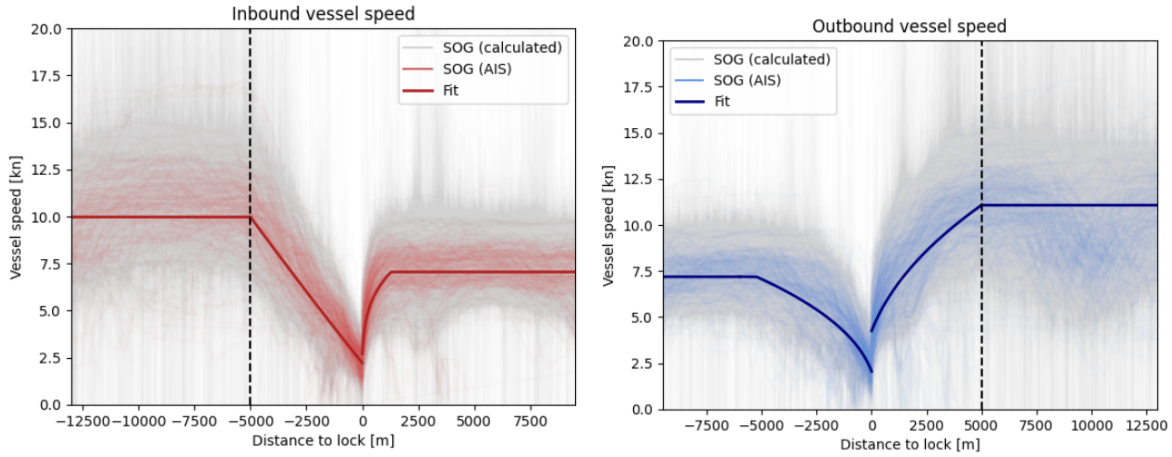

(a) Inbound vessels

(b) Outbound vessels

Figure 4.8: Port network vessels speeds

Arrival time boundaries

For each vessel, the AIS data provides the arrival time at the lock complex, but not necessarily at the boundaries of the OpenTNSim network. To estimate these boundary arrival times, the previously determined average sailing speeds are combined with the network schematization, and OpenTNSim is used to calculate how long it takes a vessel to sail from the network boundary to the lock entrance.

This computed travel time is then subtracted from the known lock arrival time to determine an estimated arrival time at the model boundaries. These boundary arrival times form the basis for defining the arrival patterns applied in the simulation scenarios.

4.2.3. Hydrodynamic data

The OpenTNSim model needs water-level data of both inland and seaside of a lock. Of the North Sea Canal it was previously discussed that a target water level of -0.4 m NAP is maintained and thus this is used as the inland water level.

The water level on the seaside of the lock is dependent on the tidal regime of the North Sea. From https://waterinfo.rws.nl/ historical water data can be retrieved from measuring stations within the IJ-muiden lock complex. Figure 4.9 illustrates the location of these stations. For the North Sea tide, the astronomical tide is retrieved for a randomly selected period of 4 months from the outer harbour station. This is done to best represent the kind of data available when making future salt intrusion predictions. The retrieved water level data has a time interval of 10 minutes. To match the 15 second time interval of the density measurements (to be discussed in Subsection 4.3.3), the data is interpolated.

Figure 4.9: Waterinfo measuring stations IJmuiden

4.2.4. Specific locking and clustering logistics

Nearly all seagoing vessels using the Sea Lock IJmuiden to access the North Sea Canal are required to be navigated by pilots. However, due to the limited use of the Sea Lock since its opening, pilots have had relatively little experience operating within it. In early 2023, an opportunity arose when the North Lock was temporarily out of service for maintenance, resulting in the Sea Lock being used exclusively for about a month. During this period, a series of tests were conducted to assess how vessels respond to density currents caused by salinity differences between the lock chamber and the harbour basins when the doors are opened. These tests aimed to increase operational knowledge and inform pilot procedures. Based on the findings, Schotman (2023) advised the CNB (Centraal Nautisch Beheer) on guidelines regarding vessel configurations in the lock.

Given the considerable size of the Sea Lock IJmuiden, it is possible to accommodate multiple vessels simultaneously, both in sequence and side by side. Typically, a maximum of four vessels are clustered per lock cycle. A key rule guiding this configuration is the requirement for a total spare length of at least 100 meters. This spare length includes the space from the lock door to the first stern, between vessels, and from the last bow to the opposite door, ensuring safe manoeuvring and adequate room for mooring lines and tugboat assistance. Additionally, during the 2023 test period, a maximum combined vessel width of 53 meters was enforced to maintain operational safety within the lock chamber. For safety reasons, vessels are not allowed to lie in a staggered formation within the lock chamber. This means that each vessel must be aligned properly, either fully behind or alongside another, to prevent hazardous positioning and to ensure clear and controlled movement during locking.

4.3. Key aspects for salt exchange modelling

As concluded in Subsection 3.2.2, the Zeesluisformulering requires input data on the lock geometry and bathymetry, water levels, salt concentrations, and operational parameters. Since the Zeesluisformulering will first be validated using measurement data in Chapter 5, before being applied to simulate locking strategies in Chapter 6, this chapter provides the data required for both types of modelling.

4.3.1. Lock geometry and bathymetry

The Zeesluisfomulering not only takes into account the main dimensions of the lock to determine the locking prism, but it also takes into account the specific bathymetry around the lock doors to determine the movement speed of the salt exchange. The main lock dimension where already provide in Figure 4.7 of Subsection 4.2.1, but the specific bathymetry of the lock is illustrated in Figure 4.10.

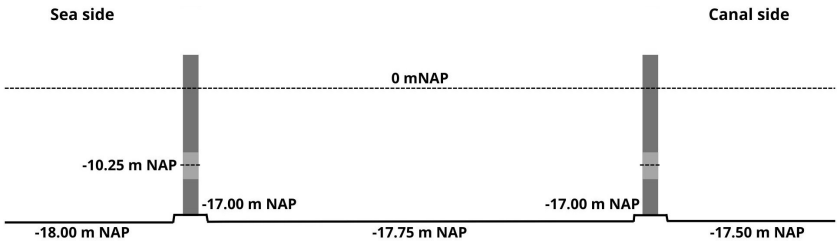

Figure 4.10: Sea Lock IJmuiden bathymetry

4.3.2. Water-levels

The Zeesluisformulering can take into account the same water-level data as OpenTNSim and for the locking strategies this is indeed the case. However, for the validation of the Zeesluisformulering it is needed to use exact water level data. From https://waterinfo.rws.nl/ the historical water data is retrieved from both the inner and outer harbour measurement stations, see Figure 4.9, for the North Sea Canal and North Sea water levels respectively. Again, the retrieved water level data has a time interval of 10 minutes, and is interpolated to match the 15 second time interval of the density measurements.

4.3.3. Measurement campaign

During February and March of 2023 the North lock of the IJmuiden lock complex was temporarily out of order due to maintenance, leaving the Sea Lock IJmuiden in full-time operation. From February 20 to March 20, density measurements were performed by Deltares in the lock chamber and the inner and outer harbour basins. The main goal was to understand the influence of the density currents on the behaviour of ships in the lock (Deltares, 2023). However, the gathered data can also be used to determine the salt mass fluxes during locking operations.

Salt concentrations

During the measuring campaign the Sea Lock was equipped with sensors measuring the conductivity, temperature and pressure of the water every 15 seconds. 20 of these sensors (D) were placed on four lines (L) on either side of the lock doors, see Figure 4.11. The top sensors of each line remained below the water level at low water, with the sensors below equally spaced 4 m from each other, and the bottom sensors at the height of the lock sills. Due to the sensors having limited memory, they were removed from the water every week, causing some gaps in the data (Deltares, 2023).

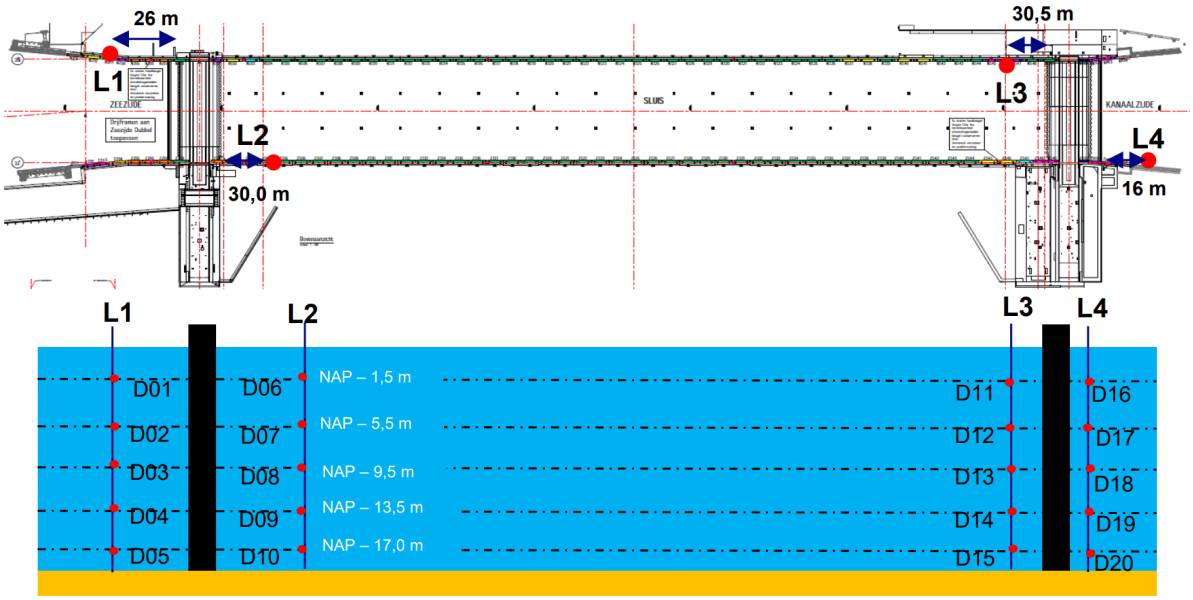

Figure 4.11: Locations of the sensors in the Sea Lock IJmuiden (Deltares, 2023).

For each sensor the conductivity σ [mS/cm], temperature T [°] and pressure P [Pa] have been measured. In the post processing of the measurement campaign, the temperature and conductivity were used to calculate the salinity S [ppm] and density ρ [kg/m^3] at the location of each sensor according to the UNESCO-1981 formulation (UNESCO, 1981). Furthermore, with the calculated density and the pressure, the averaged water levels at all four sensor lines and lock chamber average water level have been determined.

For calculations with the Zeesluisformulering the salt concentration in kg/m^3 is needed. This is different from the water density, also kg/m^3, as this concentration stands for the mass of CL^- ions per m^3 of sea water [1]. Conversion is done using the salinity [g/kg] and density [kg/m^3] according to the UNESCO-1965 formulation (UNESCO, 1965) in Equation 4.1. Even though the formulation is originally expressed in mg/L, it can also be expressed in kg/m^3.

$$C = S * \frac{\rho}{1.80655}[mg/l] = \frac{S}{1000} * \frac{\rho}{1.80655}[kg/m^3] \tag{4.1}$$

The weighted average salt concentration for each sensor line is calculated by considering the salt readings from its five sensors, with each sensor's contribution weighted according to the height of the water column it represents. The weighted average salt concentration of line L1 represents the salt concentration of the sea, while the weighted average of line L4 represents the salt concentration of the canal. Lines L2 and L3 each represent half of the lock chamber, and the salt concentration for the entire lock chamber is determined by averaging the weighted averages of these two lines.

Vessel data

The Zeesluisformulering requires the volume of vessels entering and exiting the lock chamber. For this, the main dimensions (length, width, draught) and entering and exiting times of vessels are needed. During the measurement campaign, Maritime Studies students from the Amsterdam University of Applied Sciences (Zeevaart school, Hogeschool van Amsterdam) logged the passing of vessels through the Sea Lock IJmuiden. The logbook contains the rough entering and exiting times of the vessels, as well as whether the vessel was inbound or outbound. The vessel dimensions where almost always passed on by the captains, with the exception of some vessel draughts. For the missing draughts, first

[1] In the Zeesluisformulering, the term salinity is consistently used for values in [kg/m³], but this is incorrect and should be referred to as salt concentration. In this study, salt concentration was interpreted as chloride concentration. Further analysis showed that this interpretation reduced the accuracy of the ZSF, as true salt concentration should also include the contributions of other dissolved ions in addition to chloride.

it is checked whether the vessel was logged on a previous passage with its draught. Otherwise the maximum vessel draught is taken from Marine Traffic.

Locking strategies
For the simulation of locking strategies in Chapter 6, the AIS data provided for the OpenTNSim is used, as well as the simulated entering and exiting times.

door data

During the measurement campaign any data on the operations of the doors was collected, thus for both the lock doors the start and end times of the opening and closing of the doors are known. The data is supplied in the same time step of 15 seconds as the field measurements and indicates how far the doors are opened: 0 for a closed door, 1 for an open door, values in between when the door is in movement. By looking at the change of these values, the movements of the doors can be determined: 0-1 for opening, 1-0 for closing. Furthermore, by looking at the consecutive door movements of both lock doors, the various phases of the locking cycle can be depicted. Figure 4.12 provides an example of the raw door data and demonstrates how the different locking phases can be identified based on the opening and closing actions of the lock doors. The timestamps for these door actions are placed at the midpoint of the door movement, which serves as the reference point for determining the start and end of each phase in the locking cycle.

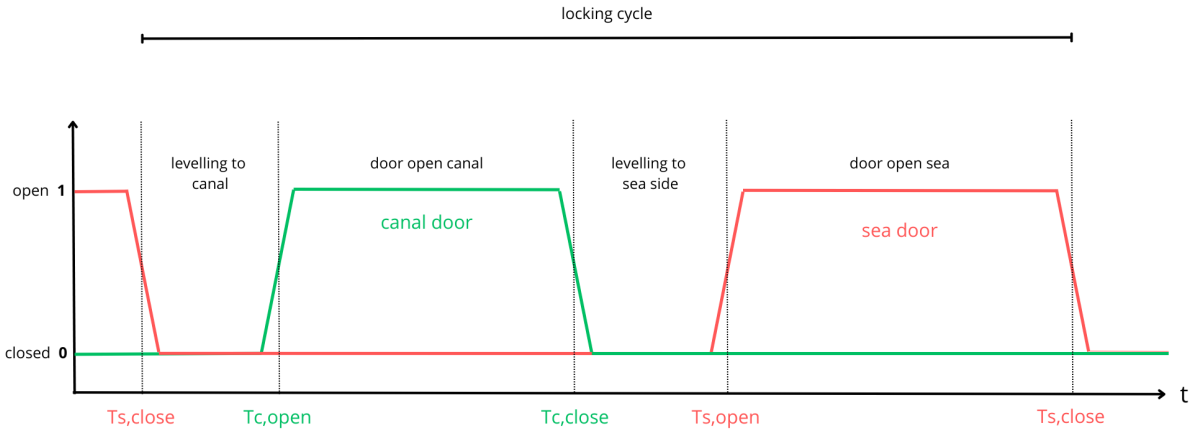

Figure 4.12: Translation of door data to locking phases

Locking strategies
For the simulation of the locking strategies in Chapter 6, the output of OpenTNSim as lock logbooks is translated into the same kind of 0-1 data as the measurement campaign and then also translated into locking phases.

4.4. Key investigation topics

4.4.1. ZSF validation

An important first step in this study is to assess whether the estimated intruding salt masses as a function of passing vessels is realistic. This is essential to verify that the model can accurately represent the contribution of ship passages to salt intrusion. Only once this has been established can scenarios involving operational strategies, such as vessel clustering, be considered reliable for further simulation. In the next chapter, the measuring campaign data and the observed vessel passages will be used to validate the model performance.

4.4.2. Clustering trade-off

Salt concentration observations at the lock complex currently form the basis for deciding when to implement operational interventions aimed at limiting salt intrusion. In this study, the focus is on investigating

vessel clustering as a mitigation measure. However, other potential measures could in principle be explored in a similar way. Once the accuracy of the Zeesluisformulering has been established through validation, the model can be applied to analyse the trade-off between salt intrusion, and vessel delays as a result of the clustering strategy. The traffic model is used to simulate how, given vessel arrival patterns and clustering strategies, lock operations influence both salt exchange and navigational efficiency.

To explore the potential of clustering as a salt intrusion mitigation strategy, a range of realistic clustering time windows could be evaluated. Currently, under normal operating conditions at the IJmuiden lock complex, clustering only occurs if the next vessel arrives within 30 minutes. However, when the z-5 salinity index exceeds certain thresholds, more stringent operational restrictions are considered, such as limiting the number of locking cycles or reducing the hours of operation. To assess the impact of such measures, clustering times ranging from 0 to 6 hours of waiting for additional vessels are simulated, assuming that the lock doors remain open whenever the lock is not levelling. The resulting vessel delays will be analysed to determine the trade-off between salt intrusion reduction and operational efficiency. Additionally, extended clustering times will be tested to identify the limits of this trade-off and provide insights into the feasibility of more aggressive mitigation strategies.

5

Zeesluisformulering validation

To determine whether the estimated salt intrusion resulting from vessel passages is realistic, it is crucial to verify that the model can accurately capture the impact of ship movements on salt intrusion. This chapter focuses on validating the Zeesluisformulering model by comparing its simulated salt intrusion through the sea lock with field measurement data. Based on this comparison, the accuracy of the model is assessed, and where necessary, a correction is applied to improve its predictive performance.

5.1. Suggested approach

The accuracy analysis of the ZSF is divided into four steps to better identify where deviations may arise.

1. Evaluating all complete locking cycles during the measurement period. This serves to verify whether the supplied ZSF Python code functions correctly and to identify and resolve any coding errors.
2. Comparing the calculated and measured salt mass exchange for the individual phases within each locking cycle. This comparison is carried out in two ways: one using the salt concentration output from the previous phase as input for the next, and another using the measured concentration as input for each phase independently. This distinction helps determine the influence of each phase on the overall deviation of the ZSF results.
3. Investigating how key parameters affect model accuracy. By comparing the modelling error to the values of specific parameters, it becomes possible to assess whether certain parameters have a disproportionate impact on the deviation and may require adjustment.
4. Comparing the cumulative calculated and measured intruded salt mass over the entire measurement period. This step provides insight into the long-term accuracy of the ZSF model.

Once the model accuracy has been assessed, a correction factor will be applied to the ZSF. The placement of this correction factor will be guided by the findings from the previous steps, and its value will be based on the observed deviations resulting from different potential adjustments.

5.1.1. Salt mass exchange comparison

To compare the calculated salt intrusion with the measured field data, both need to be expressed in terms of salt mass [kg]. The ZSF provides the total exchanged salt mass for each locking phase as output. Therefore, the field data, which consists of salt concentration measurements, must be converted into exchanged salt masses as well. This is done by calculating the total salt mass present in the lock chamber at the start and end of each locking phase. The difference between these two values gives the exchanged salt mass associated with that phase.

The total salt mass is determined by multiplying the measured salt concentration C with the effective water volume $V_{w,lock}$ in the lock. The effective volume accounts for lock chamber volume and subtracts

the volume occupied by vessels present during the phase. The salt mass M [kg] is computed using the following equation:

$$M = C \cdot V_{w,lock} = C \cdot \left((w_{lock} - z_{lock}) \cdot L_{lock} \cdot B_{lock} - V_{vessel} \right) \tag{5.1}$$

In this equation, w_{lock} is the water level in the lock chamber, while z_{lock} is the level of the lock chamber bottom. L_{lock} and B_{lock} are the lock chamber length and width respectively, and V_{vessel} is the total volume displaced by vessels inside the lock.

5.2. Execution of ZSF analysis

5.2.1. Full locking cycles

A full locking cycle is defined as a cycle where all four cycle phases follow each other as in the order illustrated in Figure 5.1. This means cycles where the lock door was temporary closed between exiting and entering of vessels are not included. During the measuring period, with the exception of the intervals during which sensors were changed, a total of 118 full locking cycles occurred. Each of these cycles is modelled with the ZSF and visualised with different subplots to include the different parameters that come into play. With the use of these figures, any issues in the ZSF python code are resolved. The results of each full locking cycle can be found in Appendix B. To clarify the structure of these locking cycles, one example is shown in Figure 5.2, with each subplot explained in the sections below.

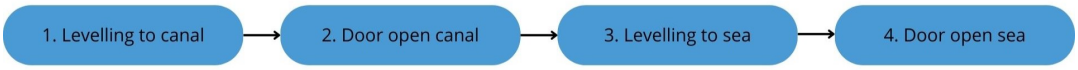

Figure 5.1: Order of locking phases in a full locking cycle

At the top in Figure 5.2a, the movement of both of the lock doors is shown. The movement and position of the doors is used to determine which locking phase is occurring. The different locking phases are distinguished by a gradient of grey tones and the border between them is marked with a vertical, dashed red line. As illustrated, each phase begins and ends halfway through a door's opening or closing motion, which corresponds to the moments when the ZSF model reads its input parameters.

In Figure 5.2b, the movement of the vessel through the lock is illustrated. Since the ZSF model assumes vessels enter the lock immediately as the doors close and exit instantaneously as the doors open, the volume of vessels present in the lock chamber is represented as a block. In reality, vessel movement takes time, and the dashed vertical lines indicate the moments when a vessel passes the threshold of the lock chamber during entry and exit.

Figure 5.2c displays the measured water levels in the lock chamber and harbour basins. An important note here is that during the *door-open-phases* the ZSF accounts for a constant water level from the moment the doors open. For the *door-open-sea phase* this has been indicated separately with a constant orange line.

The salt concentrations in the harbour basins are shown in Figure 5.2d. In addition to the measured values, the figure also displays the input concentrations used by the ZSF model. These input concentrations are treated as constant throughout each locking cycle and should not be affected by the exchange processes during that cycle. Determine appropriate values is done by selecting the most undisturbed salt concentrations: for the sea side, this is just before the start of the *levelling-to-sea phase*, and for the canal side, it is at the end of the *door-open-sea phase*.

The next plot in Figure 5.2e plots the salt concentration of the lock chamber. The purple line displays the measured lock concentration, with the accurate times of vessels entering and exiting depicted along this line as crosses. The blue line indicates the concentration calculated with the ZSF. For the calculations of these cycles the initial lock concentration of the ZSF is equal to the measured lock concentration at

the start of the *levelling-to-canal phase* when the sea door is halfway closed. The calculations in the subsequent phases is done with the calculated ZSF calculations of the previous phase.

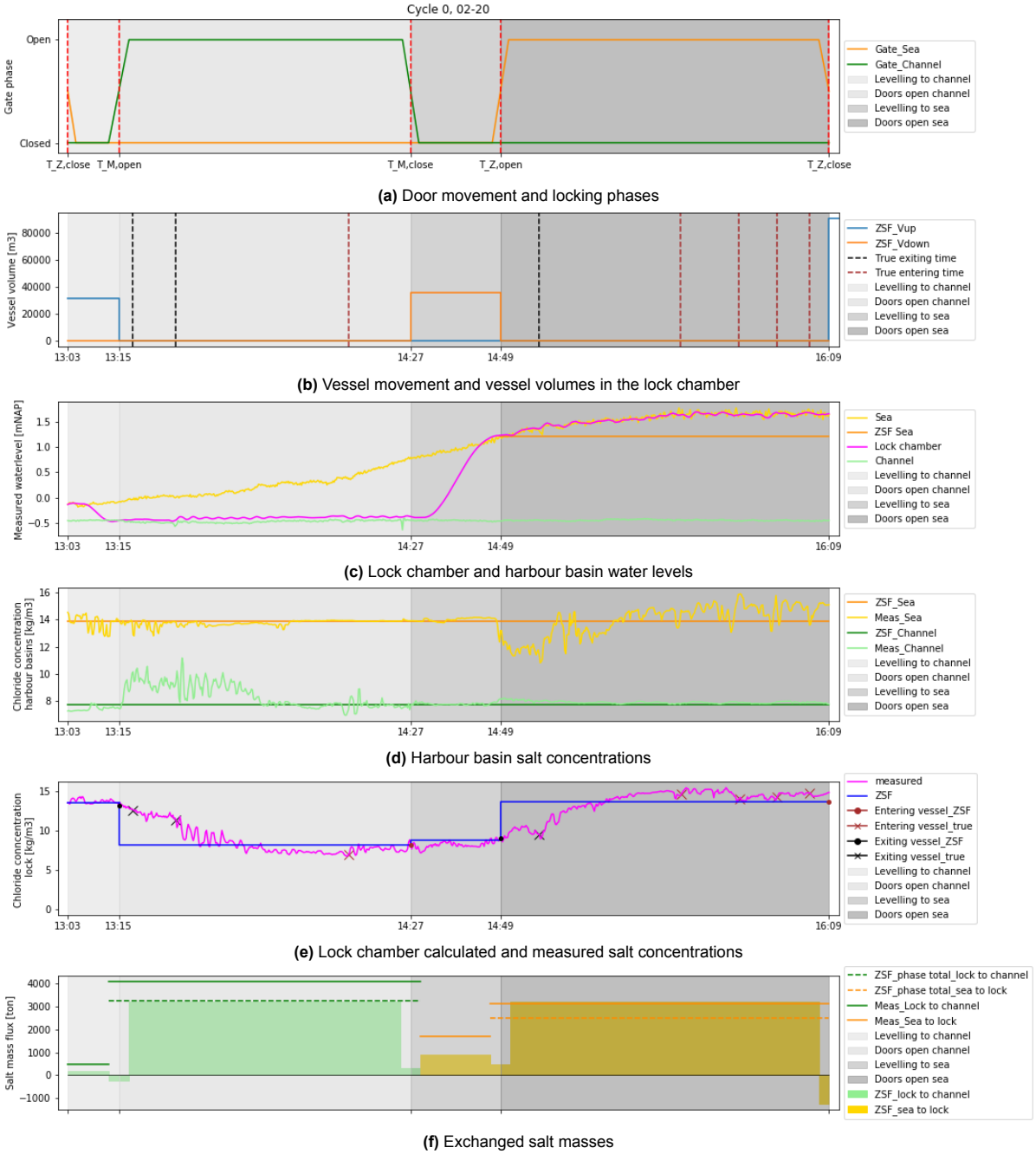

(a) Door movement and locking phases

(b) Vessel movement and vessel volumes in the lock chamber

(c) Lock chamber and harbour basin water levels

(d) Harbour basin salt concentrations

(e) Lock chamber calculated and measured salt concentrations

(f) Exchanged salt masses

Figure 5.2: Full locking cycle

The final plot, Figure 5.2f, depicts the exchanged salt mass with positive values signifying salt intrusion. For the *levelling-to-canal phase* and *door-open-canal phase*, indicated in green, this means movement from the lock chamber into the canal, and for the *levelling-to-sea phase* and *door-open-sea phase*, indicated in orange, this means from the sea into the lock chamber. The measured salt masses are displayed by solid lines. The green and orange areas display the calculated salt masses. For the calculations of the *door-open phases*, the three elements of salt intrusion (exiting vessels, lock exchange, entering vessels) are illustrated separately as solid green or orange. The summation of these elements is indicated by the dashed lines.

Figure 5.2f is the most relevant output for this study, as it provides a direct comparison between the measured and calculated salt masses exchanged per phase. To clarify how the measured and calculated salt masses are extracted, a detailed example of it is shown in Figure 5.3. The measured and calculated salt masses for each phase can be plotted against one another. When this is done for all 118 cycles, it results in the scatter plots that are discussed in Subsection 5.2.2.

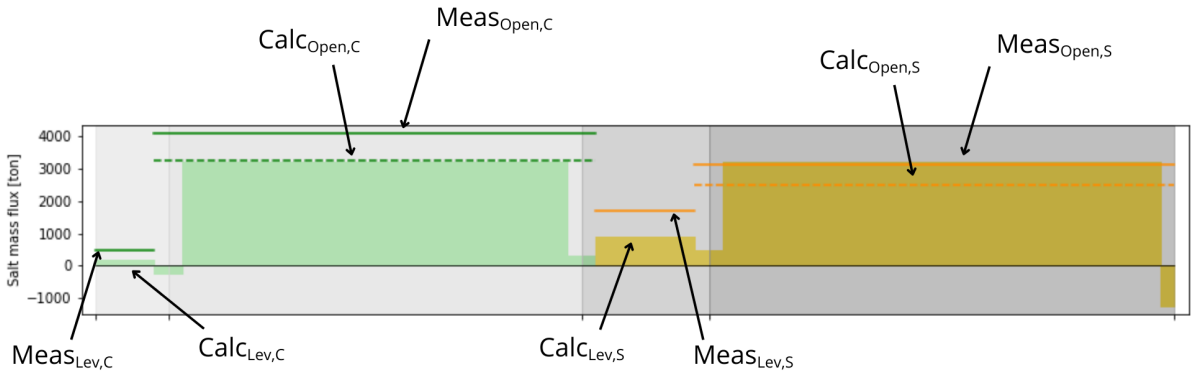

Figure 5.3: Exchanged salt mass in detail, solid lines indicating the measured exchanged salt masses and dashed lines indicating the calculated exchanged salt masses.

5.2.2. Results for individual cycle phases

This paragraph compares the exchanged salt masses of the field measurements to the model calculations per distinct locking cycle phase of the 118 locking cycles of Subsection 5.2.1. Two different versions modelled: separated phases and continued phases. In the separated phases the measured lock chamber salt concentration is used as input for each individual phase within a locking cycle, schematised by Figure 5.4a. For the continued phases the same modelling of the previous section has been used, where at the start of the *levelling-to-canal phase* the measured lock chamber salt concentration is used as initial input for the model. The other three phases then use the calculated concentrations of their previous phase as input, schematised by Figure 5.4b.

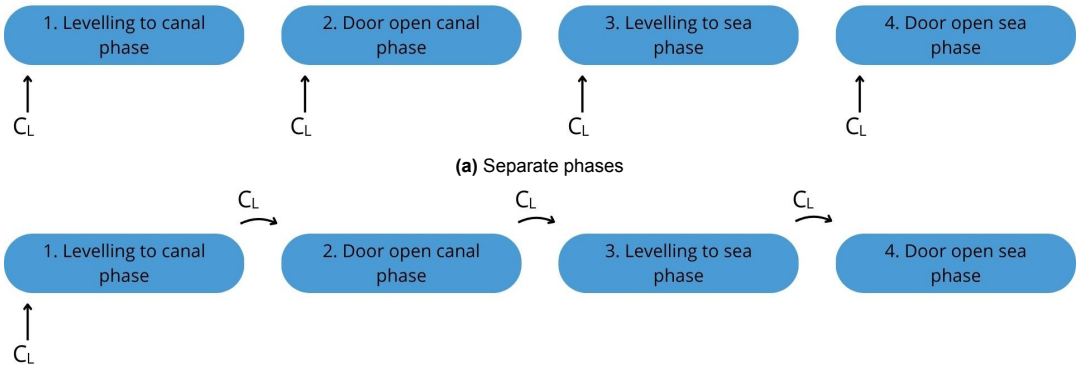

(a) Separate phases

(b) Continued phases

Figure 5.4: Input value for the lock chamber salt concentration C_L.

Figure 5.5 presents scatter plots comparing the measured and calculated exchanged salt masses. Each plot contains 118 data points, with each point representing a distinct phase from one of the 118 locking cycles described in Subsection 5.2.1.

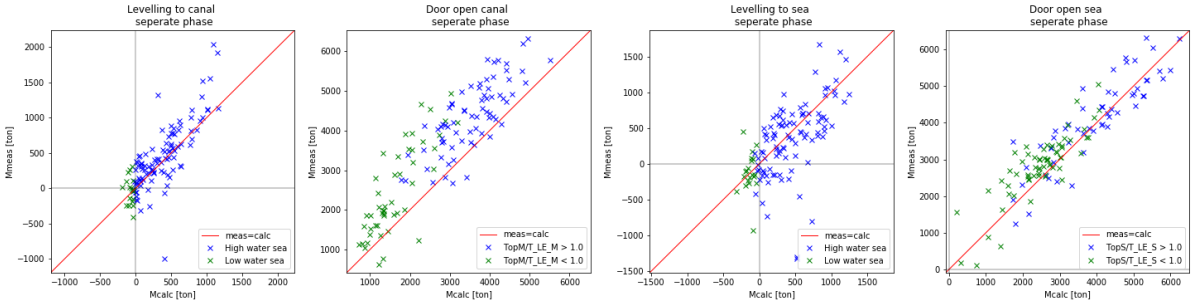

(a) Separate phases

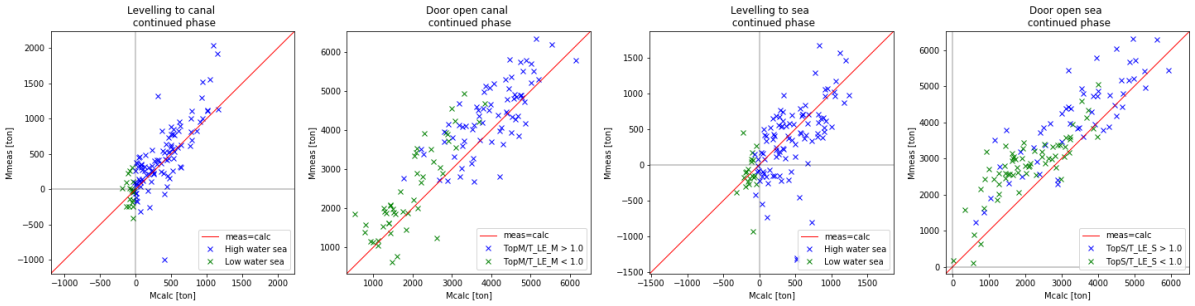

(b) Continued phases

Figure 5.5: Comparing of measured and calculated exchanged salt mass per locking phase.

In case of the *levelling-to-canal phase*, both input types give identical results as it always uses the measured concentration as input. The plots show that for this phase the plotted values of most of the marks lie around the ideal line, with the exception of some outliers. This indicates that during this phase there is both some under- and overestimating of the salt mass exchange.
When looking at the *door-open-canal phase*, it shows that in case of separate phases there is more often an underestimation of salt mass exchange. When looking at the continued phases, however, the results have shifted more towards the ideal line although still mostly underestimating.
For the *levelling-to-sea phase*, the marks are around the ideal line, although there is more overestimation. Furthermore, there is no significant difference in separate and continued phases. This is because the water at sea is more often higher than the canal, which leads to an inflow of seawater into the lock. When calculating the salt intrusion in these cases, the salt concentration of the lock chamber is not relevant. The concentration is only relevant during low tide, but because those salt masses are much smaller, the difference is less noticeable.
For the separate phases of the *door-open-sea phase*, the underestimation of salt intrusion is smaller compared to the *door-open-canal-phase*. But when continued phases are considered, the underestimation grows.

5.2.3. Most influential parameters

Using the simulations of the individual phases done in the previous section, the values of some parameters are compared to the error made in the calculated salt mass exchange. In Figure 5.6, the most relevant parameters are illustrated. Other considered parameters can be found in Appendix B.2. Figure 5.6a compares the door-open-time relative to the lock-exchange-time to the difference in measured and calculated salt mass exchange on the canal side. It indicates that for shorter door open times the error in calculations is larger, while smaller for larger door open times. This would mean that when there is (almost) full lock exchange the ZSF is most accurate. In Figure 5.6b the same parameter is plotted, but now for open doors at the sea side. There is a less noticeable correlation, but still the same can be said as for the canal side. It seems there is a smaller error in calculations for larger door open times than for smaller door open times.

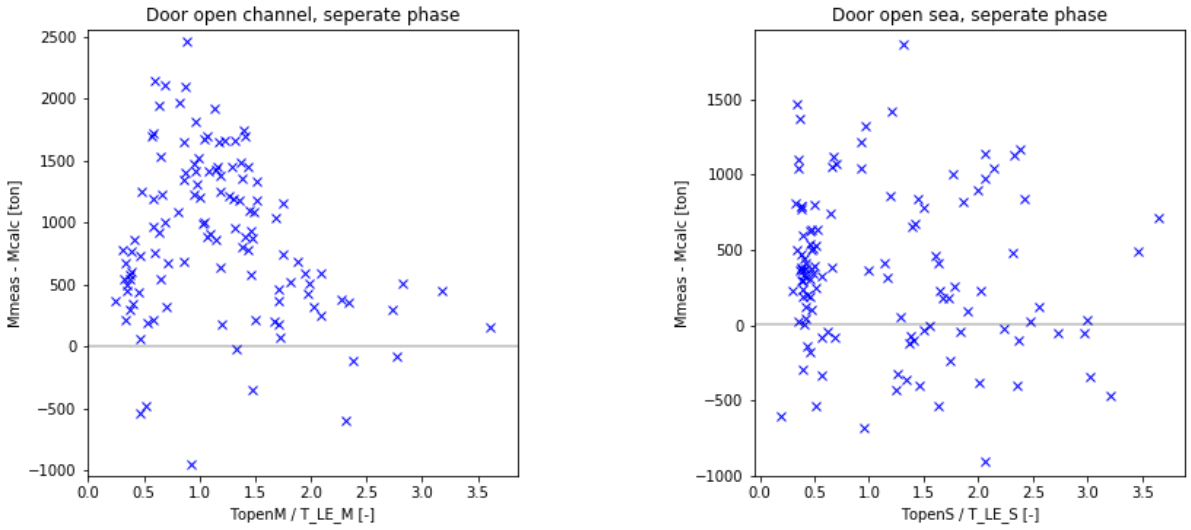

(a) Canal side

(b) Sea side

Figure 5.6: Parameter analysis: Door open time relative to lock exchange time

5.2.4. Validation results for the full measurement period

For this section the entire measurement campaign time period is assessed. This is done by comparing the cumulative calculated and measured salt intrusion for the entire duration of the measurement campaign. For the salt concentrations of the harbour basins multiple concentration variations have been considered, all of which are found in Appendix B.3. The averaged value of the rolling median of the measured concentrations is from now used as it was deemed the most accurate. Figure 5.7 illustrated the chosen salt concentrations of the harbour basins compared to the measured concentrations.

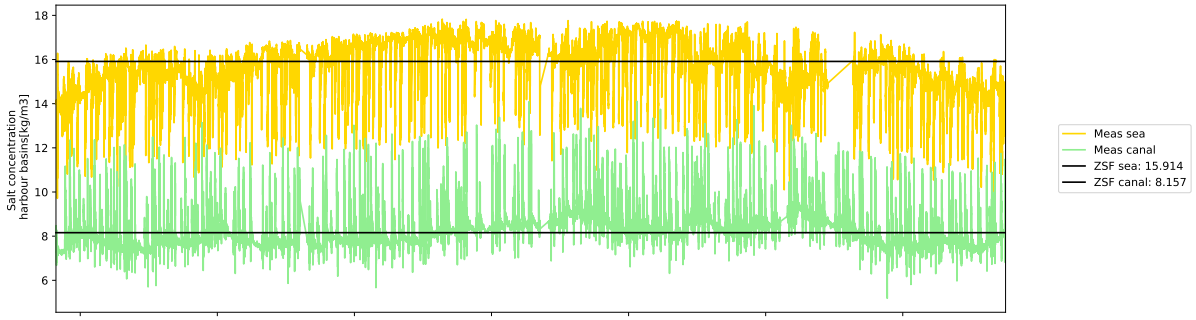

Figure 5.7: Averaged rolling median salt concentrations harbour basins.

Figure 5.11 shows the full period simulation, with the measured and calculated lock chamber salt concentrations in the top subplot. In the bottom plot the cumulative salt intrusion into the canal is plotted. A thing to point out about the figure is the vertical grey areas in all three plots. These areas depict the periods with gaps in field measurement data due to the removal of sensors. During these periods no salt intrusion was added to the cumulative as it was not possible to determine the measured salt intrusion. However, during these periods the ZSF modelling was continued as to keep predicting the salt concentration in the lock chamber.

The measured and calculated cumulative salt intrusion show that the error of the model grows over time. After the period of 4 weeks it has a value of almost 19%. The error percentage remains the constant after about 1.5 weeks, while the mass value keep increasing. When looking at the lock salt concentrations it shows that for quite some phases the measured values exceed the set harbour basin concentrations, but the ZSF calculated values do not even reach full lock exchange (when the harbour values are reached). This can partly explain the underestimation of the model since one underestimation in

the *door-open phase* gives less of an extreme salt concentration resulting in a smaller concentration difference on the next *door-open phase*, resulting in less lock exchange.

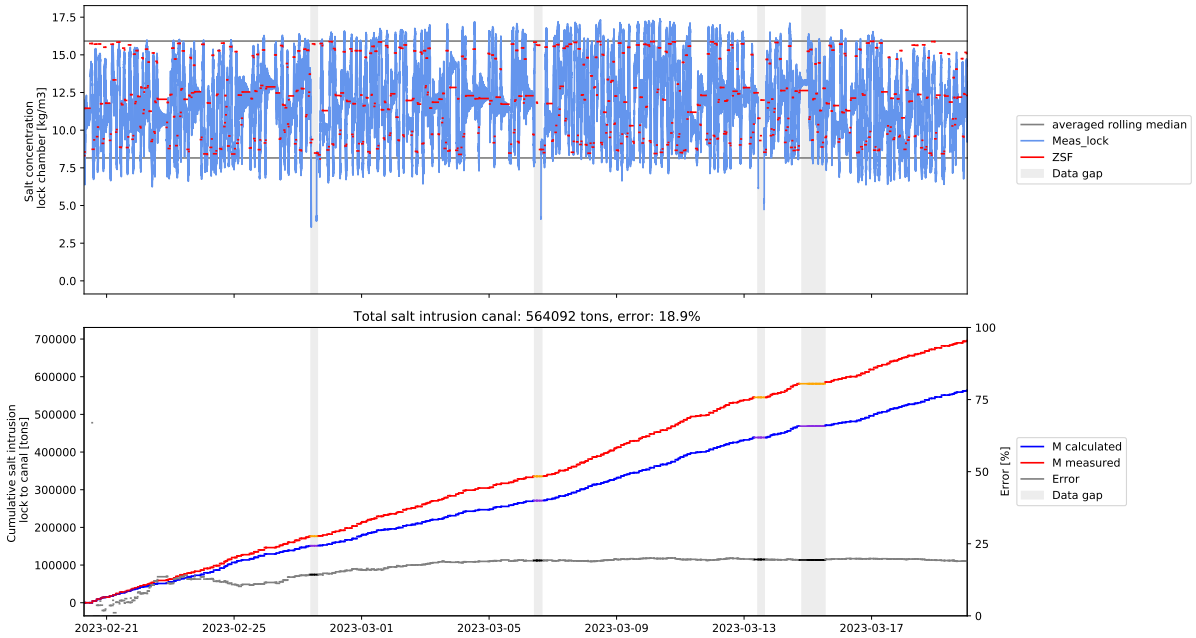

Figure 5.8: Full period validation

5.3. Correction

From the previous section it can be concluded that there is a error in the modelling of the salt intrusion at the Sea Lock IJmuiden. To be able to use the ZSF further on in this research, a correction factor is needed. This section details how the correction factor is determined, its value, location in the model, and its direct impact on the results. Subsequently, the updated model performance for the full simulation period is presented, followed by a brief discussion on the implications and limitations of the applied correction.

5.3.1. Determining correction factor

As concluded in in the previous section the largest error in the Zeesluisformulering calculations occur in the *door-open phases*, specifically in the lock exchange. Because of this, a correction factor is placed in the lock exchange calculations. Equation 5.2 holds the renewed equation for the lock exchange time, placing the correction factor such that it increases the propagation velocity of the exchange current.

$$T_{LE} = \frac{2L_L K}{c_i \cdot f_c} \tag{5.2}$$

To determine the value of the correction factor, the full measurement period is modelled again for varying correction factor values. Figure 5.9 plots the correction factors against the modelling error of the salt intrusion. With these result, the correction factor is set at 1.65.

Figure 5.10 plots the relative door open time against the volume of the exchange current. It displays the direct effect of the correction factor. It illustrates that the correction factor causes full lock exchanged being reached with shorter door open times.

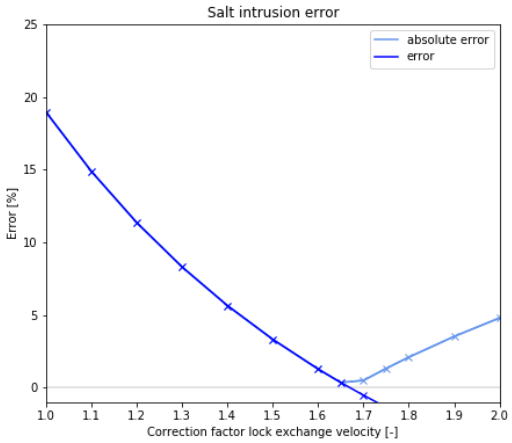

Figure 5.9: Correction factor values compared to salt intrusion error.

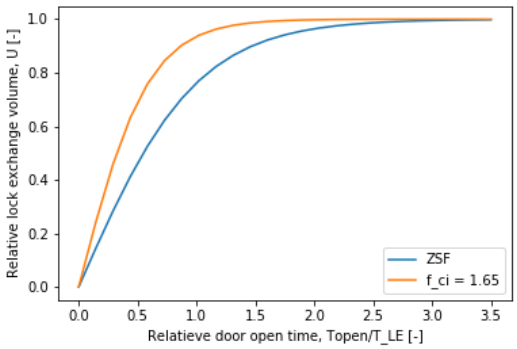

Figure 5.10: Influence correction factor on lock exchange volume.

5.3.2. Results correction factor

Figure 5.11 illustrates the results of the full period modelling with a correction factor of 1.65. The top plot shows shows far more cases of (near) full lock exchange where the lock concentration has almost reached the harbour basin salt concentrations. This has resulted in a new calculated salt intrusion with an error of only 0.4%. The calculated salt concentration follows the measured concentration closely which makes the model more balanced in over and under estimating the salt intrusion.

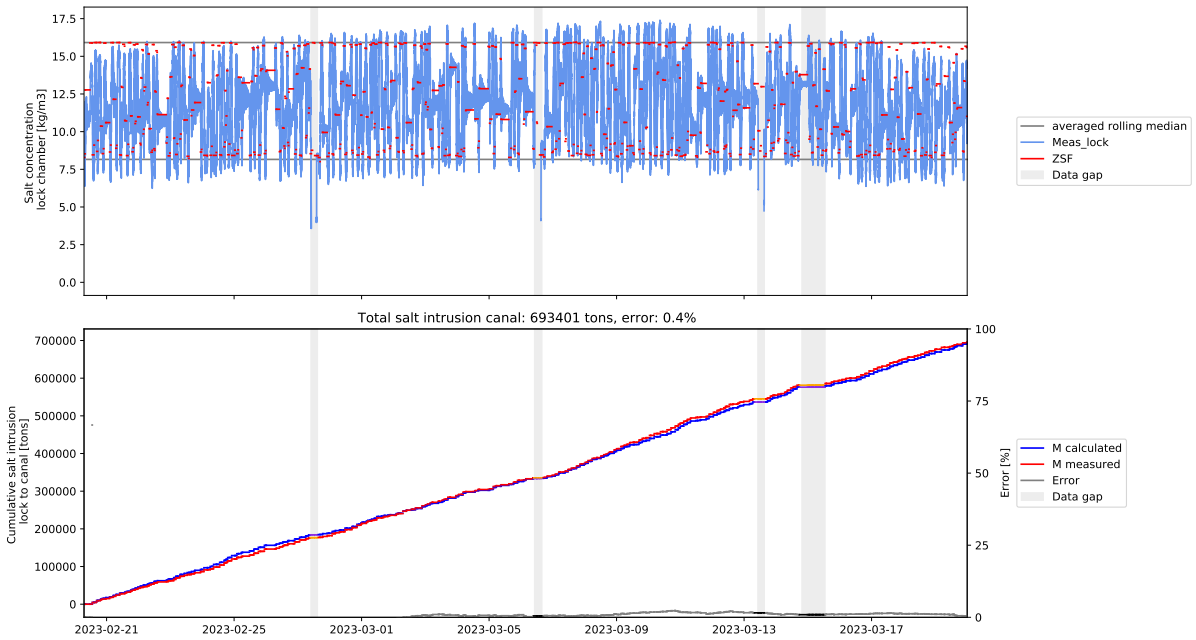

Figure 5.11: Full period modelling with correction factor of 1.65.

5.3.3. Correction factor discussion

The correction factor of 1.65 is a value specific to the Sea Lock IJmuiden. It is not only implemented to adjust the lock exchange calculations, but compensates for an array of parameters that could be the reason for the error in the salt intrusion calculations. These are however summarized into one correction factor to create a working model capable accurately predict salt intrusion in the Sea Lock

IJmuiden and cannot be implemented to every other lock in the world. Below is a list of parameters that could have an effect on the error of salt intrusion prediction:

- During the *door-open-sea phase* the changing of the tide while the doors are open are not taken into account.
- External parameters such as wind and currents can lead to an increase of salt in the harbour basins, resulting in temporary higher measured salt intrusion than in reality.
- In reality the salt concentrations of the harbour basins vary. The constant value assumed in the ZSF can lead to instances where there is a larger concentration difference in reality, thus making the measured salt intrusion larger.
- Using the weighted average of the lock chamber salt concentration can change the height and length of the salt wedge present in the lock chamber, thus creating wrong data. In the same way, the presence of waves in the lock due to wind or currents can increase the weighted height of the top sensor, influencing the measured lock chamber salt concentration.
- Add footnote info about salt concentration should have been used in stead of chloride concentration, which has since been proven to lead to a better performance of the ZSF 1

5.4. Conclusion

Now that the accuracy of the Zeesluisformulering has been assessed and an IJmuiden-specific correction factor has been applied, the model is suitable for calculating salt intrusion at the Sea Lock IJmuiden. With this adjustment, we have gained sufficient confidence in the ZSF to couple it with the logistical simulation model OpenTNSim. In the next chapter, this coupled model will be used to simulate various locking strategies, allowing us to explore the trade-off between salt intrusion and vessel delays under different clustering times.

6

Locking strategies

Building on the previous chapter, where it was shown that salt intrusion due to vessel passages can be accurately estimated, this chapter focuses on exploring the trade-off between salt intrusion and vessel waiting times for different clustering strategies using the coupled model.

6.1. Suggested approach

The simulation approach in this chapter consists of three main steps. First, vessel passages and the salt intrusion are modelled under regular clustering conditions, which include the current practice of allowing a maximum waiting time of 30 minutes. Second, alternative clustering scenarios are explored, with waiting times ranging from no clustering (0 hours) up to 2, 4, and 6 hours. These extended clustering durations reflect potential operational adjustments during drought periods when stricter measures are applied. Third, the outcomes of these scenarios are used to construct a trade-off curve, demonstrating the balance between salt intrusion and vessel delay across different clustering strategies.

To accurately represent real-world conditions, the simulations use data from the IJmuiden lock complex, with 3 months of vessel AIS data (January-March 2023) and 4 months of water level data (January-April 2023). This combined dataset provides a robust foundation for simulating 1 month of lock operations at the IJmuiden complex, allowing for a comprehensive analysis of the effects of various clustering strategies over an extended period. The month chosen is January, since during the period of February and March the field measurements were conducted, influencing the normal locking procedure (i.e. more clustering of vessels).

6.1.1. Clustering approach

The lock module in OpenTNSim supports clustering of vessels, but only in the longitudinal direction. This means it can only place vessels behind each other in the lock. Since vessels in the Sea Lock IJmuiden can also be positioned side by side, a modified clustering approach is required. For this research it is assumed that a maximum of four vessels can be accommodated in a single lock cycle.

For each vessel in the simulation, all other vessels from the same side arriving within the defined clustering window are identified, up to a maximum of four vessels in total. With a first-come-first-serve rule in place, the first arriving vessel is always included in the locking cycle. Whether the other vessels can also be included depends on whether they physically fit in the lock. To determine this, all candidate vessels are sorted by length and evaluated for their combined layout in the lock chamber, taking into account both longitudinal and side-by-side positioning, as well as safety margins and rules defined in Subsection 4.2.4. This procedure is illustrated in Figure 6.1, where the lock space is partitioned based on the largest vessel (A) and the remaining vessels (B-D) are fitted in the remaining spaces.

If not all selected vessels fit, the latest-arriving vessel is removed from the selection and the process is repeated until a valid configuration is found.

Once a valid cluster is established, each vessel gets assigned a virtual arrival time and virtual vessel length. The arrival time of the last vessel in the cluster remains unchanged, while preceding vessels are spaced at 10-minute intervals. For OpenTNSim to be able to cluster all selected vessels longitudinally in the lock, the sizes are changed in such a way that in total they fit exactly in the lock chamber. Thereby, the first arriving vessel is the largest and following vessels are smaller. This ensures a realistic configuration and prevents the first vessel from being grouped into an earlier cycle where it would not fit in reality.

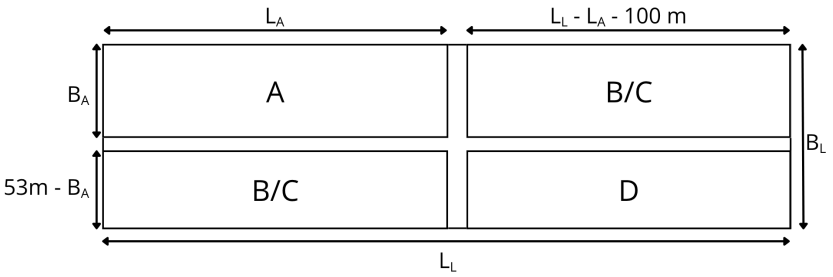

Figure 6.1: Lock partitioning for clustering of four vessels, with A the largest vessel and D the smallest.

6.2. Simulating clustering

6.2.1. Normal locking procedure

As mentioned earlier, in a normal locking procedure vessels are clustered if they arrive within a 30-minute window of one another. The first OpenTNSim simulation was carried out using this standard clustering time. Figure 6.2 shows the resulting tracking diagram for a single day of the simulation. It illustrates several instances of clustering, as well as multiple vessels that experience waiting time before being locked through.

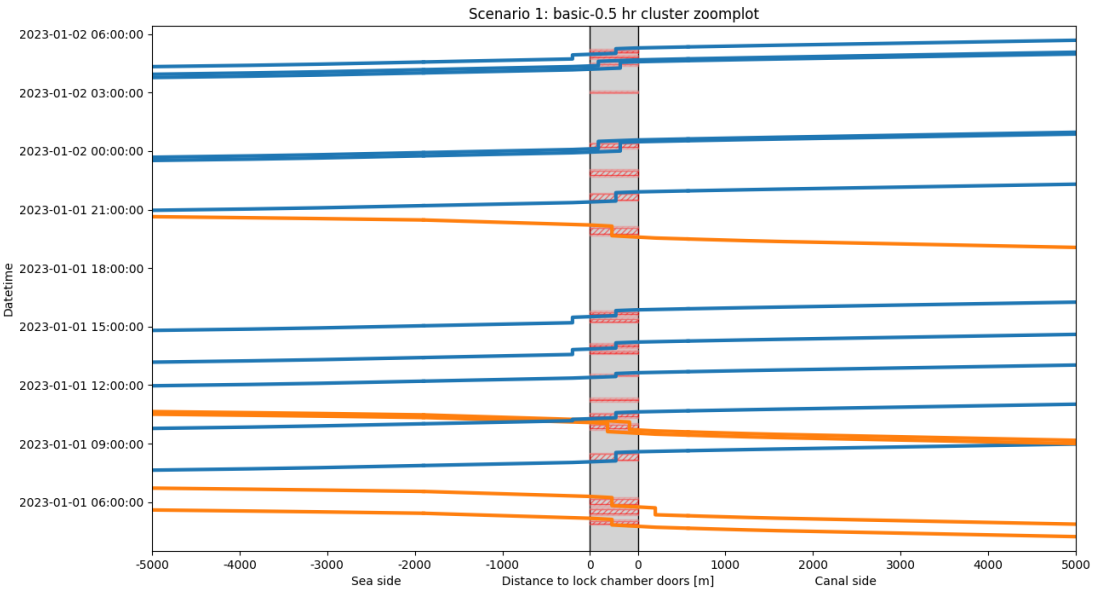

Figure 6.2: OpenTNSim tracking diagram (1 day) for the normal locking procedure

The output from OpenTNSim, including door movements and vessel passages, is translated into input for the Zeesluisformulering. This input is then used to calculate salt intrusion over the entire simulation

period. Figure 6.3 presents the resulting cumulative salt intrusion into the canal (left axis), along with the total vessel delay (right axis).

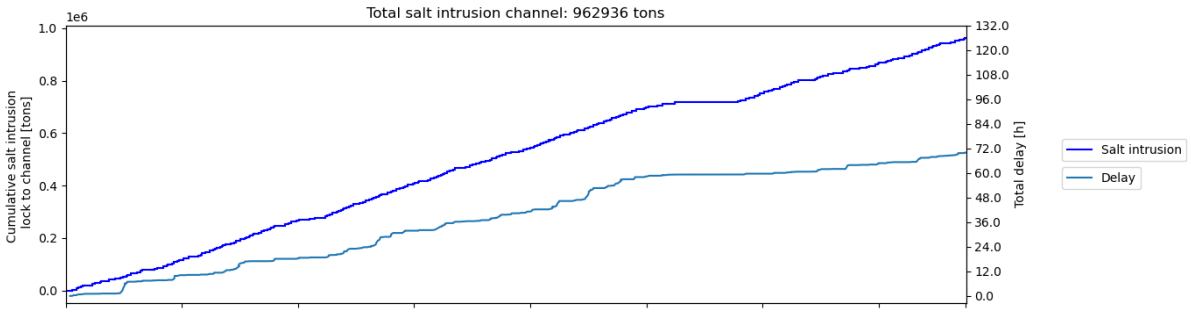

Figure 6.3: Cumulative salt intrusion and vessel delay for the normal locking procedure

6.2.2. Clustering strategies

The same simulation approach used for the normal locking procedure has also been applied to clustering times of 0 hours (no clustering, one by one locking), 2 hours, 4 hours, and 6 hours. As an example, this section compares the results of the 30-minute and 2-hour clustering strategies. The results of the other clustering simulations can be found in Appendix Appendix C.

Figure 6.4 displays the one-day tracking diagrams for both the normal locking procedure and 2-hour clustering scenario. It illustrate that more clustering occurs within the 2-hour window. It also demonstrate how the clustering approach, which uses virtual arrival times, forces clustering vessels to arrive closer together. Although the 2-hour clustering scenario appears to show minimal waiting times, this is due to the adjusted arrival times used in the clustering method. In practice, vessels would wait in the lock for all others in the cluster to arrive. Eventhough the simulations are done with virtual arrival times, the vessel delays are still calculated with the original arrival times. So the postponal of the virtual arrival time is already seen as part of the delay. Nevertheless, this comparison provides a first indication of how extended clustering lowers the total number of locking operations.

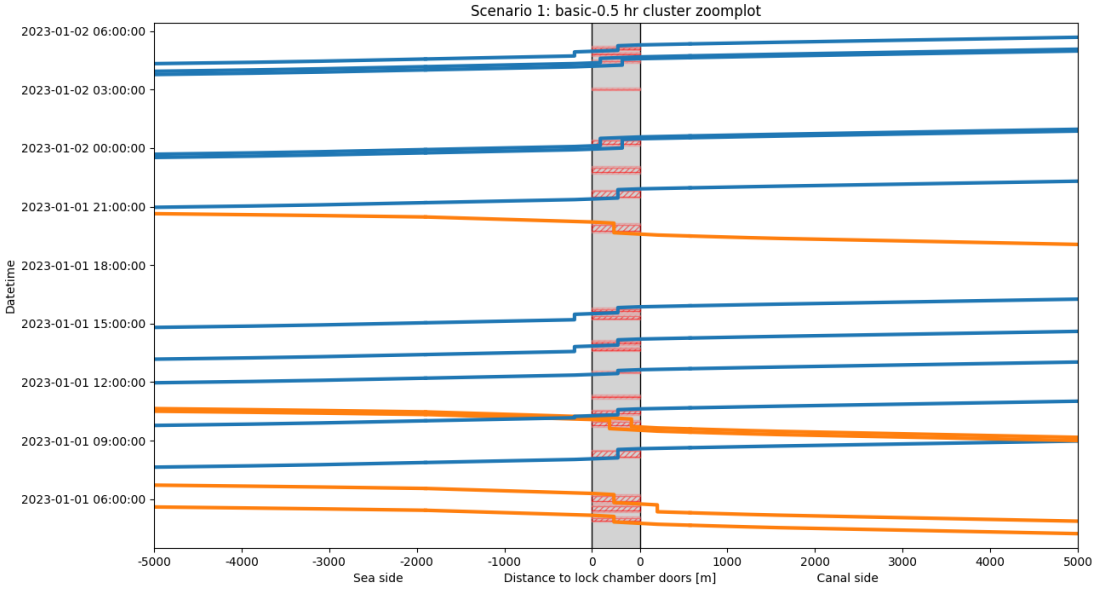

(a) Normal locking procedure

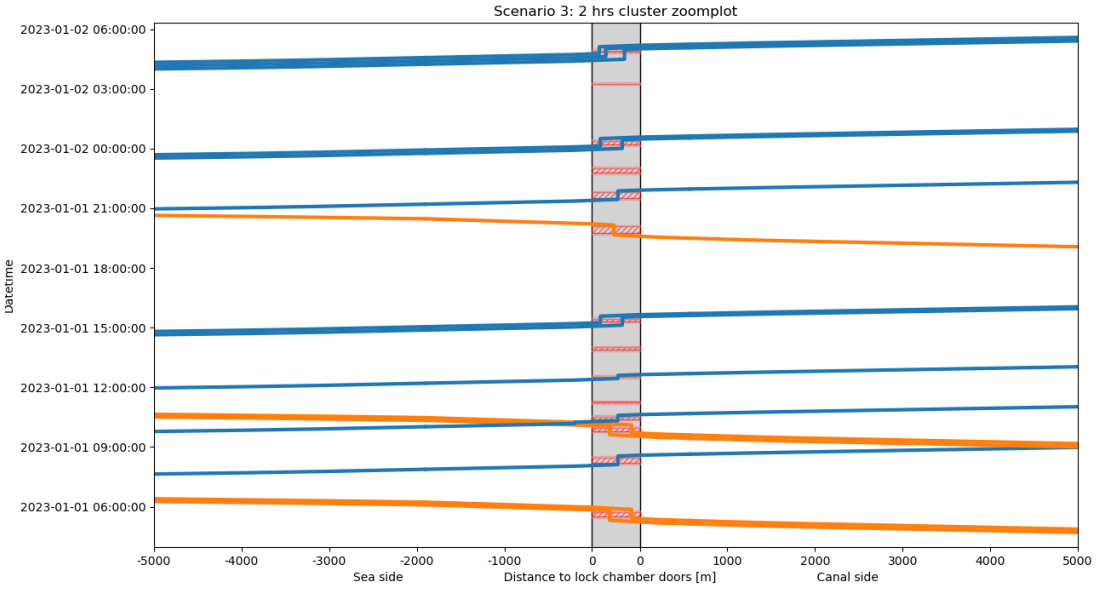

(b) 2 hour clustering

Figure 6.4: OpenTNSim tracking diagram (1 day)

Figure 6.5 illustrates the cumulative salt intrusion and total vessel delay for both the 30-minute and 2-hour clustering strategies. The figure shows that extending the clustering time results in increased vessel waiting times, while simultaneously reducing salt intrusion into the canal. This outcome highlights the central trade-off between logistical efficiency and environmental impact, which the simulation aims to quantify and explore.

The reduction in salt intrusion can be explained by the decrease in the number of locking operations. Fewer locking operations mean fewer instances of lock exchange, which is a major driver of salt in-

trusion into the canal. Although clustering often leads to longer door open times, and therefore nearly complete water exchange during each locking cycle, the decrease in number of lock operations outweighs the disadvantage of longer door openings, resulting in a net reduction of salt intrusion.

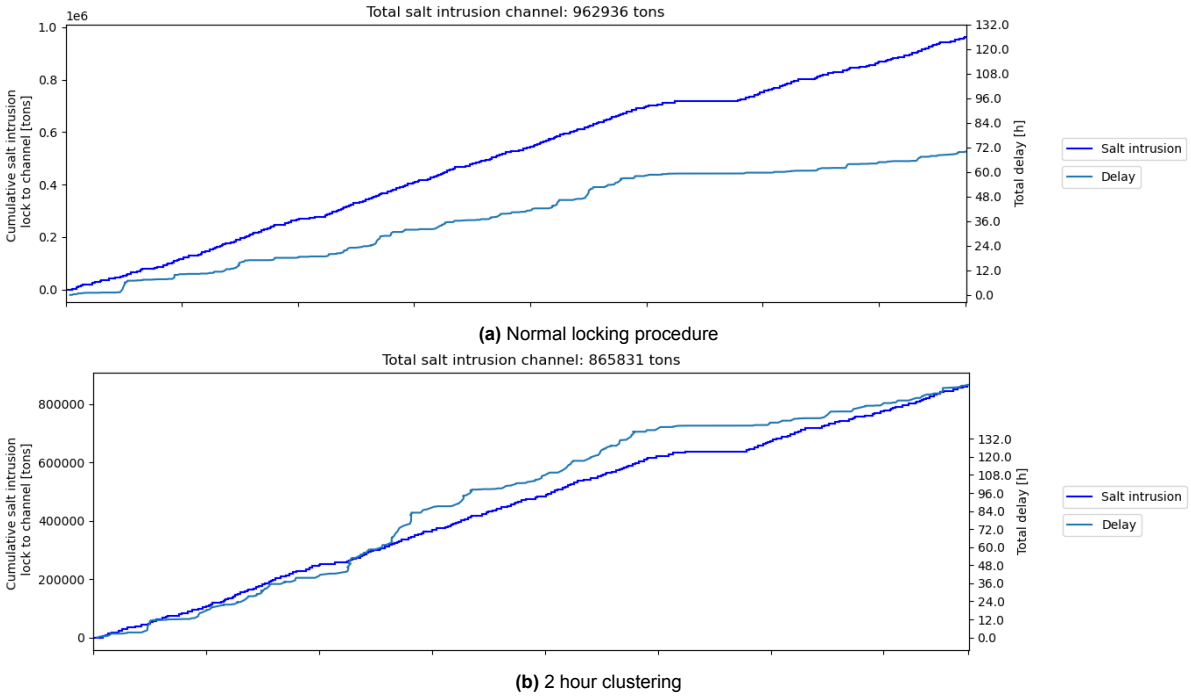

(a) Normal locking procedure

(b) 2 hour clustering

Figure 6.5: Cumulative salt intrusion and total vessel delay

6.2.3. Trade-off curve

The results of the different clustering windows can be combined into a trade-off curve that relates cumulative salt intrusion to total vessel delay. Figure 6.6 illustrates this trade-off for clustering windows ranging from 0 minutes to 6 hours. To capture the full shape of the trade-off curve, additional intermediate clustering windows were included, of which the tracking diagrams and cumulative calculation graphs can also be found in Appendix C. Interestingly, the current operational standard of 30-minute clustering appears to be the most effective at minimizing vessel delays, but it also results in the highest salt intrusion. As the clustering window increases, vessel delay grows, while salt intrusion consistently decreases. This reduction in salt intrusion is mainly due to the decrease in the number of locking operations. Fewer cycles mean fewer instances of saltwater exchange.

One might expect that reducing the clustering time would significantly worsen salt intrusion due to more frequent lock operations. However, even though a clustering window of 0 hours (no clustering), means an increase in the number of locking operations, the door open times are considerably shorter as the doors close immediately after a vessel has entered the lock. In this case, the shorter exposure during each operation outweighs the increased frequency of locking operations, leading to relatively moderate salt intrusion levels.

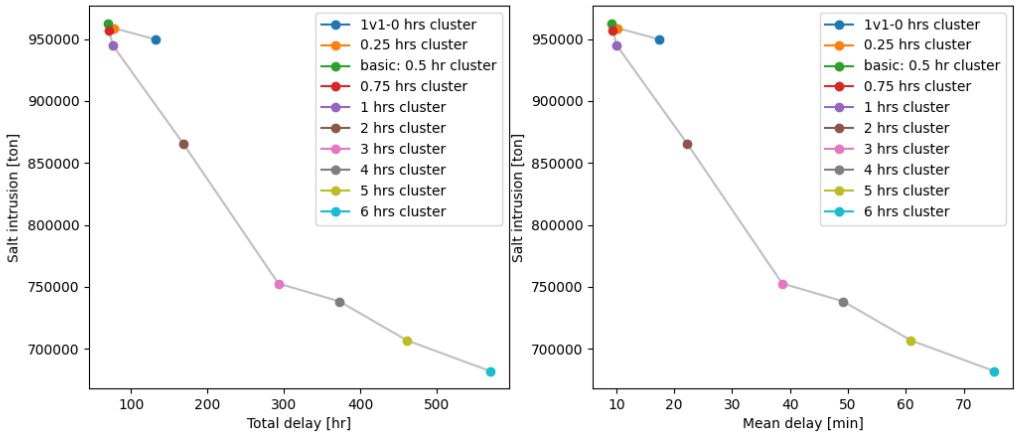

Figure 6.6: Trade-off between salt intrusion and vessel delay, 0-6 hour clustering

6.2.4. Trade-off curve for extreme clustering

The trade-off curve presented above is a valuable tool for identifying the most effective clustering window. However, it is also insightful to examine how extreme clustering durations affect this trade-off. For this reason, clustering windows have been extended up to 36 hours, even though in reality this would not be done. Figure 6.7 shows the trade-off curve for these extended durations and demonstrates that the benefits of increased clustering gradually diminish. Beyond a certain point, further increases in clustering time no longer yield significant reductions in salt intrusion.

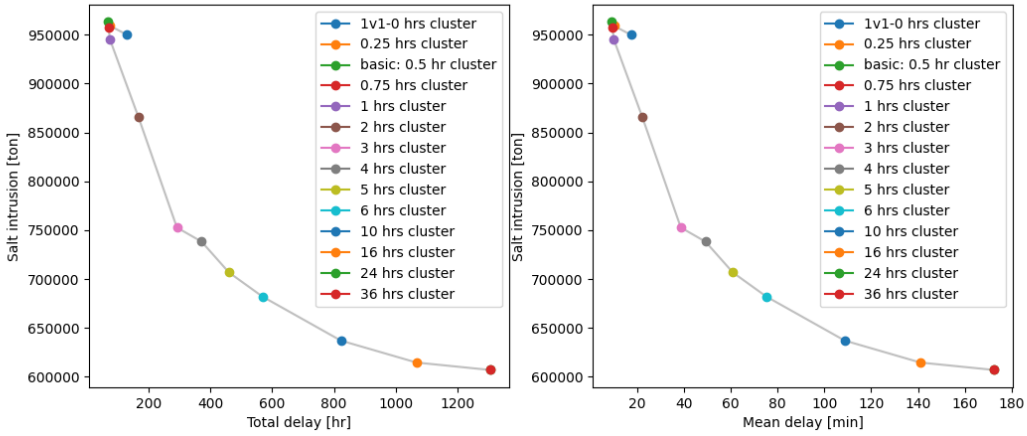

Figure 6.7: Trade-off between salt intrusion and vessel delay, 0-36 hour clustering

This trend is further supported by Figure 6.8, which shows the number of locking operations that include vessels for each clustering window. The figure indicates that beyond a certain clustering duration, the number of operations no longer significantly decreases. This is because, at some point, all feasible vessel combinations that can physically fit within the lock have already been formed. As the clustering window increases, no new vessel groups can be added, and additional cluster time does not result in larger delays. In practice, vessels that are grouped together will proceed with the locking operation as soon as the chamber is full, rather than waiting for the entire clustering window. As a result, many vessels experience little to no effect from further increases in clustering time, limiting the effectiveness of extreme clustering strategies.

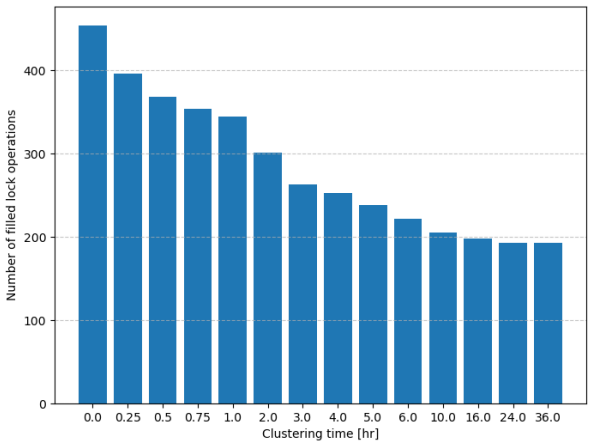

Figure 6.8: Number of vessel filled locking operations per clustering window

6.3. Conclusion

This chapter addressed how the coupled model can be used to compare the effects of alternative locking strategies by linking vessel traffic simulations with a hydrodynamic model for salt intrusion. By simulating various clustering windows, the model quantifies both vessel delays and cumulative salt intrusion, making the trade-off between them explicit.

For the IJmuiden Sea Lock, the trade-off curve shows that short clustering windows minimize vessel delays but result in higher salt loads, while longer clustering windows reduce salt intrusion at the cost of increased waiting times. The current operational standard of 30 minutes emerges as an effective compromise for minimizing delays, yet it also represents the worst case in terms of salt intrusion. Looking at the extreme, very short clustering windows (no clustering) lead to more frequent lock operations but still relatively moderate salt intrusion, as shorter door-open times limit exchange per cycle. Extending clustering beyond practical limits (e.g. >12 hours) yields diminishing returns, since the number of feasible vessel combinations reaches a limit and additional waiting no longer reduces the number of lock operations.

Overall, these results show that clustering can be a practical tool for balancing locking efficiency and water quality at IJmuiden. It helps to evaluate how operational measures perform in practice and supports their gradual implementation, reducing the need for sudden or disruptive restrictions on lock operations.

7

Discussion, conclusion & recommendations

7.1. Discussion

The coupled model provides a valuable framework for exploring the interaction between vessel traffic and salt intrusion. By linking a logistical traffic simulation with a salt exchange model, the system successfully translates vessel passages into quantifiable salt loads. This allows for meaningful comparisons between operational strategies, even if the absolute values carry some uncertainty. The results demonstrate that clustering strategies can significantly influence salt intrusion and vessel delays, and that the trade-off between these two factors can be systematically analysed. Although the model relies on simplifications, it retains enough physical and logistical realism to support strategic decision-making and identify directions for future improvements in lock operation.

Despite the meaningful results, there are some limitations to the model. A key limitation of this study lies in the application of a correction factor to the Zeesluisformulering (ZSF) during the validation phase. While the correction factor serves as a practical workaround to align model outputs with observed salt exchange, it does not address the underlying causes of the discrepancies between measured and simulated values. Specifically, the correction targets the propagation velocity of the exchange current during the door-open phases, where the model was found to deviate most strongly from the measurements. Although this solution improves numerical agreement, it bypasses the physical interpretation of flow processes in the lock. A more robust path forward would involve refining the ZSF formulation itself, potentially by incorporating more accurate representations of exchange dynamics, stratification effects, and transient flow conditions. Until such refinements are made, the model remains strongly tailored to the IJmuiden Sea Lock case, limiting its direct applicability to other lock complexes without location-specific recalibration.

Additionally, the implementation of vessel clustering in OpenTNSim has certain shortcomings. The current model setup does not support side-by-side clustering, nor does it offer a mechanism for defining flexible clustering windows. To simulate desired clustering behaviours, the vessel schedules and configurations had to be manually manipulated. This manipulation may not fully reflect operational constraints or realistic arrival patterns, potentially impacting the generalizability of the results. The deviation from reality is also enhanced by the forced order of clustering that OpenTNSim sustains, disallowing a smaller vessel to cluster in a locking operation if a too large of vessel comes before in arrival order, potentially forcing extra locking operations.

7.2. Conclusion

1. What locking processes take place during the passing of ships through locks and how do they affect the salt intrusion?

The locking cycle can be divided into four key phases, each defined by the opening and closing of lock doors and the levelling of the lock chamber: levelling to the canal, door open at canal, levelling to the sea, door open at sea. Salt intrusion occurs during multiple phases, primarily when the doors are open and during levelling, due to exchange flows and density-driven mechanisms. The passage of vessels influences salt exchange in two ways: it introduces displacement effects during entry and exit, and it determines how frequently locking operations occur and how long the lock doors need to be open at minimum. Operational decisions, such as clustering vessels into a single locking cycle, can reduce the number of operations and thereby limit total salt intrusion, albeit at the cost of increased vessel delay.

2. What models are suitable to quantify the effect of locking strategies on vessel passage and salt intrusion for a real world example, and how can these models be coupled?

To assess the impact of locking strategies on both vessel delays and salt intrusion, models are required that can capture individual vessel behaviour while remaining scalable to large port networks. A mesoscopic traffic model is therefore most suitable, as it balances detail with computational efficiency. For this purpose, OpenTNSim, an open-source, Python-based agent-based traffic model, is selected due to its ability to simulate vessel behaviour at the level of individual ships, its suitability for large-scale simulations, and its ease of integration with salt intrusion models.

On the salt transport side, a schematized salt intrusion model is necessary to simulate many lock operations over long periods without excessive computational demands. The Zeesluisformulering (ZSF) is chosen for this task because it provides a good compromise between physical realism and runtime efficiency. It captures the essential hydrodynamic processes of salt transport during lock cycles and has been shown to match measurements with reasonable accuracy.

The two models are integrated through one-way coupling, where OpenTNSim generates detailed logs of vessel movements and lock operations, including door timings and vessel sequences. These outputs are then used as inputs for the ZSF, which computes the resulting salt exchange per lock operation. This approach allows realistic, traffic-driven assessment of salt intrusion, enabling direct comparison of alternative locking strategies under real-world traffic conditions.

3. How well does the salt intrusion model perform compared to measurements and how can this performance be improved?

The Zeesluisformulering was validated against four weeks of measurement data at the IJmuiden Sea Lock. After an initial increase, the cumulative error in predicted salt intrusion stabilized at approximately 19%, meaning a consistent underestimation of in calculation. Most of the deviation comes from the *door-open phases*, specifically due to inaccuracies in the modelling of the lock exchange.

To mitigate this, a correction factor was applied in the model to artificially increase the exchange current's propagation velocity. A factor of 1.65 was found to yield the best match with observed salt exchange, improving the timing and magnitude of salt intrusion events. However, this correction is empirical and makes the model site-specific, limiting its transferability to other lock systems without recalibration.

4. How can the coupled model be used to compare the effect of alternative locking strategies?

The coupled model allows for systematic evaluation of operational strategies by simulating the impact of different clustering windows on both salt intrusion and vessel delay. By altering the waiting time allowed for clustering, the trade-off between operational efficiency and environmental impact can be explored. Results show that while larger clustering windows reduce salt intrusion by decreasing the number of locking cycles, they also increase vessel delays. The model can quantify this trade-off curve, allowing decision-makers to weigh different priorities and explore the feasibility of more restrictive or flexible operational regimes.

Main research question: How can shipping delays and salt intrusion as a result of locking operations be quantified, to be able to compare the effects of realistic locking strategies?

Shipping delays and salt intrusion resulting from locking operations can be quantified by coupling a mesoscopic vessel traffic model with a schematized salt intrusion model. In this study, OpenTNSim was used to simulate vessel movements and locking sequences with high temporal resolution and across a large fleet, allowing for the assessment of delays at the level of individual ships. To quantify the corresponding salt intrusion, the Zeesluisformulering (ZSF) was used—a simplified yet effective model that estimates salt exchange during each locking phase based on water volumes and salinity differences.

Through one-way coupling, key operational parameters such as levelling durations, door movements, and vessel volumes were extracted from OpenTNSim and used as input for the ZSF. This approach made it possible to evaluate how different locking strategies, such as vessel clustering, affect both cumulative salt intrusion and vessel delays over time. By running strategy scenarios with varied clustering windows, a trade-off curve was developed that shows how operational decisions can reduce salt intrusion at the cost of increased waiting times. Despite some simplifications and the use of a correction factor in the ZSF, this coupled modelling framework enables meaningful comparison of realistic strategies and provides valuable insight into operational impacts on both logistics and saltwater management.

7.3. Recommendations

Based on the findings of this study, several recommendations can be made for future research.
First, the Zeesluisformulering currently relies on a correction factor to align model output with observations. Further research is needed to better understand the physical sources of model inaccuracies. This would enable refinement of the model formulation itself, improving its general accuracy.
Second, the current approach was limited to the IJmuiden Sea Lock, but the methodology could be applied to other lock complexes, either using location-specific correction factors or with an improved ZSF. Application on other locks can help generalize the results.
Third, the implementation of clustering in OpenTNSim could be improved, particularly in how vessel positions within the lock are handled in two dimensions. Side by side clustering allows more automatic and realistic modelling of the cluster behaviour, which would improve simulation accuracy. Also implementing the option to set a clustering window would improve the model as it would need less manipulation to reach the desired clustering behaviour of simulations.
Finally, while this study focused on clustering of vessel as a salt intrusion mitigation measure, the coupled model could also be used to evaluate other mitigation measures such as limiting lock door open times or restricting operational hours.

References

Baart, F., Jiang, M., Bakker, F., van Gijn, M., Frijlink, T., & van Koningsveld, M. (2022, September). *Opentnsim* (Version v1.2.0). Zenodo. https://doi.org/10.5281/zenodo.7053274

Bakker, F. (2025). *Quantifying water transport performance in estuaries: An agent-based method to facilitate system modification trade-offs in multi-stakeholder settings* [Dissertation (TU Delft)]. Delft University of Technology. https://doi.org/10.4233/uuid:1ea910c2-a69c-4b65-a2dd-8570240e8675

Bakker, F., & van Koningsveld, M. (2024). Tool to evaluate countermeasures at locks to limit freshwater losses and saltwater intrusion while minimizing waiting times for shipping. *35th PIANC World Congress 2024: Future Ready Waterborne Transport–Unlocking Africa*, 1558–1563. https://resolver.tudelft.nl/uuid:3188cdf9-5206-4b36-a57c-dd550e0bde5b

Bakker, F., van der Werff, S., Baart, F., Kirichek, A., de Jong, S., & van Koningsveld, M. (2024). Port accessibility depends on cascading interactions between fleets, policies, infrastructure, and hydrodynamics. *Journal of Marine Science and Engineering, 12(6), 1006*. https://doi.org/10.3390/jmse12061006

Bijlsma, R. A., & van der Schelde, T. (2019). *Simulation of waterway infrastructure*. https://www.simio.com/case-studies/simulation-of-waterway-infrastructure/

Buitendijk, M. (2025). *New Lock Terneuzen promises economic benefits*. https://swzmaritime.nl/news/2025/05/02/new-lock-terneuzen-promises-economic-benefits

Cruise Port Amsterdam. (2022). *Adjusted passage regime at ijmuiden sea lock affects calls at cruise port amsterdam*. Retrieved May 23, 2024, from https://sea.cruiseportamsterdam.com/adjusted-passage-regime-at-ijmuiden-sea-lock-affects-calls-at-cruise-port-amsterdam/

de Groot, I., & Vreeken, T. (2016). *Validatierapport wanda-locks, het nieuwe zoutlekmodel* (tech. rep.). Deltares.

Deltares. (2011). *Ontwerpstudie en praktijkproef zoutlekbeperking volkerak sluizen - beschrijvingen resultaten praktijkproef stevin sluis en evaluatie maatregelen stevin sluis.* (tech. rep. No. 1201226-005). Deltares. Delft, The Netherlands.

Deltares. (2019). *Zeesluisformulering* (Version v0.1.3).

Deltares. (2023). *Dichtheidsmetingen zeesluis ijmuiden 2023* (tech. rep.). Arne van der Hout.

Deltares. (2025a). *Delft3d fm suite 2d3d software*. Retrieved June 10, 2025, from https://www.deltares.nl/software-en-data/producten/delft3d-fm-suite

Deltares. (2025b). *Sobek*. Retrieved June 3, 2025, from https://nhi.nu/modelcode/sobek/

IPLO. (2025). *Waqua*. Retrieved June 10, 2025, from https://iplo.nl/thema/water/applicaties-modellen/watermanagementmodellen/waqua/

Jongeling, T. H. G. (2003). *Salt water intrusion analysis panama canal locks: Existing situation. report a: Field data collection, development and validation of simulation model, analysis of salt water intrusion* (Technical Report No. Q3039). WL | Delft Hydraulics.

Jourquin, B. (2022). *Nodus, the transportation network modeling software designed for multimodal and intermodal freight transport*. https://doi.org/10.5281/zenodo.3634540

Kerstma, J., Kolkman, P., Regeling, H., & Venis, W. (1994). *Water quality control at ship locks: Prevention of salt- and fresh water exchange*. AA Balkema.

Kooman, C., & De Bruijn, P. (1975). *Lock capacity and traffic resistance of locks* (tech. rep.). Rijkswaterstaat.

Kortlever, W., van der Hout, A., O'Mahoney, T., de Loor, A., & Wijdenes, T. (2018). Levelling the new sea locks in the netherlands; including the density differences. *PIANC World Congress Panama City*.

MARIN & Deltares. (2025). *Shipma*. Retrieved July 29, 2025, from https://www.marin.nl/en/about/facilities-and-tools/software/shipma

MercoPress. (2024). *Panama canal authority to explore desalinization plant's potential*. Retrieved December 16, 2024, from https://en.mercopress.com/2024/05/01/panama-canal-authority-to-explore-desalinization-plant-s-potential

Merk, O., Busquet, B., & Aronietis, R. (2015). The impact of mega-ships. *International Transport Forum OECD, Paris*.

PIANC. (2021). *Saltwater intrusion mitigation in inland waterways* (tech. rep.). Permanent International Commission for Navigation Congresses (PIANC).

Port of Amsterdam. (2023). *Sea lock: Built for the future*. Retrieved December 18, 2023, from https://www.portofamsterdam.com/en/zeesluis-ijmuiden

Rijkswaterstaat. (1973). *In- en uitvaarttijd van schepen als onderdeel van het schutproces* (tech. rep.). Rijkswaterstaat. https://resolver.tudelft.nl/uuid:270f8ef9-67aa-4b96-83de-36d35498d01c

Rijkswaterstaat. (1986, January). *Beschrijving generatieprogramma voor het algemeen scheepvaart simulatiemodel simdas 05* (tech. rep. No. 185443) (Nota S84.125(52), 12 p.; 30 cm). Ministerie van Verkeer en Waterstaat, Rijkswaterstaat, Dienst Verkeerskunde (RWS, DVK). https://open.rijkswaterstaat.nl/zoeken/@128574/beschrijving-generatieprogramma-algemeen

Rijkswaterstaat. (2021). Operationeel watermanagement amsterdam-rijnkanaal en noordzeekanaal. https://iplo.nl/thema/water/beheer-watersysteem/infographics-operationeel-watermanagement

Rijkswaterstaat. (2022). *Informatiescherm ark-nzk*. Retrieved December 4, 2023, from https://www.arcgis.com/apps/MapSeries/index.html?appid=fd64fe585cd240599360f45458e97f68

Rijkswaterstaat. (2023a). *Selectieve onttrekking bij zeesluis ijmuiden*. Retrieved December 14, 2023, from https://www.rijkswaterstaat.nl/water/projectenoverzicht/selectieve-onttrekking-bij-zeesluis-ijmuiden

Rijkswaterstaat. (2023b). *Sluizencomplex ijmuiden*. Retrieved December 13, 2023, from https://www.rijkswaterstaat.nl/water/waterbeheer/bescherming-tegen-het-water/waterkeringen/dammen-sluizen-en-stuwen/sluizencomplex-ijmuiden

RVW. (2020). *Waterway Guidelines 2020* (tech. rep.). Rijkswaterstaat, Ministerie van Infrastructuur en Waterstaat. https://puc.overheid.nl/rijkswaterstaat/doc/PUC_632307_31/1/

Schotman, A. (2023). Webinar onderzoek zeesluis [Powerpoint Slides].

UNESCO. (1965). Second report of the joint panel on oceanographic tables and standards. *UNESCO technical papers in marine science*, *4*.

UNESCO. (1981). Tenth report of the joint panel on oceanographic tables and standards. *UNESCO technical papers in marine science*, *36*.

United Nations. (2024). *Review of maritime transport 2024: Navigating maritime chokepoints*.

Van Koningsveld, M., Verheij, H., Taneja, P., & De Vriend, H. (2023). *Ports and waterways– navigating the changing world*. Delft University of Technology, Hydraulic engineering, Ports; Waterways, Delft, The Netherlands. Revision no. 1349 logged at 2023-02-08 17:29. https://doi.org/10.5074/T.2021.004

Webuild Worldwide. (2025). *Expansion of the Panama Canal - Third set of locks*. Retrieved July 23, 2025, from https://www.webuildgroup.com/en/projects/dams-hydroelectric-plants/expansion-of-the-panama-canal-third-set-of-locks/

Weiler, O., & Burgers, R. (2018). Zoutindringing door schutsluizen: Overzicht projecten en aanzet formulering t.b.v. netwerkmodellen.

Wijsman, J. (2011, January). Panama canal extension: A review on salt intrusion into gatun lake.

List of Figures

List of Tables

A

ZSF equations overview

This appendix lists all equations used for modelling with the Zeesluisformulering and all input parameters that are needed. For the use of the ZSF in this report all figures have been displayed with the sea side on the left and the canal side of the right as that is how the lock complex in IJmuiden is located. The actual ZSF is however oriented with the canal side to the left and the sea side to the right as to accommodate the river flow in the positive direction from left to right. The equations in this appendix are stated as in the original ZSF and thus salt intrusion is seen as a negative. For the use within the models the salt mass exchange value have been inverted.

A.1. Input parameters

In table A.1, the input parameters of the Zeesluisformulering are listed. Some parameters are predetermined for the IJmijden Sea Lock and are valid in every lock cycle or they have a default value, these values are listed in the last column of the table. Other values are to be determined for each lock cycle or lock cycle phase.

Table A.1: Input parameters for the Zeesluisformulering, with some set values for the IJmuiden Sea Lock

Parameter	Description	Unit	IJmuiden value
L_L	Length of lock chamber	m	545 m
B_L	Width of lock chamber	m	70 m
z_L	Bottom level lock chamber	mNAP	-17.75 mNAP
z_S	Bottom level sea side	mNAP	-18.00 mNAP
z_C	Bottom level canal side	mNAP	-17.50 mNAP
$z_{S,S}$	Bottom level sill sea side	mNAP	-17.00 mNAP
$z_{S,C}$	Bottom level sill canal side	mNAP	-17.00 mNAP
T_{Open}	Door open time	min	
T_{Niv}	Levelling time	min	5 min
$V_{Ship,up}$	Volume of upstream-bounded vessel	m^3	
$V_{Ship,down}$	Volume of downstream-bounded vessel	m^3	
h_C	Water level at canal side	mNAP	
h_S	Water level at sea side	mNAP	
S_C	Salt concentration at canal side	kg/m^3	
S_S	Salt concentration at sea side	kg/m^3	

A.2. Equations

In this subsection, the Zeesluisformulering equations are stated as they are used in the validation model. Some general lock operation and geometrical equations are stated first. Further equations are grouped per lock cycle phase and the needed input parameters per lock cycle are stated.

Beware of the direction of the exchange, positive is regarded as the exchange from the sea toward the canal.

A.2.1. General equations

Lock volume at levelled situation with sea:

$$V_{L,S} = L_L B_L (h_S - z_L) \quad [m^3] \quad (A.1)$$

Lock volume at levelled situation with canal:

$$V_{L,C} = L_L B_L (h_C - z_L) \quad [m^3] \quad (A.2)$$

Effective depth of lock entrance at levelled situation with sea:

$$H_{S,Eff} = (h_S - z_{S,S}) + 0.2\text{min}(z_{S,S} - z_S; z_{S,S} - z_L) \quad [m] \quad (A.3)$$

Effective depth of lock entrance at levelled situation with canal:

$$H_{C,Eff} = (h_C - z_{C,S}) + 0.2\text{min}(z_{C,S} - z_C; z_{C,S} - z_L) \quad [m] \quad (A.4)$$

Average water density over the lock complex:

$$\overline{\rho_{CS}} = 1000 + 0.8\left(\frac{S_C + S_S}{2}\right) \quad [kg/m^3] \quad (A.5)$$

A.2.2. Levelling to canal

LW1: Low water at sea

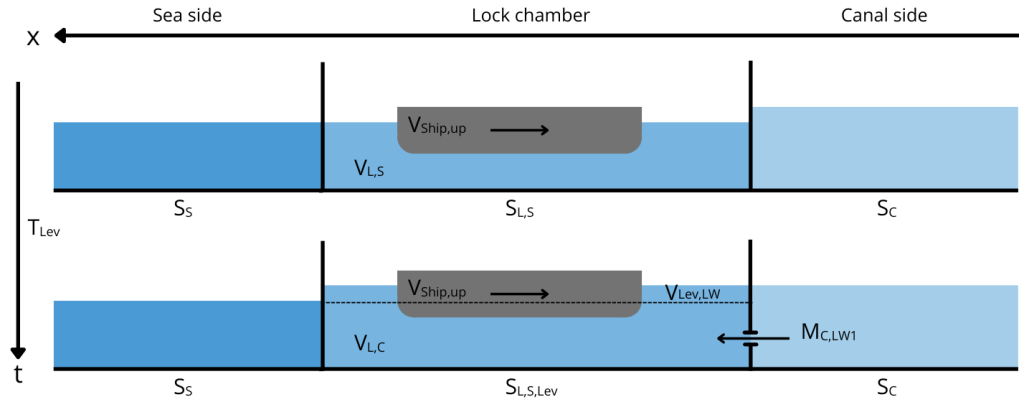

Figure A.1: ZSF LW1: Levelling to canal, low water

Levelling volume:

$$V_{Lev,LW} = L_L B_L (h_C - h_S) \quad [m^3] \quad (A.6)$$

$$V_{Lev,HW} = 0 \quad [m^3] \quad (A.7)$$

Mass exchange of salt from canal to lock chamber after levelling to the canal:

$$M_{C,LW1} = V_{Lev,LW} S_C \quad [kg] \quad (A.8)$$

Lock chamber salt concentration after levelling to the canal:

$$S_{L,S,Lev} = \frac{S_{L,S}(V_{L,S} - V_{Ship,up}) + M_{C,LW1}}{V_{L,C} - V_{Ship,up}} \quad [kg/m^3] \quad (A.9)$$

HW1: High water at sea

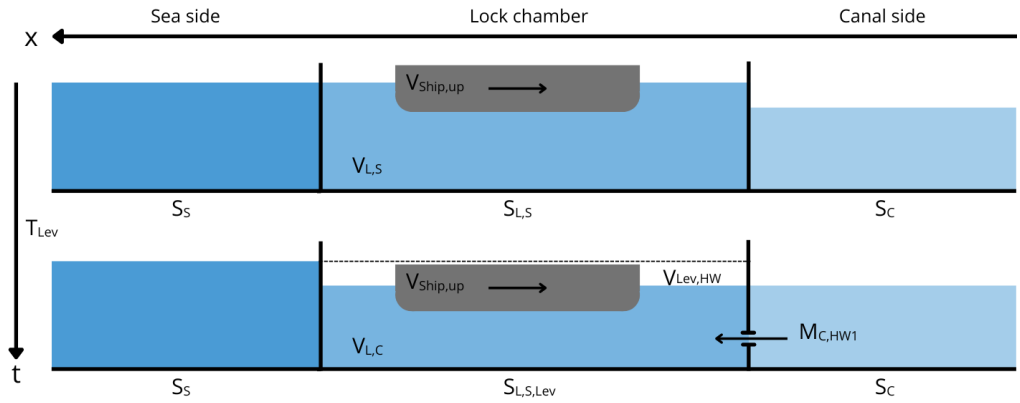

Figure A.2: ZSF HW1: Levelling to canal, high water

Levelling volume:

$$V_{Lev,LW} = 0 \quad [\text{m}^3] \quad \text{(A.10)}$$

$$V_{Lev,HW} = L_L B_L (h_S - h_C) \quad [\text{m}^3] \quad \text{(A.11)}$$

Mass exchange of salt from canal to lock chamber after levelling to the canal:

$$M_{C,HW1} = -V_{Lev,HW} S_S \quad [\text{kg}] \quad \text{(A.12)}$$

Lock chamber salt concentration after levelling to the canal:

$$S_{L,S,Lev} = S_{L,S} \quad [\text{kg/m}^3] \quad \text{(A.13)}$$

Total

Total mass exchange of salt from canal to lock chamber after levelling to the canal:

$$M_{C,1} = V_{Lev,LW} S_C - V_{Lev,HW} S_{L,S} \quad [\text{kg}] \quad \text{(A.14)}$$

A.2.3. Door open phase canal

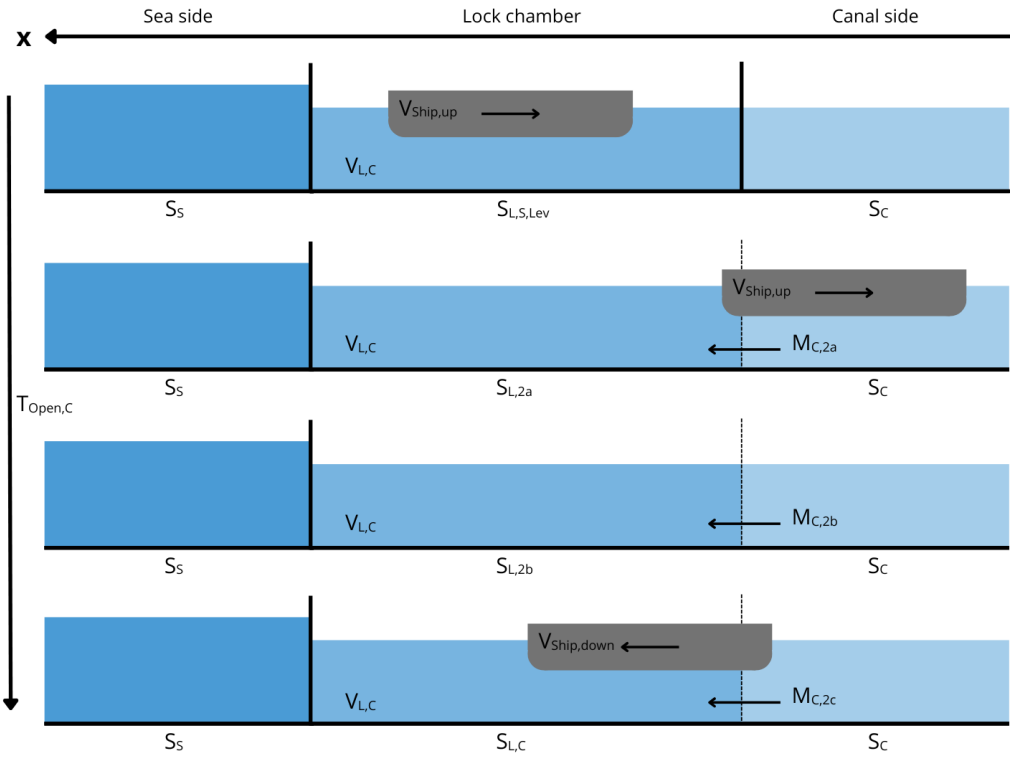

Figure A.3: ZSF LW2/HW2: Door open canal

Exiting vessels

Mass exchange of salt from canal to lock chamber after vessels exit the lock toward the canal:

$$M_{M,2a} = V_{Ship,up} S_M \quad \text{[kg]} \quad \text{(A.15)}$$

Lock chamber salt concentration after vessels exit the lock:

$$S_{L,2a} = \frac{S_{L,S,Niv}\left(V_{L,M} - V_{Ship,up}\right) + M_{M,2a}}{V_{L,M}} \quad \text{[kg/m}^3\text{]} \quad \text{(A.16)}$$

Exchange current

Propagation velocity of the exchange current during open doors at the canal:

$$c_{i,M} \approx \frac{1}{2}\sqrt{g\frac{0.8\left(S_{L,2a} - S_M\right)}{\overline{\rho_{CS}}} H_{C,Eff}} \quad \text{[m/s]} \quad \text{(A.17)}$$

Time required for exchange current to fully exchange during open doors at the canal:

$$T_{LE,C} = \frac{2L_L}{c_{i,C}} \quad \text{[s]} \quad \text{(A.18)}$$

Effective depth of lock entrance at levelled situation with canal:

$$H_{C,Eff} = (h_C - z_{D,C}) + 0.2\text{min}(z_{D,C} - z_{V,C}; z_{D,C} - z_L) \quad \text{[m]} \quad \text{(A.19)}$$

Effective lock volume at levelled situation with canal:

$$V_{L,C,Eff} = L_L B_L H_{C,Eff} \quad \text{[m}^3\text{]} \quad \text{(A.20)}$$

Volume of exchange current during open doors at the canal:

$$V_{U,C} = V_{L,C,Eff} \cdot \tanh\left(\eta \frac{T_{Open,C}}{T_{LE,C}}\right) \quad [m^3] \quad (A.21)$$

Mass exchange of salt from canal to lock chamber due to salt exchange during open doors at the canal:

$$M_{C,2b,LE} = S_M \cdot V_{U,C} - S_{L,2a} \cdot V_{U,C} \quad [kg] \quad (A.22)$$

Lock chamber salt concentration after exchange current during open doors at the canal:

$$S_{L,2b} = \frac{S_{L,2a} \cdot K_{L,C} + M_{C,2b,LE}}{V_{L,C}} \quad [kg/m^3] \quad (A.23)$$

Entering vessels

Mass exchange of salt from canal to lock chamber after vessels enter the lock from the canal:

$$M_{C,2c} = -V_{Ship,down} S_C \quad [kg] \quad (A.24)$$

Lock chamber salt concentration after vessels enter the lock:

$$S_{L,C} = \frac{S_{L,2b} V_{L,C} + M_{C,2c}}{V_{L,C} - V_{Ship,down}} \quad [kg/m^3] \quad (A.25)$$

Total

Total mass exchange of salt from canal to lock chamber during open doors at the canal:

$$M_{C,2} = M_{C,2a} + M_{C,2b,LE} + M_{C,2c} \quad [kg] \quad (A.26)$$

A.2.4. Levelling to sea

LW3: Low water at sea

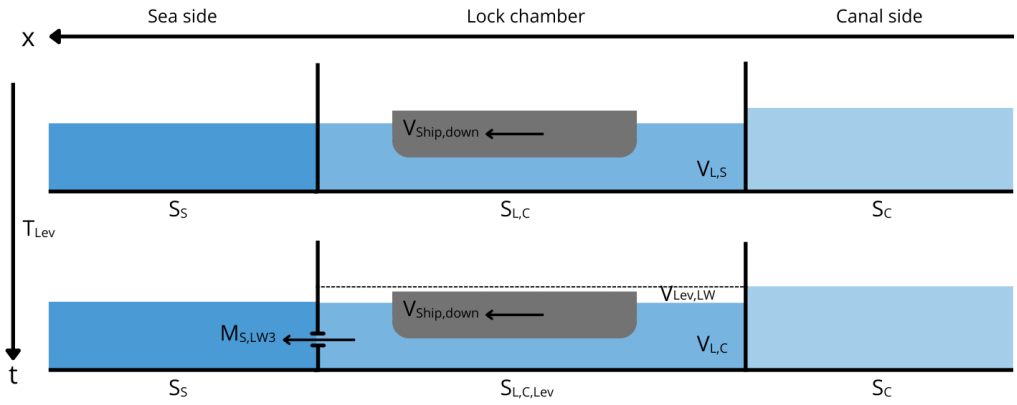

Figure A.4: ZSF LW3: Levelling to sea, low water

Levelling volume:

$$V_{Niv,LW} = L_L B_L (h_C - h_S) \quad m^3] \quad (A.27)$$

$$V_{Niv,HW} = 0 \quad [m^3] \quad (A.28)$$

Mass exchange of salt from lock chamber to sea after levelling to the sea:

$$M_{L,LW3} = V_{Niv,LW} S_{L,C} \quad [kg] \quad (A.29)$$

Lock chamber salt concentration after levelling to the sea:

$$S_{L,C,Niv} = S_{L,C} \quad [kg/m^3] \quad (A.30)$$

HW3: High water at sea

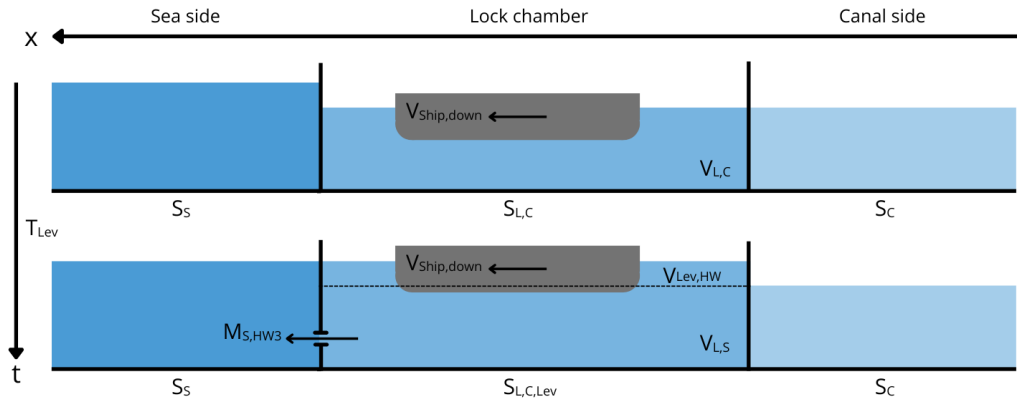

Figure A.5: ZSF HW3: Levelling to sea, high water

Levelling volume:

$$V_{Niv,LW} = 0 \quad [m^3] \quad (A.31)$$

$$V_{Niv,HW} = -L_L B_L (h_S - h_C) \quad [m^3] \quad (A.32)$$

Mass exchange of salt from lock chamber to sea after levelling to the sea:

$$M_{S,HW3} = -V_{Niv,HW} S_S \quad [kg] \quad (A.33)$$

Lock chamber salt concentration after levelling to the sea:

$$S_{L,C,Niv} = \frac{S_{L,C}\left(V_{L,C} - V_{Ship,down}\right) - M_{S,HW3}}{V_{L,S} - V_{Ship,down}} \quad [kg/m^3] \quad (A.34)$$

Total

Total mass exchange of salt from lock chamber to sea after levelling to the sea:

$$M_{S,3} = V_{Niv,LW} S_{L,C,Niv} - V_{Niv,HW} S_S \quad [kg] \quad (A.35)$$

A.2.5. Door open phase sea

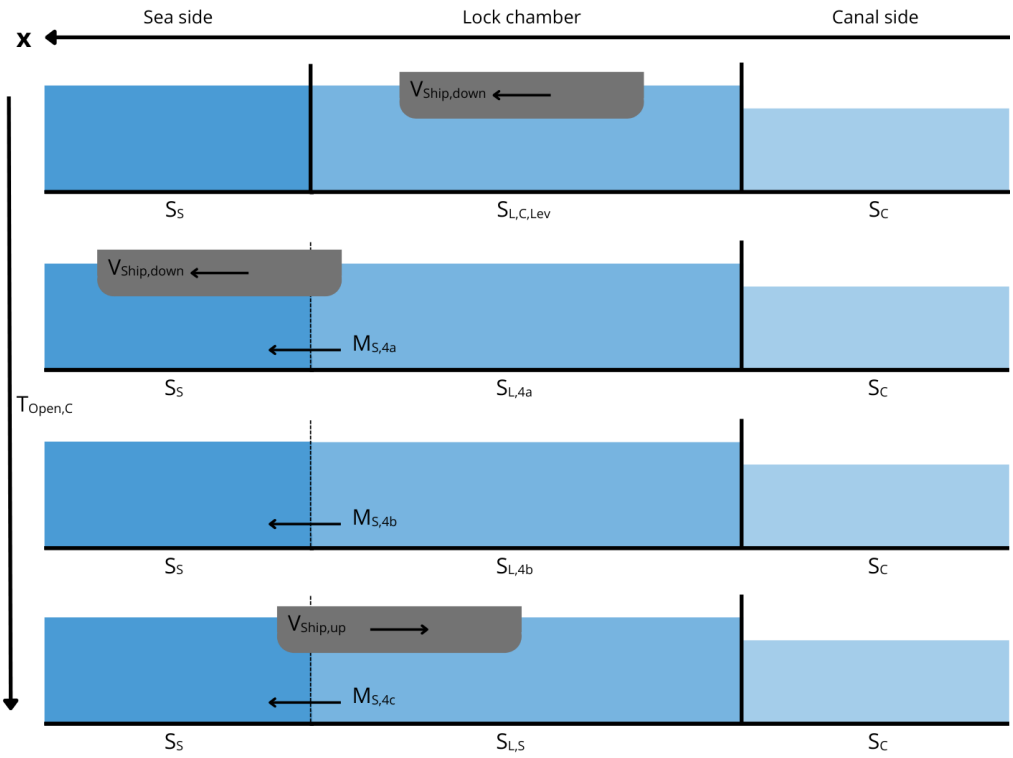

Figure A.6: ZSF LW4/HW4: Door open sea

Exiting vessels

Mass exchange of salt from lock chamber to canal after vessels exit the lock toward the sea:

$$M_{S,4a} = -V_{Ship,down} S_S \quad \text{[kg]} \quad \text{(A.36)}$$

Lock chamber salt concentration after vessels exit the lock:

$$S_{L,4a} = \frac{S_{L,C,Niv}\left(V_{L,S} - V_{Ship,down}\right) - M_{S,4a}}{V_{L,S}} \quad \text{[kg/m}^3\text{]} \quad \text{(A.37)}$$

Exchange current

Propagation velocity of the exchange current during open doors at sea:

$$c_{i,S} \approx \frac{1}{2}\sqrt{g\frac{0.8\left(S_S - S_{L,4a}\right)}{\overline{\rho_{CS}}} H_{S,Eff}} \quad \text{[m/s]} \quad \text{(A.38)}$$

Effective depth of lock entrance at levelled situation with sea:

$$H_{S,Eff} = \left(h_S - z_{D,S}\right) + 0.2\text{min}\left(z_{D,S} - z_{V,S}; z_{D,S} - z_L\right) \quad \text{[m]} \quad \text{(A.39)}$$

Effective length of lock at levelled situation with sea:

$$L_{L,Eff} = L_L \frac{h_S - z_L}{H_{S,Eff}} \quad \text{[m]} \quad \text{(A.40)}$$

Time required for exchange current to fully exchange during open doors at sea:

$$T_{LE,S} = \frac{2L_{L,Eff}}{\eta c_{i,S}} \quad \text{[s]} \qquad \text{(A.41)}$$

Effective lock volume at levelled situation with sea:

$$V_{L,S,Eff} = L_{L,Eff} B_L H_{S,Eff} \quad \text{[m}^3\text{]} \qquad \text{(A.42)}$$

Volume of exchange current during open doors at sea:

$$V_{U,S} = V_{L,S,Eff} \cdot \tanh\left(\eta \frac{T_{Open,S}}{T_{LE,S}}\right) \quad \text{[m}^3\text{]} \qquad \text{(A.43)}$$

Mass exchange of salt from lock chamber to sea due to salt exchange during open doors at sea:

$$M_{S,4b,LE} = V_{U,S} S_{L,4a} - V_{U,S} S_S \quad \text{[kg]} \qquad \text{(A.44)}$$

Lock chamber salt concentration after exchange current during op doors at the canal:

$$S_{L,4b} = \frac{S_{L,4a} V_{L,S} - M_{S,4b,LE}}{V_{L,S}} \quad \text{[kg/m}^3\text{]} \qquad \text{(A.45)}$$

Entering vessels

Mass exchange of salt from the lock chamber to sea after vessels enter the lock from the sea:

$$M_{S,4c} = V_{Ship,up} S_{L,4b} \quad \text{[kg]} \qquad \text{(A.46)}$$

Lock chamber concentration after vessels enter the lock:

$$S_{L,S} = \frac{V_{L,S} S_{L,4b} - M_{S,4c}}{V_{L,S} - V_{Ship,up}} \quad \text{[kg/m}^3\text{]} \qquad \text{(A.47)}$$

Total

Total mass exchange of salt from lock chamber to sea during open doors at sea:

$$M_{S,4} = M_{S,4a} + M_{S,4b,LE} + M_{S,4c} \quad \text{[kg]} \qquad \text{(A.48)}$$

B

Extra ZSF validations graphs

B.1. Full lock cycles

This appendix section hold the full lock cycle figures. Due to the extensive number of locking cycles, namely 118, only 3 will be presented in this document. The complete set of figures is provided as a supplementary appendix.

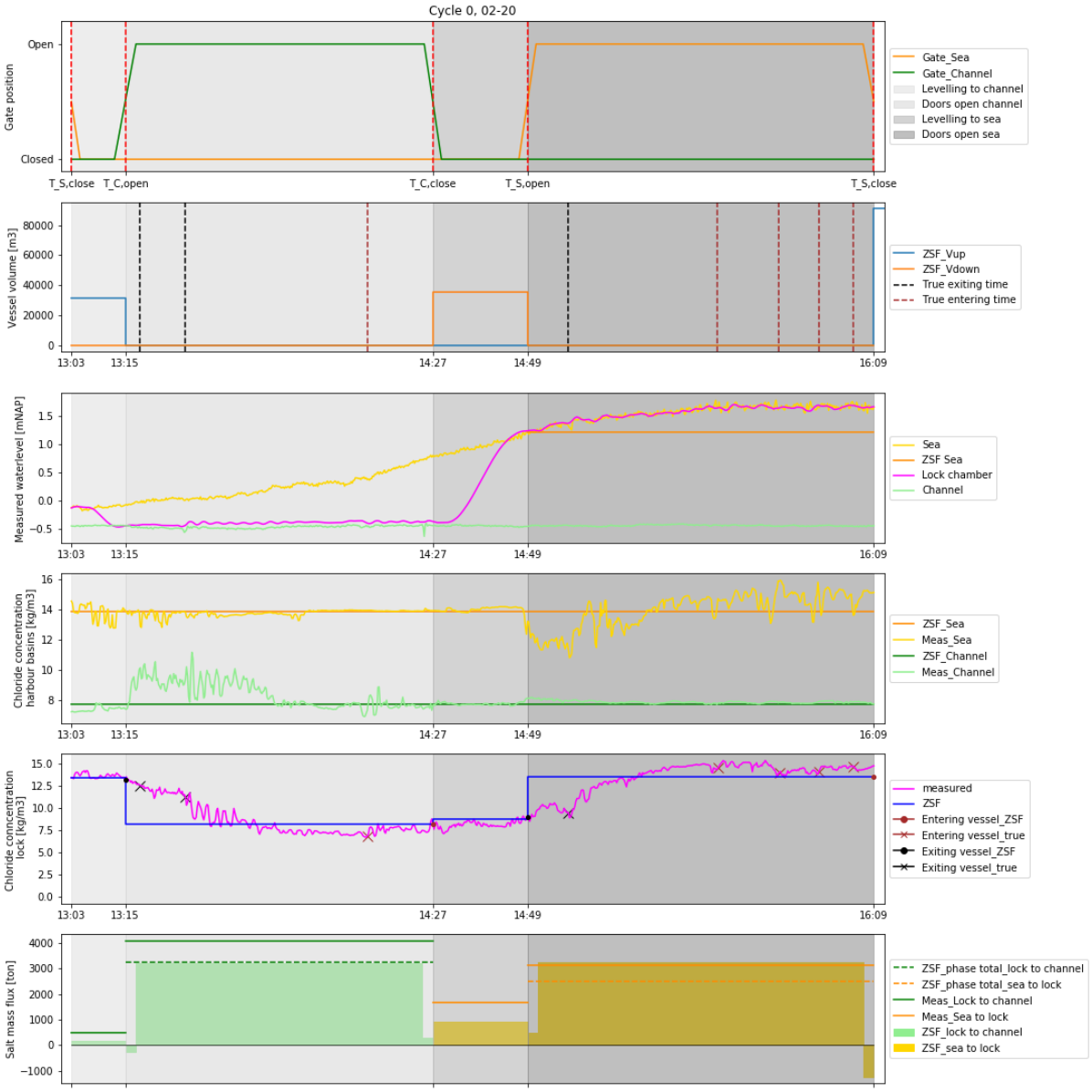

Figure B.1: Full cycle 0

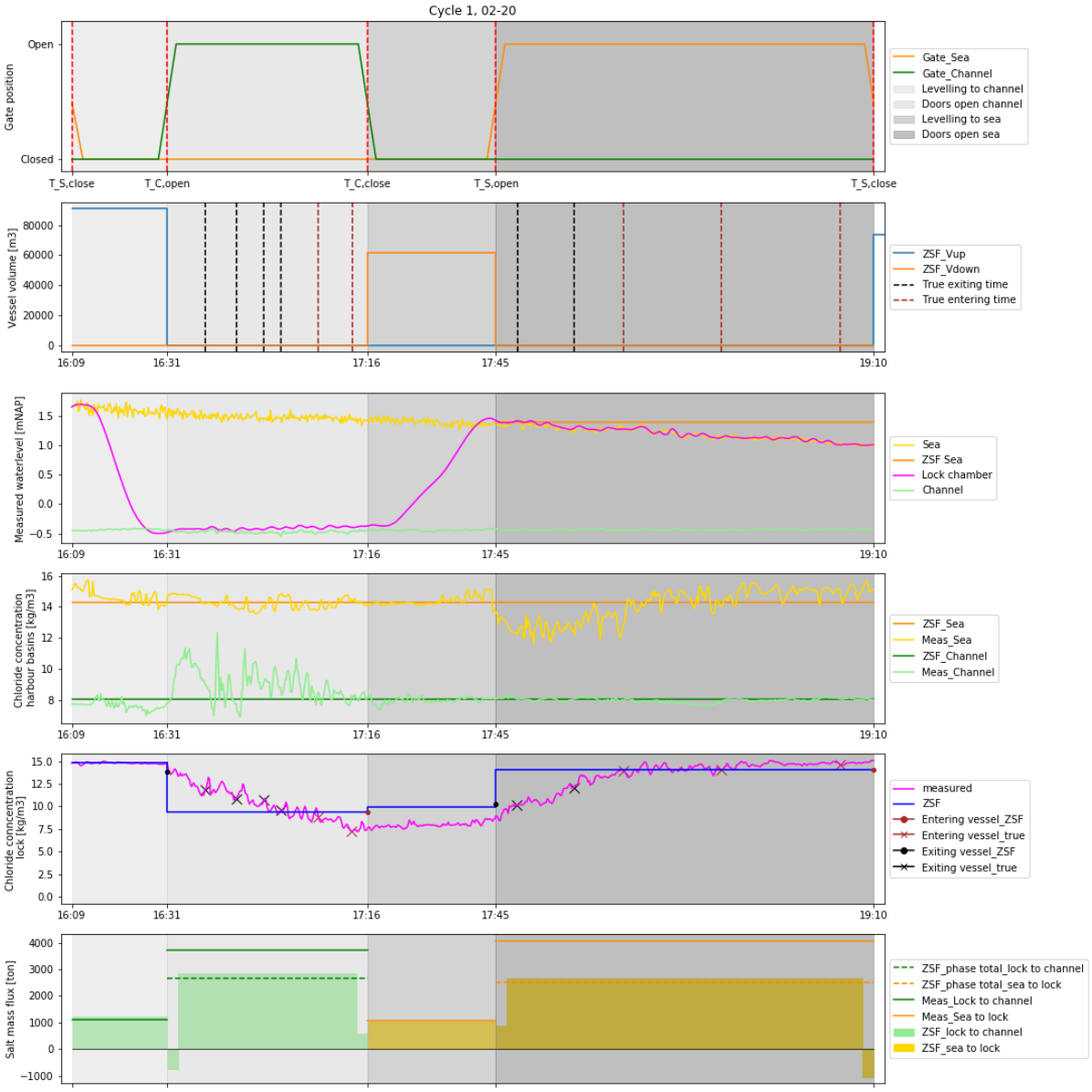

Figure B.2: Full cycle 1

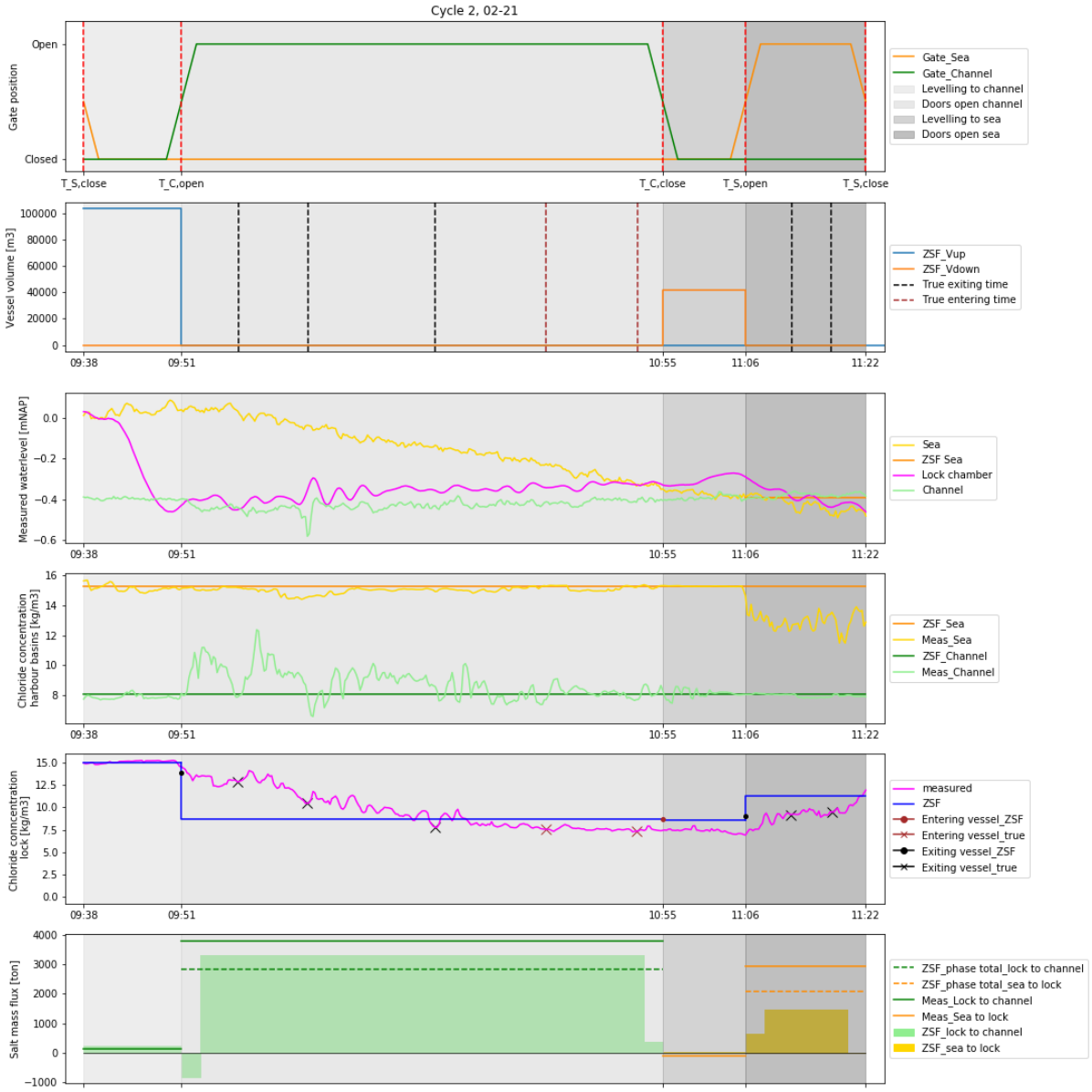

Figure B.3: Full cycle 2

B.2. Parameters

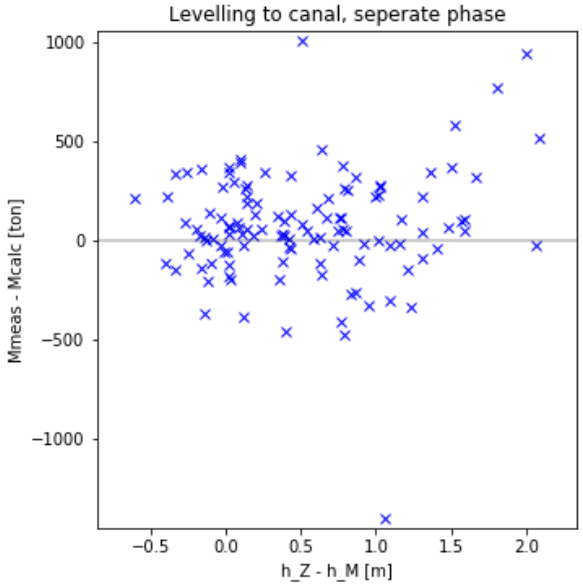

Figure B.4: Water level difference, levelling to canal

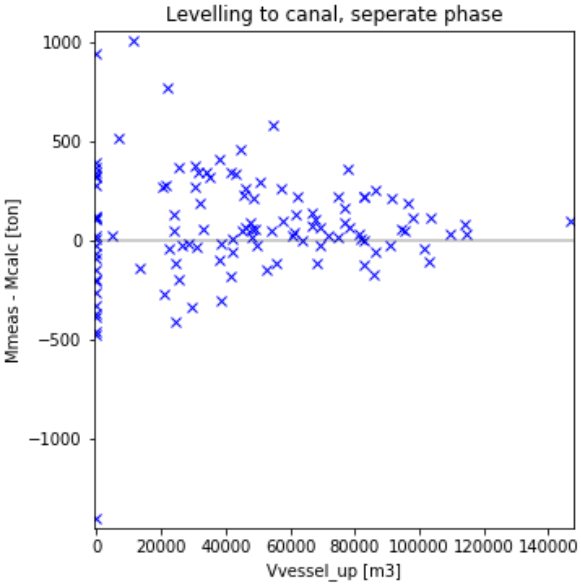

Figure B.5: Vessel volume, levelling to canal

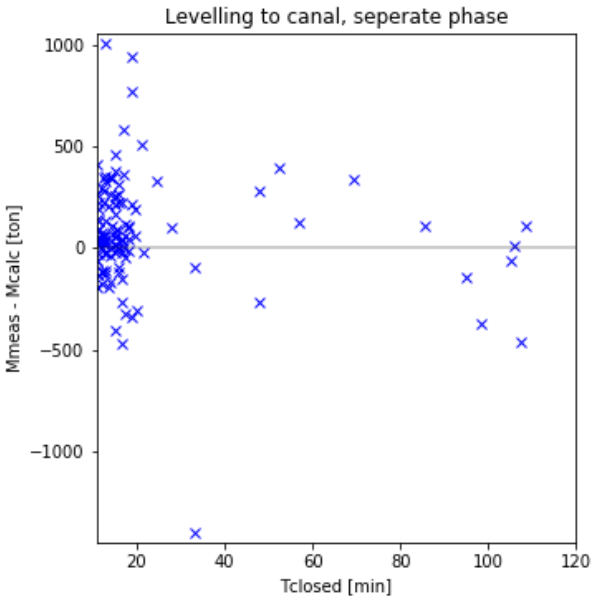

Figure B.6: Door closed time, levelling to canal

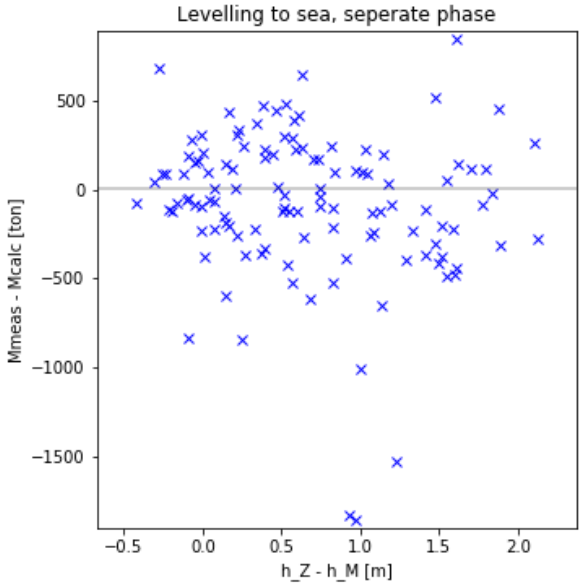

Figure B.7: Water level difference, levelling to sea

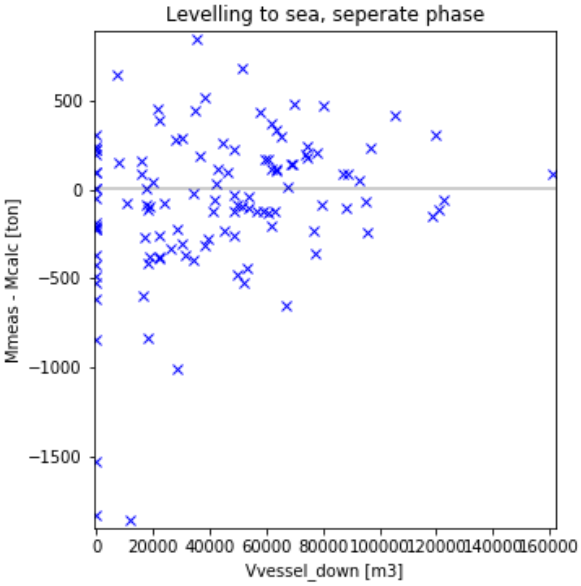

Figure B.8: Vessel volume, levelling to sea

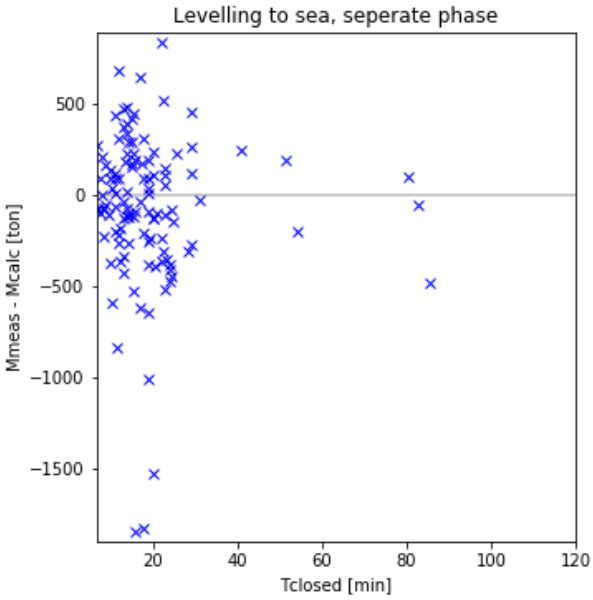

Figure B.9: Door closed time, levelling to sea

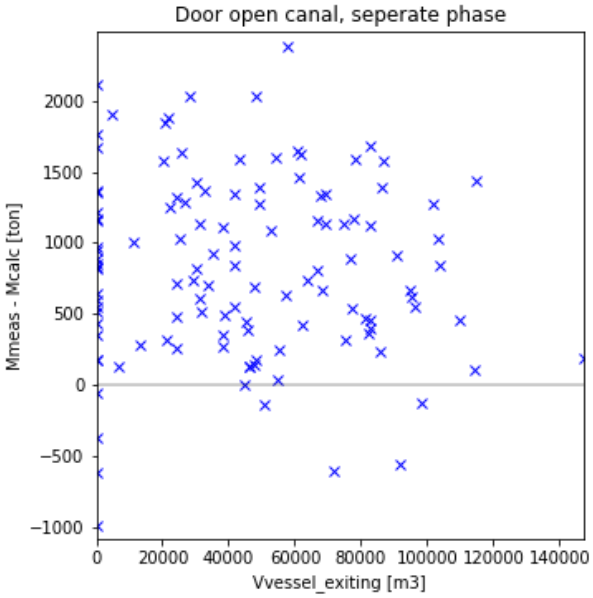

Figure B.10: Exiting vessel volume, door open canal

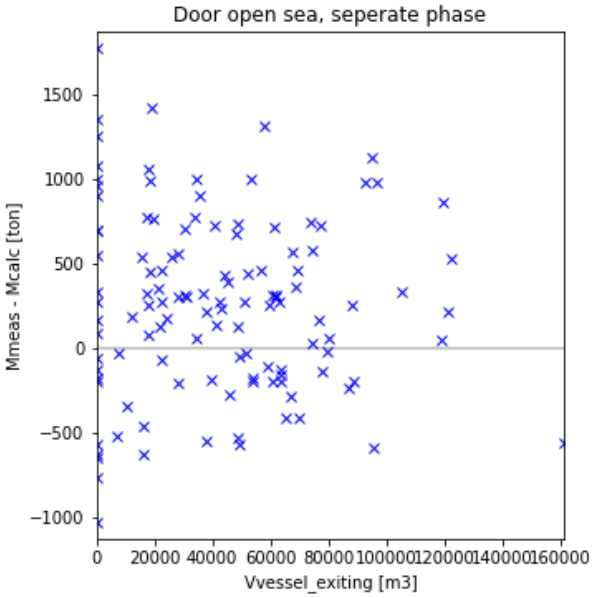

Figure B.11: Exiting vessel volume, door open sea

B.3. Harbour basin salt concentration variations

Figure B.12 illustrates the ZSF modelling during the full campaign period. The plot in Figure B.12a indicates the variations of the field measurement salt concentration: the rolling mean, the rolling median, the averaged rolling mean, the averaged rolling median; as well as the field data itself. As can be seen in Figure B.12b, using the rolling mean and averaged rolling mean result in the most accurate cumulative salt intrusion. Even though the averaged rolling mean results in a slightly larger error, this is the harbour basin salt concentration chosen to continue with. This is because when predicting the salt intrusion with the ZSF model, there is no influence of the harbour concentrations taken into account and thus a constant value is more realistic to have to work with.

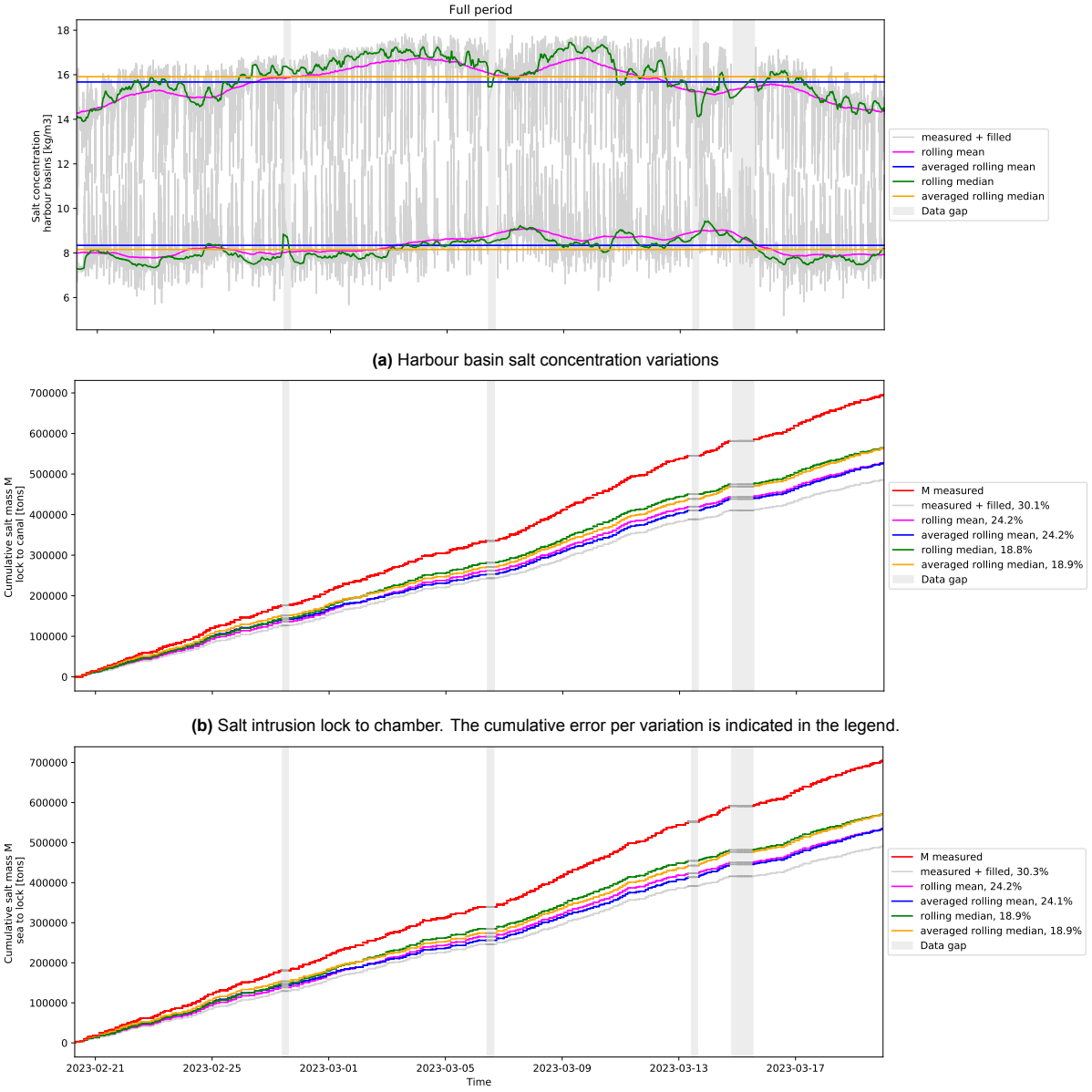

(a) Harbour basin salt concentration variations

(b) Salt intrusion lock to chamber. The cumulative error per variation is indicated in the legend.

(c) Salt intrusion sea to lock. The cumulative error per variation is indicated in the legend.

Figure B.12: Full period cumulative salt intrusion for variations of salt concentrations.

C

Locking strategies

This appendix contains the tracking diagrams and salt intrusion-vessel delay results of all clustering windows from Chapter 6.

Normal locking procedure - 30 minute clustering

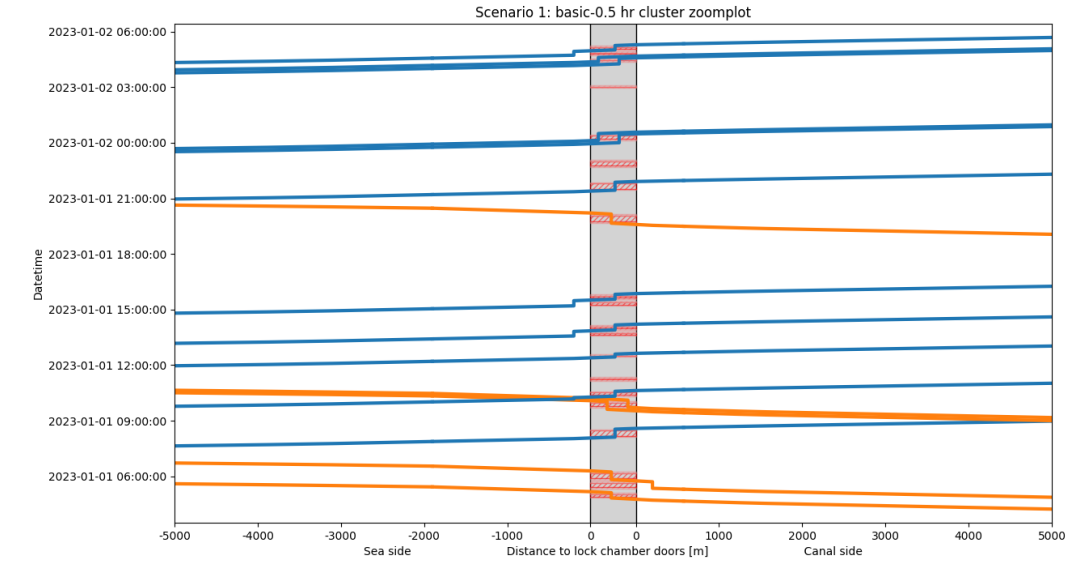

(a) Tracking diagram

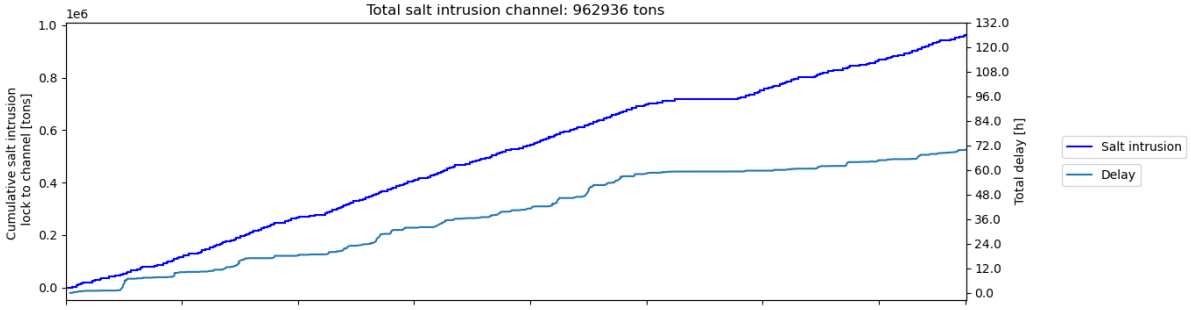

(b) Cumulative salt intrusion and total vessel delay

Figure C.1: Normal locking procedure - OpenTNSim and ZSF calculations

no clustering - 0 hours

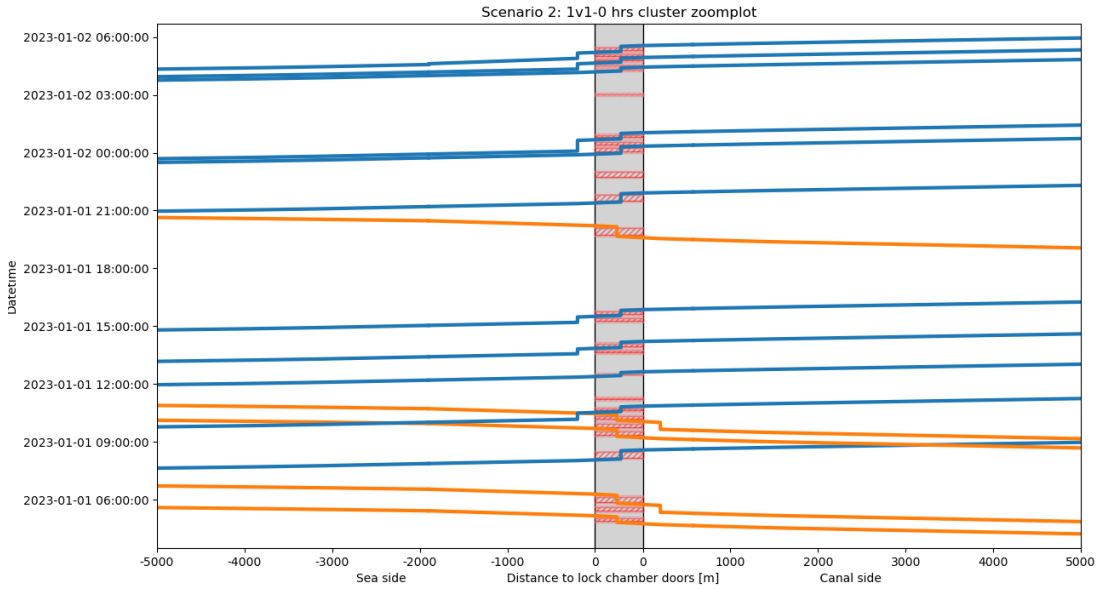

(a) Tracking diagram

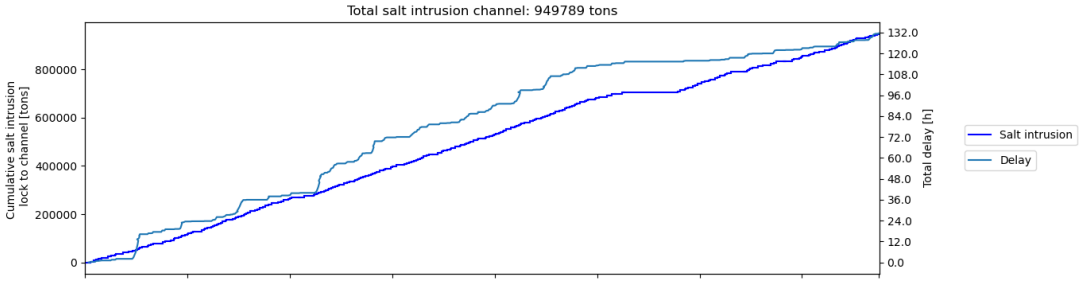

(b) Cumulative salt intrusion and total vessel delay

Figure C.2: No clustering - OpenTNSim and ZSF calculations

2 hour clustering

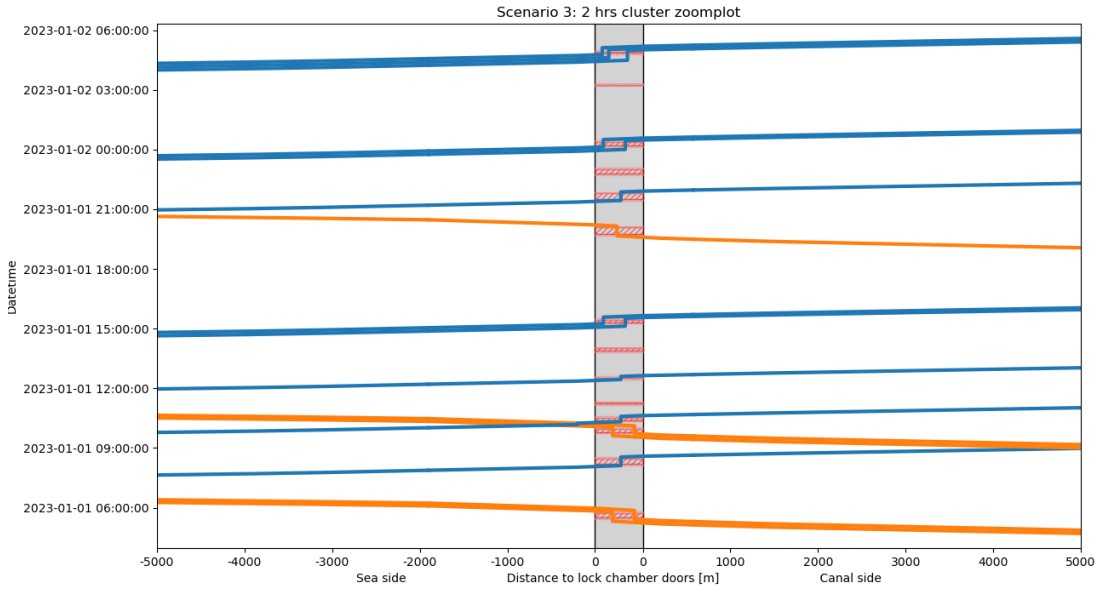

(a) Tracking diagram

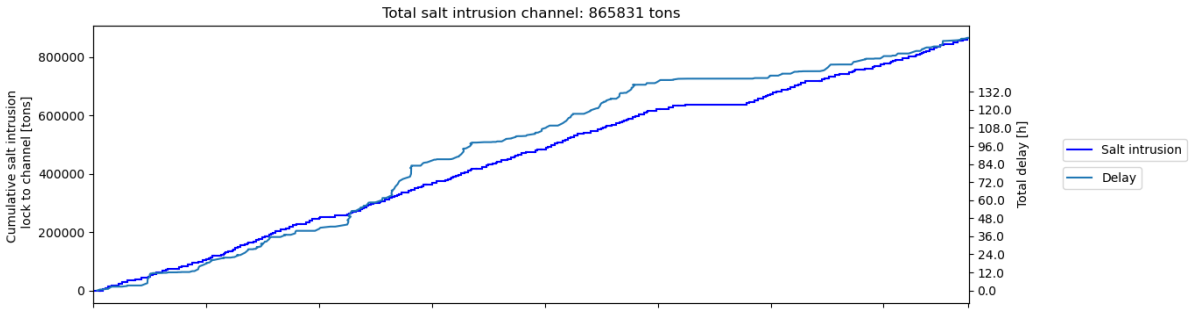

(b) Cumulative salt intrusion and total vessel delay

Figure C.3: 2 hour clustering - OpenTNSim and ZSF calculations

4 hour clustering

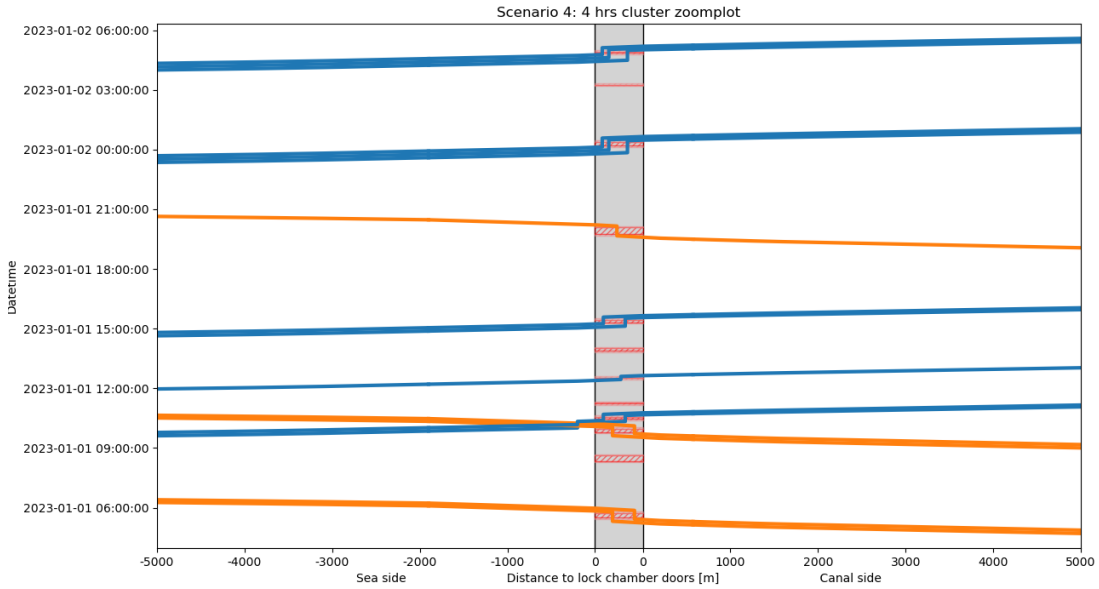

(a) Tracking diagram

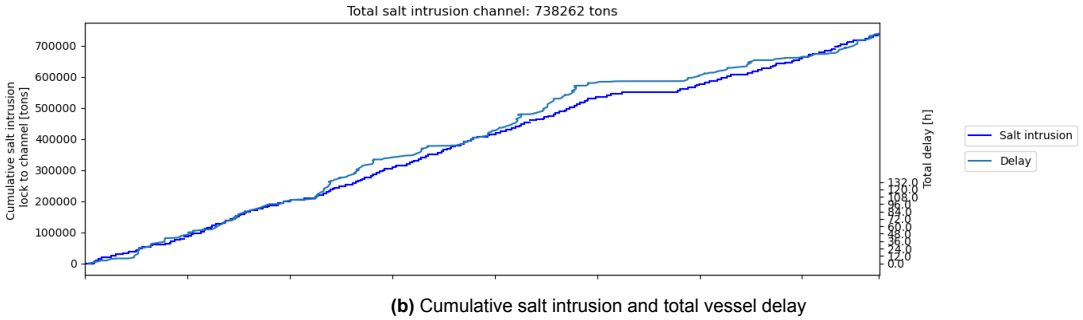

(b) Cumulative salt intrusion and total vessel delay

Figure C.4: 4 hour clustering - OpenTNSim and ZSF calculations

6 hour clustering

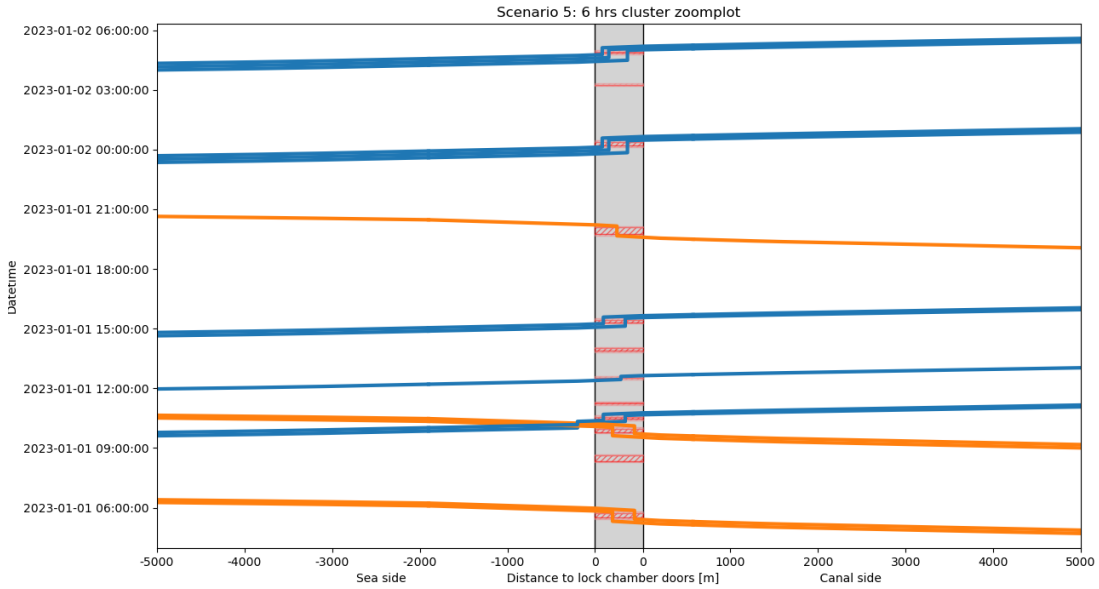

(a) Tracking diagram

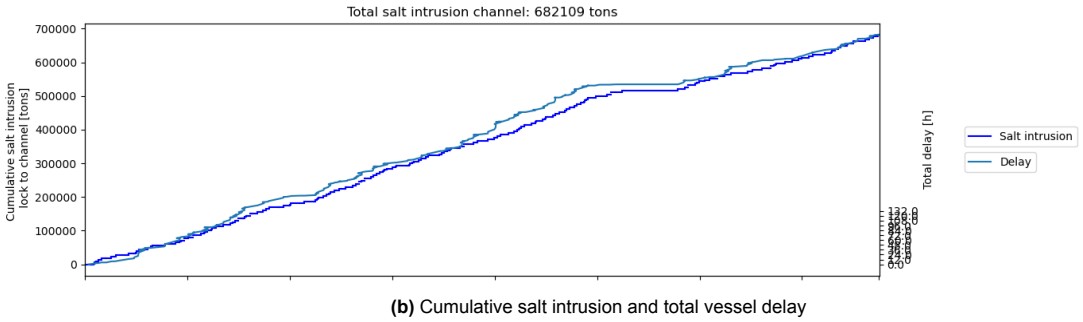

(b) Cumulative salt intrusion and total vessel delay

Figure C.5: 6 hour clustering - OpenTNSim and ZSF calculations

1 hour clustering

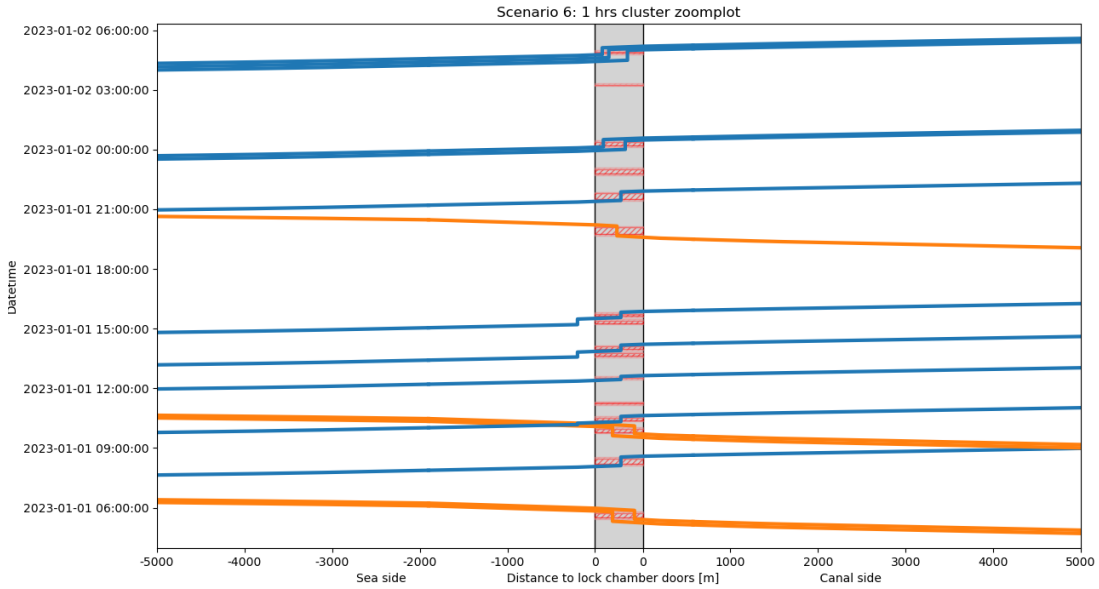

(a) Tracking diagram

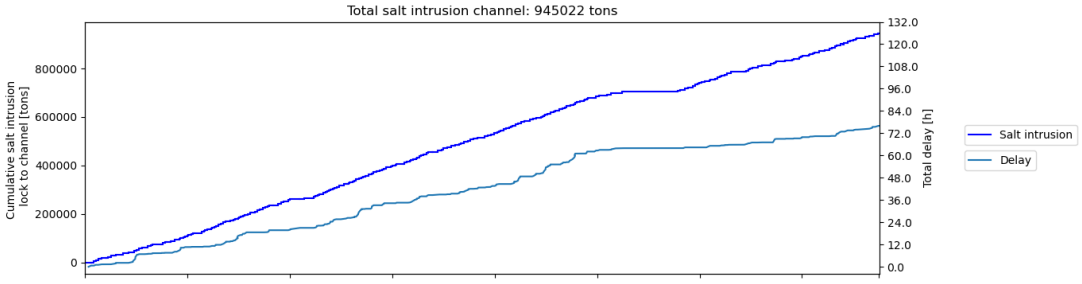

(b) Cumulative salt intrusion and total vessel delay

Figure C.6: 1 hour clustering - OpenTNSim and ZSF calculations

15 minute clustering

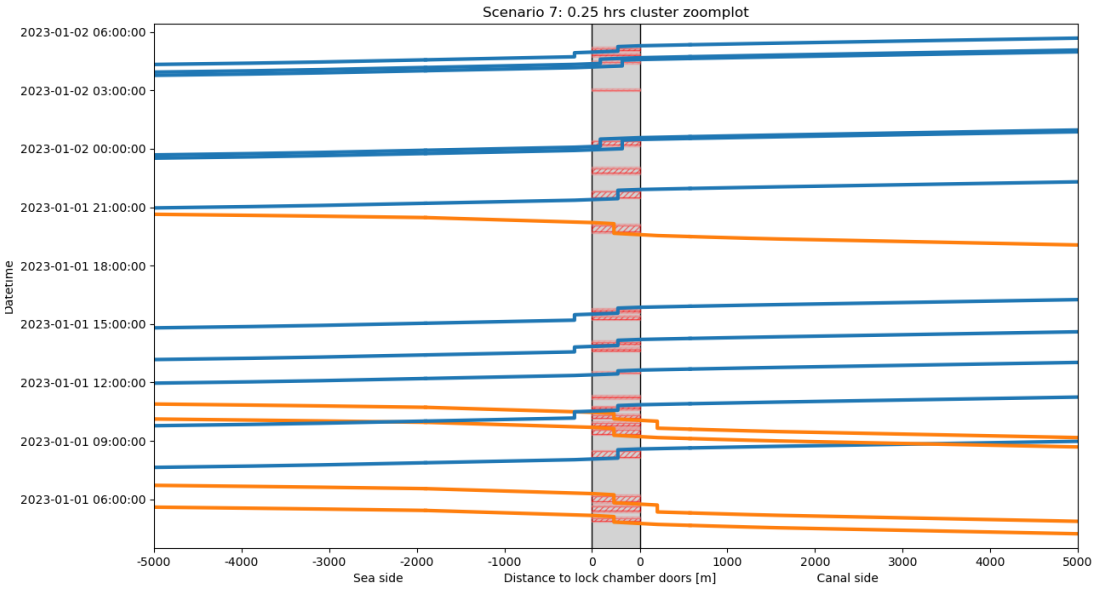

(a) Tracking diagram

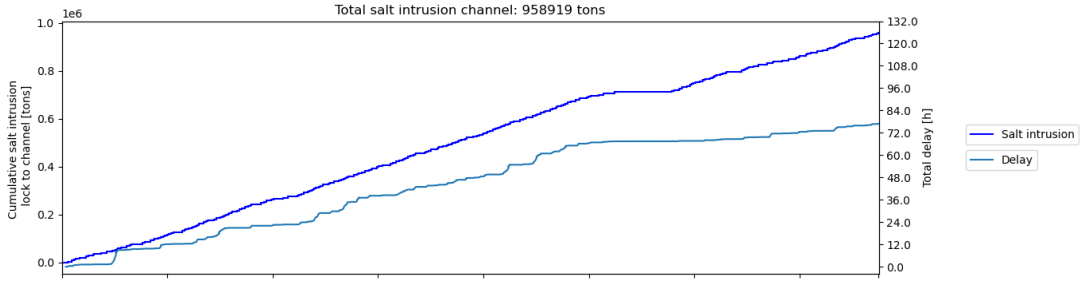

(b) Cumulative salt intrusion and total vessel delay

Figure C.7: 15 minute clustering - OpenTNSim and ZSF calculations

45 minute clustering

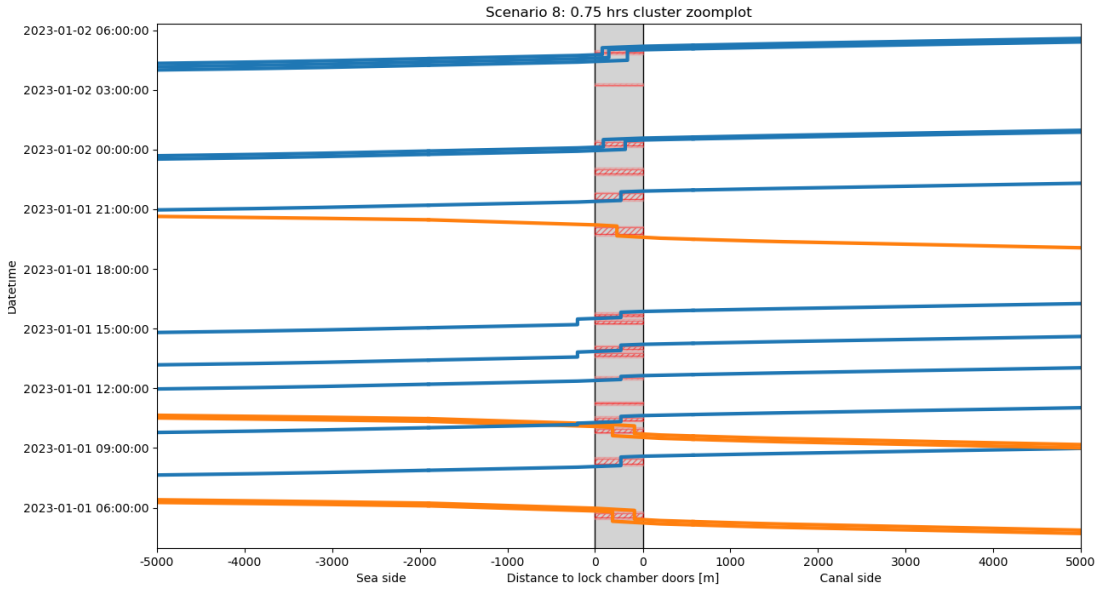

(a) Tracking diagram

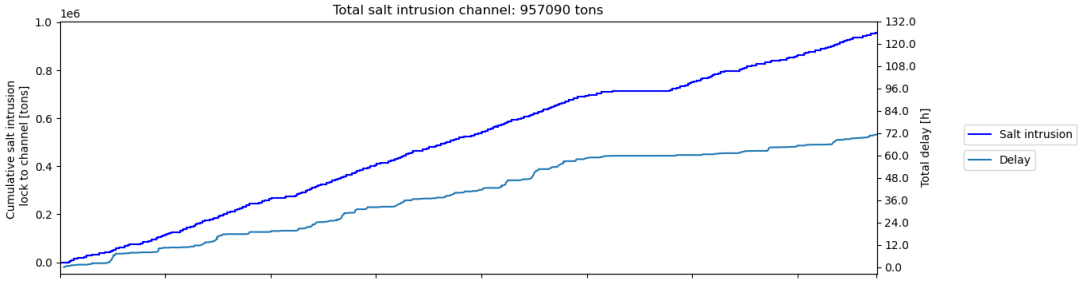

(b) Cumulative salt intrusion and total vessel delay

Figure C.8: 45 minute clustering - OpenTNSim and ZSF calculations

3 hour clustering

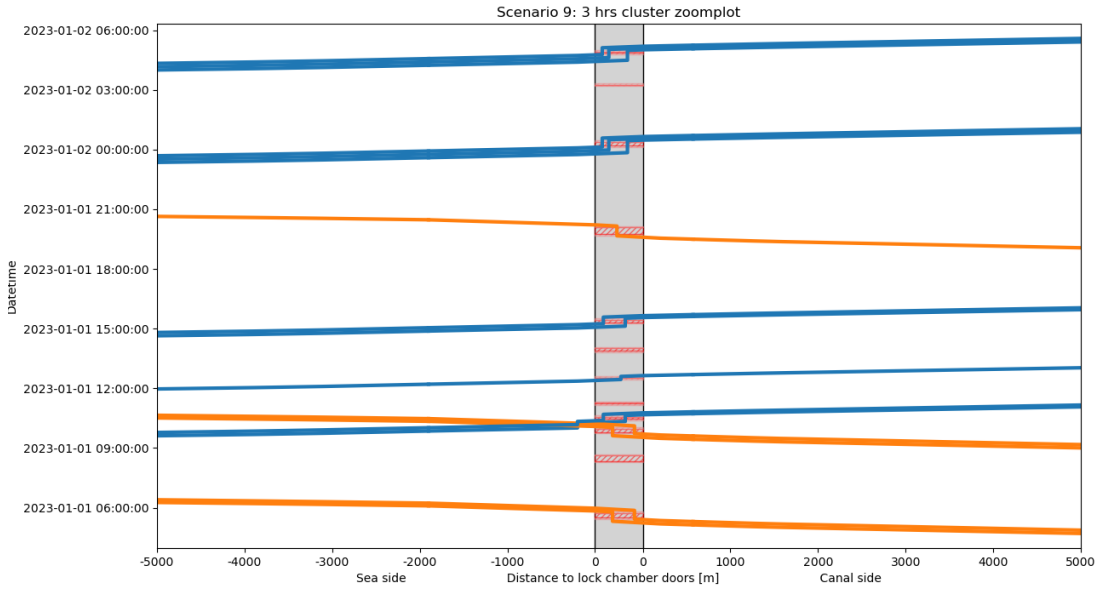

(a) Tracking diagram

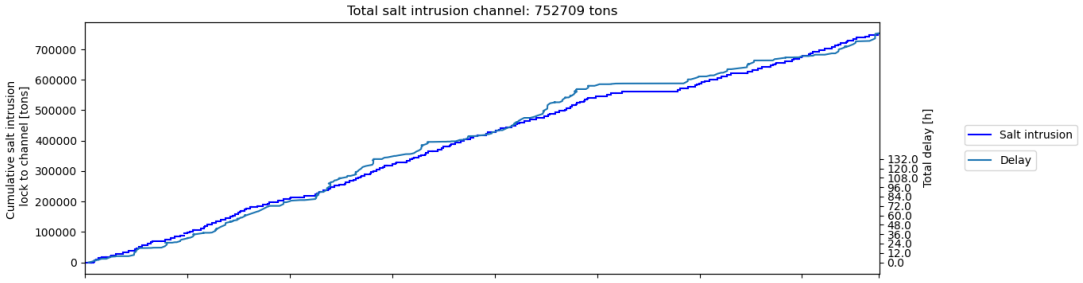

(b) Cumulative salt intrusion and total vessel delay

Figure C.9: 3 hour clustering - OpenTNSim and ZSF calculations

5 hour clustering

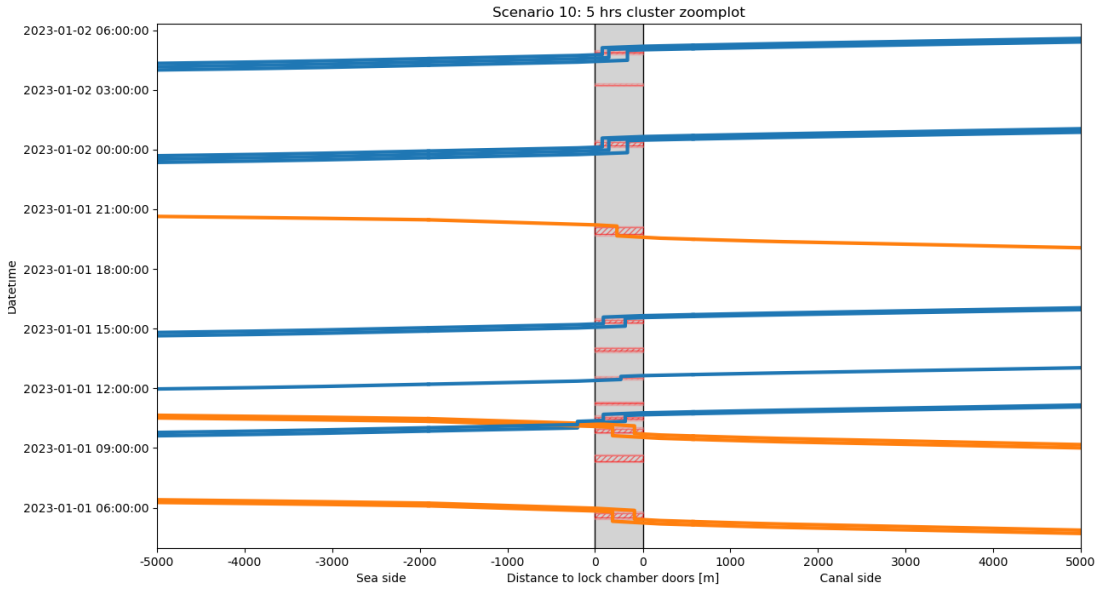

(a) Tracking diagram

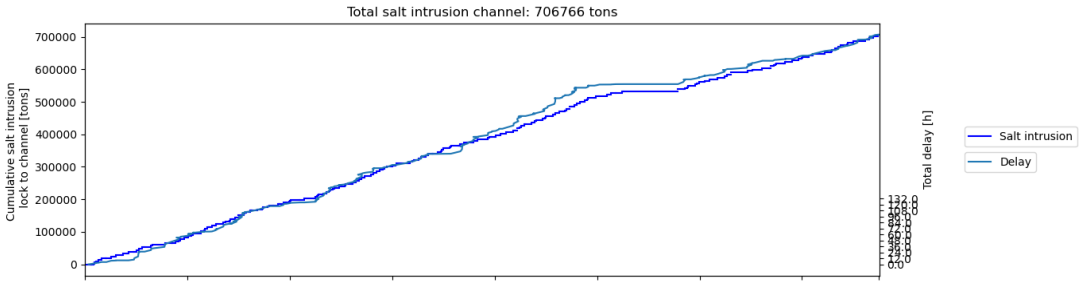

(b) Cumulative salt intrusion and total vessel delay

Figure C.10: 5 hour clustering - OpenTNSim and ZSF calculations